Assessment of calcium sulphate dihydrate on spontaneous combustion at Khwezela Colliery

Thapelo Wilfred Ngoepe

A research report was submitted to the Faculty of Engineering and the Built Environment, University of the Witwatersrand, Johannesburg, in partial fulfilment of the requirements for the degree of Master of Science in Engineering.

Johannesburg, 2021

DECLARATION

I declare that this report is my own, unaided work. I have read the University Policy on Plagiarism and hereby confirm that no plagiarism exists in this report. I also confirm that there is no copying, nor is there any copyright infringement. I willingly submit to any investigation in this regard by the School of Mining Engineering, and I undertake to abide by the decision of any such investigation.

_____ 17/10/2021

Signature of Candidate Date

On this.....17.....day of.....October.....

.....2021..... (Year), at .....Wits University.....

ABSTRACT

Coal spontaneous combustion (CSC) is a major concern in the exploitation and utilisation processes of coal. Various methods for prohibiting the spontaneous combustion of coal have been developed. This study aimed to determine the causes of spontaneous combustion of coal and assess the effectiveness of calcium sulphate dihydrate (gypsum) on spontaneous combustion at Khwezela Colliery in Mpumalanga, South Africa.

In order to exploit coal at favourable costs at Khwezela Colliery, gypsum was applied to two drill holes and one coal stockpile affected by spontaneous combustion. Temperature changes of the three drill holes and coal stockpiles were measured daily for 21 days from 06h00 to 16h00. Data from the holes and stockpiles were represented graphically and analysed using one of the statistical techniques called *t*-test. Furthermore, a *t*-test of two samples assuming unequal variances was used, and the significance level of 0.05 was chosen. The test statistic critical value was 2.1 for the stockpiles and 2.0 for the holes. The absolute value of test statistics obtained from comparing the hot holes ranged from 0.0 to 1.7. At the same time, the absolute value of test statistics for comparisons of the same sides of the stockpiles ranged from 3.6 to 4.3. The treated stockpile produced an absolute value of test statistic of 2.0.

The analysis has revealed that gypsum is effective in managing the spontaneous combustion of stockpiles. An increase in the concentration of gypsum resulted in a decrease in the spontaneous combustion of the treated stockpile. Similarly, an increase in the concentration of gypsum resulted in a decrease in the in-hole temperature fluctuation. The use of gypsum in managing spontaneous combustion results in a decrease in the operation costs, safety and productivity of mining operations affected by spontaneous combustion.

ACKNOWLEDGEMENTS

I would like to acknowledge the following:

- Prof Bekir Genc (School of Mining Engineering, University of the Witwatersrand) for his passion to my research topic and patience through all phases of this research report.
- Mr Mogodi Mahapa for motivating and supporting me during data collection.
- Anglo American Coal for permitting me to use its' site for performing the experiment.
- University of the Witwatersrand for giving me an opportunity to enrol for Msc Mining Engineering.

DEDICATION

To my late Grandfather Thamaga Zacharia Ngoepe, my late uncles Kgotso David Ngoepe, and my late cousins Mpho and Kgaugelo Ngoepe for being there for me we were young.

To my Grandmother Jeanette and my Mother Anna for supporting me financially and emotionally.

To my Siblings Lerato and Tebogo for putting their trust in me.

And the Almighty God (The Father, the Son and Holy Spirit).

!!Bakone Wee!!

Contents

LIST OF FIGURES

LIST OF TABLES

LIST OF EQUATIONS

LIST OF ABBREVIATIONS

AEL	Africa Exploration Limited
AHR	Average Heating Rate
CSC	Coal Spontaneous Combustion
DSC	Differential Scanning Calorimetry
DTA	Differential Thermal Analysis
FCC	Feng Chakravorty and Cochrae
FT	Flammability Temperature
LCD	Liquid Crystal Display
ROM	Run Off Mine
TCM/HR	Total cubic meters per hour
TGA	Thermogravimetric Analysis
WOP	Wet Oxidation Potential
XPT	Crossing-Point Temperature
XRF	X-Ray Fluorescent

1 INTRODUCTION

The Khwezela Colliery lost thousands to millions of tonnes of coal due to spontaneous combustion. This loss included machines worth millions of Rands that caught fire in hot areas. Additionally, this resulted in low productivity of 2 200 tcm/h from the dragline compared to the target of 3 800 tcm/h target due to poor drilling and blasting from working in extremely hot areas. There have been incidents where holes filled with explosives have detonated prematurely, resulting in injuries. Thus, in order to mitigate the occurrence of premature detonation, mines have developed standard operating procedures. In addition, numerous researches are conducted to understand the mechanism of spontaneous combustion of coal (Onifade et al., 2020); for example, Hao et al. argue that the self-heating of coal occurs if the heat produced during oxidation exceeds the heat emitted to the environment (Hao, et al., 2013; Zhang, et al., 2016). Various chemicals have been tested to determine their ability to inhibit spontaneous combustion. For instance, Tsai et al. (2017) investigated and quantified the inhibition effects of Zn/Mg/Al-CO_3 layered double hydroxide, thermo-sensitive hydrogel, di-ammonium phosphate, and sodium phosphate and magnesium chloride. The results demonstrated that Zn/Mg/Al–CO_3 LDHs are extremely highly compatible with coal and form a crystalline structure on the surface of coal, which interrupts the diffusion of oxygen for combustion and, consequently, inhibits spontaneous coal combustion.

1.1 Background of the study

The chemistry of carbonaceous materials such as coal and coal shales make them undergo self-heating when exposed to atmospheric conditions; with an increase of pyrite content, the characteristic parameters of CSC decrease (Wen & Zhang, 2011). These characteristic parameters of coal include the release of CO, CO_2 and CH_4. The activation energy of coal decreases with increasing pyrite content; hence coal with a higher pyrite content tends to be more susceptible to spontaneous combustion (Fuqiang, 2019). The self-heating of coal shales which can start spontaneous combustion, has been reported in South African coalfields (Onifade & Genc, 2019a, b, c). Reactive sedimentary material has pores embedded in the solid together with the carbon-rich elements. This renders the rock porous to different fluids like water and air.

It also increases its surface area, thus making the organic particles reactive as it permits oxygen to get through (Dullien, 1979).

Many researchers have focused more on the self-heating of coal, with few studies determining the self-heating of coal shales (Onifade, 2018). To expose coal, the coal shale material above coal, which often experiences spontaneous combustion, must be drilled, charged, blasted, and moved away. During charging, the extreme heat in the drill hole affects the explosives leading to premature detonation. In order to prevent premature detonation, the extreme heat in the drilled holes must be suppressed before and during charging. Multiple heat-suppressing products have been developed; however, not all have been tested successfully in mining operations. However, calcium sulphate dihydrate (gypsum) has been found to provide excellent fire protection because it dehydrates at temperatures around 120^0C (Belmiloudi, 2005). Dehydration is an endothermic chemical reaction absorbing energy and thus acting as a barrier to heat transfer. It is the effectiveness of this barrier to suppress heat that is investigated in this research.

1.2 Description of the study area

Khwezela Colliery is a coal mine owned by Anglo American. It was formed as a result of the merger between Landau and Kleinkopje Collieries in 2016. It is situated in the South-Eastern part of eMalehleni in Mpumalanga Province, South Africa (Miningdata, 2019). Khwezela Colliery coal area is in the Witbank. Witbank Coalfields has been the heart of coal mining in South Africa since the mining began in the early 1890s (Miningdata, 2019). The initial mining method of coal was bord and pillar, usually with a very low coal recovery ratio of 45%, leaving a substantial amount of coal as pillars. The remaining pillars are currently being mined using the strip-mining method.

Khwezela Colliery is situated in the Northern part of the Witbank Coalfields. The coal forms part of the Vryheid Formation of the Ecca group. Witbank Coalfields has coals with different characteristics, suitable for different applications, such as power generation, metallurgical, liquefaction, domestic and chemical sectors (Onifade, 2018). The Witbank Coalfields consists of five seams with a thick sedimentary sequence (shale, mudstone, sandstone, and siltstone), as shown in Figure 1.1. The seams are numbered from 1 to 5, following the order from the base upwards.

The 5-seam is 2m thick, 4-seam is 3m thick, 2-seam is 7m thick, and 1-seam is 2m thick. The 5-seam and 2-seam are previously mined using bord and pillar, while the other coal seams have not been mined previously. The 2-seam coal is intensely affected by spontaneous combustion, while the remaining coal seams are not affected by spontaneous combustion.

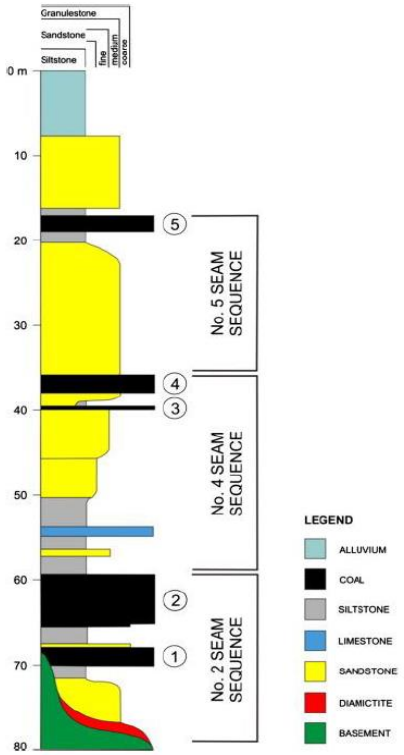

Figure 1.1: Stratigraphic column for the Vryheid Formation in the Witbank Coalfields. ***(Hancox & Gotz, 2014)***

Figure 1.2 illustrates the stratigraphic column of the study area. The No.2 seam coal is approximately 7m thick and overlain by a combination of sandstone and siltstone together referred to as interburden. The interburden is predominantly grey in colour and is affected by spontaneous combustion as illustrated in Appendix A. the No.2 seam coal is underlain by a 1.35m thick 1 seam parting and 3m thick No.1 seam coal. The No.1 seam coal is underlain by a coarse grained and massive sandstone.

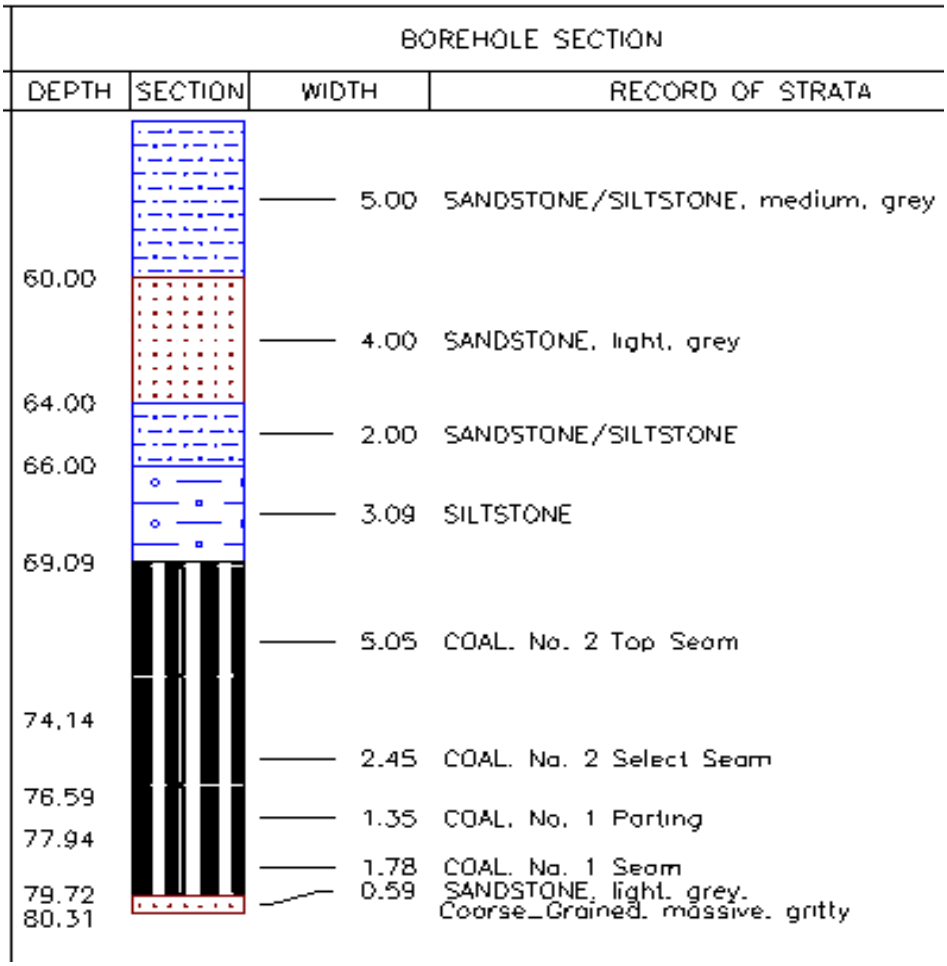

Figure 1.2: Stratigraphic column of the study area

1.3 Problem statement

Khwezela Colliery has been experiencing spontaneous combustion since the opencast mining of 2-seam started in 1978. This has resulted in a loss of coal, the creation of excessive dust, noxious gases, burning of machines, premature explosives detonation, high maintenance costs, and loss of revenue. Based on the financial analysis of the mine, the colliery has incurred costs amounting to over 25% above the budget, which in most cases exceeded revenue as maintenance costs exceeded the budget. These problems were caused by spontaneous combustion, specifically during the drilling and blasting of hot holes.

During the charging of blast holes, the temperature of the holes was measured for all the holes that were to be blasted. Any hole whose temperature was not more than 80^0C was considered safe to be charged by the mine. Some of the holes were measured to have temperatures above 80^0C and could not be charged. This created

a large burden between the charged holes due to the wide scattering holes with unsafe temperatures across the drilled benches. Consequently, poor blasting fragmentation would be produced, resulting in low production of loading machinery.

Blasted coal was observed to be burning, and it required to be sprayed with water before it was loaded to stockpile. This was done to reduce the temperature of the coal and avoid burning the loading and hauling machinery. In order to prevent this loss of coal, a chemical substance inhibiting spontaneous combustion was required.

1.4 Aims and objectives of the research

This research aimed to assess the effectiveness of gypsum in managing spontaneous combustion of blast holes and coal stockpiles at Khwezela Colliery. The following objectives were used to achieve the aim:

- Investigate the causes of spontaneous combustion at Khwezela Colliery.
- Assess the effectiveness of gypsum in managing temperature of the drill holes.
- Assess the effectiveness of gypsum in managing the temperature of coal stockpiles affected by spontaneous combustion.

1.5 Justification for research

Numerous researches have focused on laboratory tests to determine the extent to which various chemical products suppress heat. While many of them yielded positive results, their application to the mining industry in hot holes has not produced satisfactory results. The inhibitors tested in hot holes have only proven effective in suppressing heat from the bottom of the hole. This was observed from the thermocouple reading before and after applying heat treatment products in hot holes at Khwezela Colliery and Tweefontein Colliery.

Khwezela Colliery has experienced poor fragmentation resulting in poor dragline productivity and subsequently low coal exposure rates. This made it impossible to achieve the required targets of saleable coal products and loss of revenue. Additionally, there have been blasting incidents due to the premature detonation of explosives. The success of this research has helped to understand the effectiveness of gypsum to suppress spontaneous combustion of blast holes and coal stockpiles. Other mining operations experiencing hot holes will also benefit from the success of this research.

1.6 Structure of the research report

This report consists of seven chapters which are structured as follows:

Chapter 1: Introduction

Chapter 1 placed into context the foundation on which this study is rooted. This was done by capturing the study's background, including some of the researchers' previous work. It also described the Khwezela Colliery in detail then formulated a clear and complete problem statement. The justification of the study was done by indicating specific reasons to conduct this study and the impact of the study. This chapter ended with the structure of the report to show a coherent and logical flow from one chapter to the next.

Chapter 2: Literature review

Chapter 2 explored and critically reviewed the past and present investigations on the mechanisms of spontaneous combustion, including factors that affect it. It then focused on gypsum, intending to describe how it is used and can be used, including the chemistry of gypsum. Controversial issues arising from different researchers are explored, and proposals are made on harmonising the different issues.

Chapter 3: Research methods

Chapter 3 described in detail the instruments and the methodology used for data collection. It also explained the statistical analysis done to assess the significance of gypsum in managing the spontaneous combustion of hot-holes and coal stockpiles. The use of 64-Channel, thermocouples, and FLIR thermal cameras to collect data was discussed in detail. The use of samples assuming unequal variance and the choice of 0.05 significance level to assess gypsum is also explained in detail.

Chapter 4: Results and discussion on coal stockpile

Chapter 4 showed the graphs of measurements taken daily for each side of the stockpile. It also described the observed pattern between the daily stockpile temperature and atmospheric temperature. The same sides of the stockpile were compared and discussed in order to describe meaningful relationships observed. Statistical analysis was also performed and discussed on the different sides and the same sides of the stockpiles.

Chapter 5: Results and discussion of in-hole temperature

Chapter 5 showed the graphs used for the measurements taken on the hot holes. The effect of gypsum on the management of in-hole temperature was assessed and described in detail. Statistical analysis of data was also done to determine the effectiveness of gypsum in managing in-hole temperature.

Chapter 6: Conclusion and recommendations

Chapter 6 summarised the observed relationships between measurements of the stockpiles and hot holes. It also indicated the extent to which gypsum managed the temperature of the coal stockpiles and in-hole temperature. The limitations of the research were also outlined, including how research can be improved in future.

Chapter 7: References

Chapter 7 used the Harvard referencing style to indicate all the sources which were used in this study.

2 LITERATURE REVIEW

2.1 Introduction

This chapter defines what spontaneous combustion is and it probes into the various causes of spontaneous combustion. It also looks at various methods of predicting the spontaneous combustion liability of coal. The thermal decomposition of gypsum is reviewed in detail in terms of the thermochemistry of gypsum and the heat of dehydration.

2.2 Definition of spontaneous combustion

Genc & Cook (2015) reported spontaneous combustion risks in South African coalfields and the Witbank Coalfields of Mpumalanga Province in South Africa, and the mines which experience intense spontaneous combustion are Khwezela Colliery of Anglo-American Coal and Tweefontein opencast mine of Glencore. Other mines around the Witbank area are also experiencing spontaneous combustion. Spontaneous combustion of coal can occur when coal with relatively low ignition temperature begins to release heat. This occurs in several ways, either by oxidation in the presence of moisture and air; or by bacterial fermentation, which generates heat (Zang, et al., 2019). The generated heat is unable to escape resulting in an increase in the temperature of the coal. The temperature of the coal rises above the ignition point, thus causing spontaneous combustion. When the oxidiser such as oxygen and fuel are present in the required proportion in the reaction, the system experiences thermal runaway.

2.3 Causes of spontaneous combustion

Self-heating of coal and coal shales has been reported to be one of the causes of spontaneous combustion (Onifade & Genc, 2019a, b, c). In most of the coal mines in the Witbank area of Mpumalanga Province in South Africa, the burning of coal is easily observed. These include coal stockpiles, in-situ coal, coal shales above coal layers, especially in the previously mined-out coal seams, high walls and spoil heaps (Onifade, 2018). All these coal constituents are known to be undergoing self-heating and distinguish large open-pit mines. These coal constituents, often containing uneconomic amounts of coal and other carbonaceous material, are exposed to the atmosphere for extended periods from which low-temperature oxidation can take place. Low-

temperature oxidation occurs whenever carbon-containing material is exposed to oxygen in the air. The oxidation rate for a particular material depends on temperature, particle size, oxygen partial pressure, water content and extent of previous oxidation (Carras, 1994). The rate of this reaction increases exponentially with temperature. When the temperature increases sufficiently to be beyond the ignition temperature of the carbonaceous material, ignition starts which lead to spontaneous combustion.

Numerous researches have focused on the spontaneous combustion of coal seams without looking at the spontaneous combustion of coal shales (Onifade & Genc, 2020). Spontaneous combustion of both coal seams and coal shales in the Witbank area has been extensively studied by Onifade & Genc (2018a, b, c). Aforementioned studies looked at 14 coals and 14 coal shales in the Witbank area. The study by Onifade & Genc (2018a, b, c) concluded that coal shales found in association with coal seams vary considerably in their intrinsic properties and spontaneous combustion liability (Onifade & Genc, 2019a, b, c; Onifade et al., 2019). From this observation, the study established the interrelationship between the spontaneous combustion liability and properties of coal and coal shales.

Alpern & Lemos de Sousa (2002) stated that coal shale consists of 50% to 90% ash. This usually provides a clear indication of the coal quality. Coal and coal shales, consisting of varying proportions of organic matter and inorganic material, mainly crystalline, may undergo spontaneous combustion (Onifade & Genc, 2019a, b, c; Onifade, et al., 2019). This enables the rock to be porous to air, and with the increased surface area, the organic particles have reactive oxidation sides (Dullien, 1979). The implication is that oxygen will occupy the pores, increasing the likelihood of the organic material oxidation leading to spontaneous combustion.

Coal shale may undergo spontaneous combustion due to the amount of pyrite, organic composition, reactive nature and coal rank (Onifade, et al., 2018). The effects of the intrinsic properties of coal shales such as ash content, moisture, volatiles, carbon, nitrogen, hydrogen, sulphur, and mineral composition causing the start of self-heating in coal is complicated and may be the reason for the difficulties in understanding the mechanisms of spontaneous combustion (Beamish & Hamilton, 2005). The spontaneous combustion liability of coal shales differs between bands of coal seams when exposed to oxygen in the air (Onifade & Genc, 2019a, b, c).

2.4 Factors affecting spontaneous combustion of coal

Low-temperature oxidation of coal can be affected by several factors such as oxygen concentration, temperature, inherent moisture content, particle size and surface area (Zhang, 2001). It can also be affected by maceral composition, coal rank, volatile matter and chemical composition of coal (Scott, 2002). Eroglu (1992) supported by Onifade & Genc (2018), posited that spontaneous combustion could also be affected by coal's geological, environmental, mining, and physical and chemical composition. Phillips, et al. (2011) mentioned geological factors consisting of seam thickness, seam gradient, organic matter and geological discontinuities. Other factors which affect the spontaneous combustion of coal include ambient temperature, oxygen concentration, humidity, metamorphic grade, composition, moisture content, bulk density and particle size (Wang, et al., 2016).

The mining of 2-seam using the strip-mining method often leaves the high-wall side of the strip exposed to air, thereby allowing the ingress of oxygen into the coal and coal shales to initiate spontaneous combustion (Onifade, 2018). At Khwezela Colliery, the coal left on benches and the cracks visible on the benches also affect spontaneous combustion (Onifade, 2018). Ozdeniz et al. (2015) classified air pressure, relative humidity, wind speed, wind direction, moisture and sun radiation as some of the environmental factors affecting spontaneous combustion. The presence of water on the 2-seam bords and the proximity to Olifant River could provide the moisture that exacerbates spontaneous combustion.

Particle size and porosity of coal and coal shales affect the spontaneous combustion of coal, as illustrated by Mastalerz, et al. (2010) and supported by Onifade, et al. (2018). Coal with large particle sizes experiences lower spontaneous combustion liability than coal with a smaller range of particle distribution (Hansel, et al., 2004). Large particles have a smaller surface area and higher density, while smaller particles possess a bigger surface area and lower density. The liability of spontaneous combustion of coal was increased with decreasing particle size, increasing the moisture content of the coal, and decreasing air humidity (Kucuk, et al., 2003). This is evident after a 2-seam of Khwezela Colliery is mined and put on stockpile; it tends to undergo spontaneous combustion rapidly and intensely, as observed by the researcher. The 2-seam and 1-seam of Witbank Coalfields in South Africa have

different particle sizes and densities. The 1-seam has a higher granular and density than the 2-seam. The 1-seam at Khwezela Colliery is not affected by spontaneous combustion as it is not mined previously using board and pillar mining, while the 2-seam is affected by spontaneous combustion as it was previously mined using the board and pillar mining method. This could be the reason for 2-seam to be adversely affected by spontaneous combustion, while 1-seam coal is not adversely affected by spontaneous combustion.

Uludag (2007) explained that the extent of self-heating could be based on a complex relationship between various intrinsic and extrinsic factors of coal. Arisoy & Akgun (2000) found that the moisture content and oxygen in the air influence the spontaneous combustion liability of coal. Their studies are supported by Beamish & Hamilton (2005), who discovered that a low moisture content might support spontaneous combustion liability of coal while a high moisture content impedes spontaneous combustion liability of coal. This view agrees with the Khwezela Pit observation, where the areas observed to have reddish water accumulation are affected by spontaneous combustion, especially the lithology immediately above the water level. Khwezela Pit has high moisture due to the water observed on the No. 2 seam bords. This could be another reason for the No.2 seam being affected by spontaneous combustion. It is also observed that the moisture content of coal affects the initial stages of coal self-hearting (Ren, et al., 1999).

2.4.1 Atmospheric effects on coal stockpile

Self-heating of coal stockpiles poses a serious problem for both coal producers and users. Spontaneous ignition occurring in coal stores leads to the loss of precious coal resources and the emission of greenhouse and toxic gases (Carras & Young, 1994). Coal stockpiles are mainly studied in relation to recognizing basic variables affecting the process of self-heating (Zhu, et al., 2013). Thus, using mathematical models, the effects of coal characteristics such as reactivity or particle size, the effects of coal characteristics such as bed porosity, slope angle and stockpile height, as well as meteorological conditions such as solar radiation, oxygen concentration and wind speed on the self-heating of coal stockpiles were studied in more detail (Taraba & Michalec, 2014).

Figure 2.1 illustrates that the exposure of a coal stockpile to atmospheric winds reduces the safety margins. A wind speed of 1 m s^{-1} can be considered critical because when exceeded, temperature runaway occurs, and the spontaneous heating process in the stockpile begins to turn into uncontrolled combustion. The dynamics of self-heating are positioned between the curves of 2 m s^{-1} and 3 m s^{-1}, which corresponds well with the monthly average wind speed from the SW–NE direction of 2.35 m s^{-1}. Obviously, concerning the progress of the spontaneous heating of the stockpile pile, the fluctuating character of the wind manifests itself by the average value of the wind speed from the prevailing direction (Taraba & Michalec, 2014).

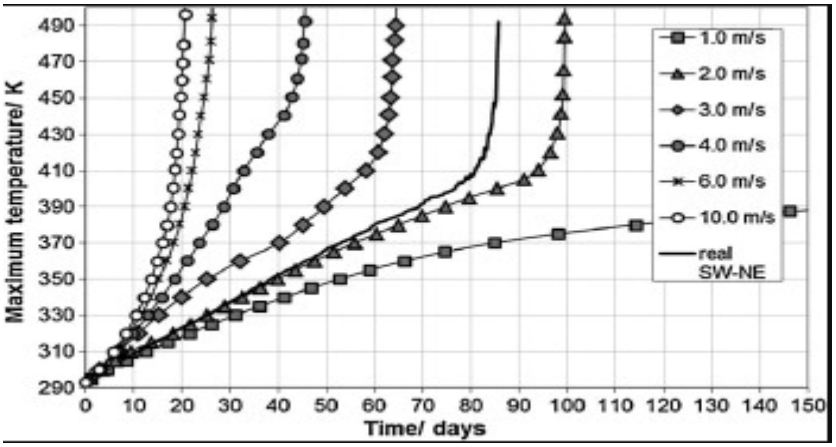

Figure 2.1: Variation of the coal stockpile maximum temperature vs time for different wind speeds ***(Taraba & Michalec, 2014)***

Air entering a stockpile play a more complex role. On the one hand, it cools the stockpile by taking away the generated heat, while on the other hand, the oxidation process becomes more intense. Both aspects immediately affect the development of the maximum temperature inside the stockpile, which is considered a key parameter characterising the risk of self-heating in coal stockpiles (Srinivasan & Pradeep, 1996).

2.4.2 Wind-driven forced convection and natural conduction

Stockpiles consisting of coarse and fine coal particles are affected by wind differently and to different extents, and different equations also govern them. Most of the investigations of coal stockpiles have focused on experimental methods of fine particles, which are about a few millimetres in diameter (Sipila & Auerkari, 2012). The gas flow within fine particles coal stockpile follows Darcy's Law (Sipila & Auerkari,

2012). However, the diameters of coarse coals are much greater than those fine-particle coals, ranging from 3cm to 20cm. This indicates that the gas flow within the coarse coal stockpile is inappropriate to be governed by Darcy's Law because of the high Darcy's parameter and Reynolds number. Coarse particles are more prone to spontaneous combustion than fine particles (Zhu, et al., 2013).

Figure 2.2 illustrates Contours of temperature within the coal stockpile at different stages of the spontaneous combustion heating process when the wind blows with a speed of 3 m s^{-1}. Hot spot temperature is of (a) 346 K; (b) 370 K; (c) 397 K; (d) 475 K. Numerical simulations with both fixed direction and real fluctuations of the airflow confirmed the promoting role of wind on the dynamics of the development of spontaneous heating as illustrated in Figure 2.2. Concerning progress in the spontaneous heating of the pile, the fluctuating character of the wind manifests itself by an average value of the wind speed from the prevailing direction.

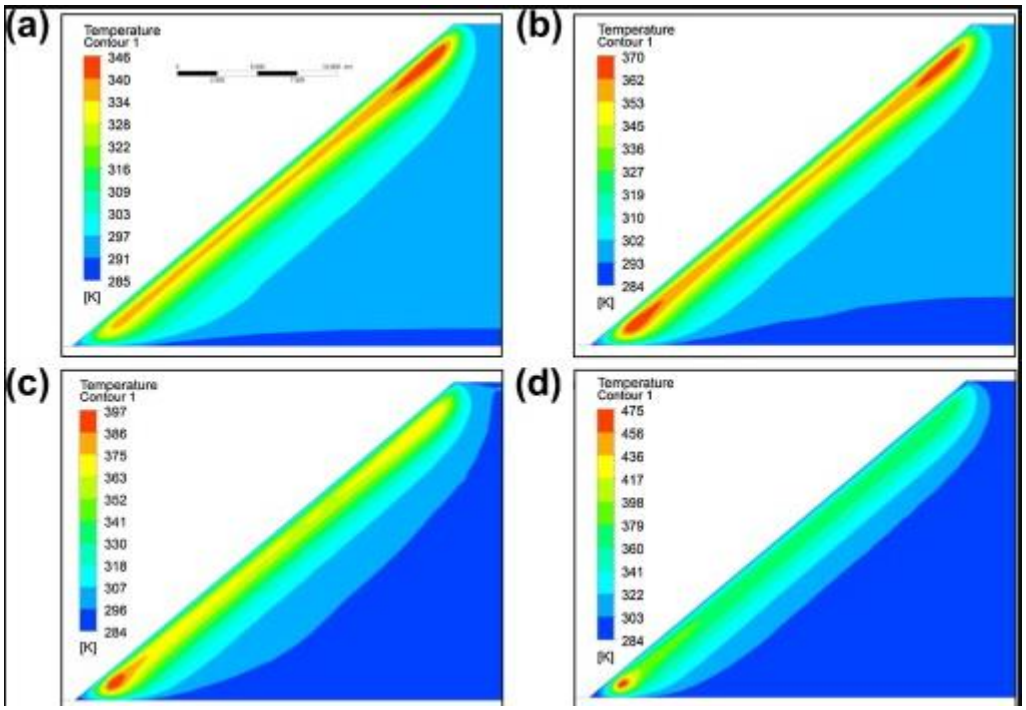

Figure 2.2: contours of coal stockpile temperature at different stages of spontaneous combustion heating process ***(Taraba & Michalec, 2014)***

Wind-driven forced convection affects the gas flow within the stockpile greatly. Therefore, the temperature distribution of the coarse coal stockpile is influenced by wind velocity. On the one hand, with a wind blowing on the left side of a stockpile, there could be one hot spot in the coarse coal stockpile, and the temperature distribution is asymmetric. On the other hand, the self-ignition location in a coal stockpile moves towards the downstream and upper part of the coal stockpile when wind velocity increases. When the wind is gentle, the ignition occurs on the lower part of the coal stockpile, close to the surface of the windward side, which is consistent with the location of the hottest spot in a fine-particle coal stockpile (Akgun & Essenhigh, 2001). When the wind blows moderately at a velocity of 0.05m/s to 0.5m/s, the self-ignition takes place nearly on the centre of the stockpile, but with a wind velocity of 1m/s, the combustion location is at the upper part of the stockpile (Akgun & Essenhigh, 2001).

2.4.3 Influence of pyrite on spontaneous combustion of coal

The presence of sulphur in coal can be classified into organic and inorganic sulphur. Organic sulphur is hard to distinguish from other forms of sulphur due to its ability to combine with macromolecular structures in the form of covalent bonds with a complex structure (Beamish, et al., 2012). The inorganic sulphur in coal occurs in the form of pyrite and sulphate. Olivella, et al. (2002) quantified the sulphur content in coal seams to be between 0.3% to 15.1%. An excess amount of sulphur in coal promotes self-heating, which lead to CSC. Hsieh & Wert (1985) measured the content of pyrite on lignite, sub bituminous, bituminous and anthracite coals of the United States of America to be from 0.59% up to 3.9%. Olivella, et al. (2002) measured the South African coal and some coal samples from around the globe to contain from 5.4% up to 15.1% pyrite. The study of Waterberg Coal revealed coal as medium sulphur type coal with pyritic and organic sulphurs accounting for the bulk of the total sulphur (Makgato & Chirwa, 2017). Maceral analyses of coal showed that vitrinite is the dominant maceral (up to 51.8 vol. %), whereas inertinite, liptinite and reactive semifusinite occurred in proportions of 22.6 vol. %, 2.9 vol. % and 5.3 vol. % respectively. The ratio of fixed carbon to volatile matter, commonly referred to as fuel ration which indicates the combustion characteristics of the coal was determined.

Mastelerz (2010) indicated that pyrite as a major constituent of inorganic sulphur has significant influences on the spontaneous combustion liability of coal. Yang, et al. (2019) also noted that pyrite as an impurity is generally considered the main form of inorganic sulphur and has a notable impact on CSC. Pyrite reacts with oxygen in the presence of water to form hydro-peroxide (H_2O_2) and therefore initiates oxygen (Huffman & Huggins, 1985). Bhattacharya (1971) argues that pyrite with a concentration of 2% promotes the spontaneous combustion liability of coal. The type of pyrite within the coal determines whether rapid self-heating would occur (Beamish, et al., 2012), and coal consisting of high pyritic sulphur does not reach thermal runaway fast enough in a dry state compared to coal in a moist state.

Arisoy & Beamish (2015) conducted an adiabatic oven test to measure the accelerating effect of pyrite and moisture on coal self-heating rates and reaction rate data for pyrite oxidation. This study found that coals of similar intrinsic spontaneous combustion reactivity can show quite dissimilar behaviours regarding the time taken to reach thermal runaway. In some circumstances, the moderating effect of moisture can delay thermal runaway considerably due to the heat loss from evaporation. Conversely, thermal runaway can be accelerated due to the presence of reactive pyrite. The pyrite reaction with oxygen also consumes moisture, which creates an additional drying effect that does not consume heat, unlike the normal moisture removal that takes place through evaporation. Consequently, the self-heating of the coal is accelerated, and a feedback mechanism develops that produces a dramatic self-heating behaviour not shown by previous studies (Arisoy & Beamish, 2015).

Deng, et al. (2015) evaluated the effects of pyrite contents on one factor affecting the spontaneous combustion liability of coal. Coal samples with pyrite contents of 0%, 3%, 5%, 7%, and 9% were produced by blending coal and pyrite. The DSC was used to determine the intensity of heat discharged during coal oxidation for the different pyrite contents. The study indicated that the presence of pyrite could accelerate the propensity of CSC. The DSC showed that the coal sample with a 7% pyrite content has the highest rate of heat flow. Samples with pyrite contents of 5% to 7% have the most significant influence on spontaneous combustion liability within the range of the study.

Sunjati & Zhang (1999) investigated the effect of inorganic matter on the spontaneous combustion behaviour of Victorian brown coal. Each of the fourteen samples they used was tested in an isothermal reactor to obtain its critical ambient temperatures with those of raw coal and the acid-washed coal. Potassium chloride, montan powder and sodium chloride were the most effective inhibitors, followed by magnesium acetate and calcium chloride. The presence of sodium nitrate and ammonium chloride in the coal samples did not significantly influence spontaneous combustion. However, calcium carbonate, sodium acetate, potassium acetate, and pyrite promoted spontaneous combustion. The effect of additive loading was also investigated for an inhibition agent (KCl) and a promotion agent (NaAc). It was revealed that the effectiveness of these promotion and inhibition agents was enhanced with an increase in the additive loading. Low-temperature oxidation kinetics were also estimated by an energy balance approach and compared with the self-heating potential of these samples. The effects of reactor size and reactor specific surface area on the critical ambient temperatures are also discussed.

A simultaneous thermal analysis experiment was likewise conducted by Yang, et al. (2019) to understand the influence of pyrite on the tendency of coal to undergo spontaneous combustion. This study found that with a higher pyrite content, characteristic parameters, the temperature corresponding to the maximum weight loss and peak temperatures of coal samples are lowered. They concluded that the activation energy of coal samples decreases with increasing pyrite content. Coal with high pyrite content tends to be more liable to spontaneous combustion. All the investigations found that pyrite promoted the spontaneous combustion of coal. Lain (2009) expressed the pyrite oxidation as illustrated in Equation 2.1:

$$Fe_2S + 7O_2 + 16H_2O = 2H_sSO_4 + 2FeSO_4.7H_2O + 1321KJ \qquad (2.1)$$

The equation above is an exothermic reaction that occurs at low temperatures, which generate heat that is double that of coal with the same oxygen (Martinez, 2009). This indicates that the presence of pyrite is a contributing factor towards the spontaneous combustion liability of coal.

2.5 Methods of predicting spontaneous combustion liability of coal

There is currently no specific standard method of evaluating spontaneous combustion liability of coal due to the inherent variability of coal properties. Various organizations

have used various techniques to evaluate the spontaneous combustion liability of coal. A brief description of the methods to predict spontaneous combustion of coal are discussed:

2.5.1 Differential scanning calorimetry (DSC) method

This method determines the changes in energy inputs provided to a substance and a reference material as a function of temperature when both materials are kept at a controlled temperature. Sahu, et al. (2004) used DSC to evaluate the spontaneous combustion liability of coal. Thirty coal samples from seven different Indian Coalfields were investigated and their initial temperature determined. The study indicated that an increase in the temperature indicates the spontaneous combustion liability of coal.

Zhang, et al. (2016) used the DSC to determine the intrinsic reaction of Ximeng brown coal oxidation at low temperatures. The heat evolution of the intrinsic reaction after eliminating the water evaporation and thermal decompositions of the inner oxygen-containing functional groups was obtained by subtracting the DSC curve in N_2 from the DSC curve in the air. It is considered that the intrinsic reactions between coal and oxygen could be divided into three stages, including the slow oxidation, accelerated oxidation and rapid oxidation stages. Compared with the DSC-air curve, the DSC-sub curve based on the subtracting results elucidated the exothermic characteristics of an intrinsic oxidation reaction in each stage more clearly. In addition, the DSC-sub curve reduced the experimental errors inborn from the heating rate and the sample mass, so it had a more practical application value than DSC-air curves. Activation energies obtained from DSC-sub curves can better reflect intrinsic oxidation reaction and be used as important indicators for the evaluation of CSC (Zhengfeng, et al., 2016).

2.5.2 Thermogravimetric analysis (DGA)

This method estimates the loss in weight of coal samples at variable temperatures due to self-heating. A specific coal sample is heated through a programmed heating process and plotted against the time/temperature. The results are termed Thermogravimetric (TG) curves. The created TG curve is referred to as the differential Thermogravimetric (DTG) curve and is the difference between the coal curve and the inert material curve. Choudhury et al. (2007) and Onifade et al. (2020) used the TGA technique to assess spontaneous combustion characteristics of different coal samples. Choudhury, et al. (2007) found that the amount of vitrinite and lipnite showed high

spontaneous combustion liability. The parameters used in the method were observed to have a strong relationship with the petrographic composition that combines the effect of coal rank and mineral matter (Choudhury, et al., 2007).

Chen, et al. (2019) used Thermogravimetric (TGA) and in-situ Fourier transform infrared spectroscopy to study spontaneous combustion in bituminous coal. The results show that the coal's spontaneous combustion can be divided into five stages. The spontaneous combustion of Gubei bituminous coal (Chen, et al., 2019) is divided into five stages. Stage I is the water evaporation and minimal mass loss stage (30 °C–135.7 °C), Stage II is the oxygen absorption weight increase stage (135.7 °C–294.6 °C), Stage III is the slow chemical reaction stage (294.6 °C–419.5 °C), Stage IV is the combustion stage (419.5 °C–574.3 °C), and Stage V is the burnout stage (temperatures > 574.3 °C).

2.5.3 Russian U index

This method estimates the amount of oxygen absorbed by individual coal samples over 24 hours (Banerjee, 2000). The gases obtained under the experimental conditions may be quantified by evaluating gas composition. The oxygen absorbed during the testing is directly proportional to the spontaneous combustion liability of coal (Banerjee, 2000). The problem with this method is that the volume of oxygen absorbed by the coal sample during testing is not reproducible when repeated with the same coal.

Panigrahi, et al. (1997) studied and presented the experimental setup for determination of the Russian U index. Ten coal samples from Jharia coalfield have been analysed using this method. The carbon, hydrogen, nitrogen and sulphur contents for these samples were determined using Fenton`s method of ultimate analysis modified at the Central Fuel Research Institute, Dhanbad, India. In addition to this, the XPT of these samples were also determined. Attempts were made to correlate the Russian U index and XPT of coal samples with its basic constituents, viz., carbon, and hydrogen and ash contents. It was also observed that from the point of susceptibility of spontaneous combustion the Russian U index shows a similar relationship with the basic constituents of coal as that of the crossing point temperature. (Panigrahi, et al., 1997)

2.5.4 Differential thermal analysis (DTA)

This method involves heating a small coal sample at a constant temperature and keeping records of the temperature difference within the material and similar inert material as a function of temperature existing in the medium. This indicates the changes in a material's chemical and physical properties at the particular temperature and the properties of the material used (Mohalik, et al., 2010). Uludag (2007) used this method to study the spontaneous combustion liability of South African coals with a small-scale laboratory testing apparatus. Each sample tested for the analysis has different characteristics in terms of calorific value, volatiles, moisture content, and porosity. It is impossible to isolate a single property of coal and analyse it individually. DTA analysis results are a combined effect of the inherent characteristics of coal. A certain sequence of events occurs during the heating process, which can be analysed using various regions of the DTA thermogram. The first stage of the heating process involves oxygen absorption and loss of inherent moisture. This is evident from the decline of temperature and the slope of the curve. The DTA curve rapidly accelerates during the second stage due to volatiles. Since most of the moisture is lost during the first stage, no temperature decrease is observed in the second stage. The volatiles and the constant increase in coal temperature catalyse the self-heating process, occurring at temperatures around 70–90°C. This minimum point is believed to be one of the most important aspects of the DTA curve. Therefore, a more detailed analysis of DTA should be used when describing the behaviour of coal in a standard testing environment. The Wits-Ehac Index should be modified to include the minimum point of acceleration and inherent moisture content as factors in self-heating (Uludag, 2007). Nimaje & Tripathy (2016) used DTA to assess the liability of some Indian coals to spontaneous combustion. Their studies found that the flammability temperature, Wet oxidation potential, and DTA studies used to assess the spontaneous combustibility character indicated no significant correlation with the intrinsic properties (Nimaje & Tripathy, 2016).

2.5.5 Crossing-point temperature (XPT)

The experimental tests of this method involve heating coal in an oxidised condition to cause low-temperature oxidation either at an automatic heating rate or at a certain temperature from the ambient temperature to the ignition temperature of the coal

(Onifade, 2018). This method is extensively used in South Africa, Poland, Turkey and India to categorize spontaneous combustion liability of different coal seams. Coal with a lower liability index has a higher XPT. Humphreys (1979) argues that this method is not suitable because it does not consider the inherent properties of coal and the design of the experiment. Issues have been raised on the crossing-point temperature (CPT) techniques due to the variation in the setting of a reference point, which is partly reflected in the disputes among the developers of the individual techniques (Wang, et al., 2011). As reported in the literature (Chen, 1999), the CPT determined by Chen's technique departs from the oven temperature, with a variation ranging from several to a few tens of kelvin. The extent of departure depends on the temperature of the oven and the properties of the sample tested. These two techniques are almost identical in nature but yield different test results even under the same experimental conditions. The obvious question is which results are more reliable. Generally speaking, in the utilisation of the CPT techniques, there are two basic impending issues:

1. How does the temperature of the crossing-point and its corresponding rate of temperature rise relate to the kinetics of the exothermic reactions?
2. How do the crossing-point temperatures measured contain essential information for reliable determination of the kinetic parameters associated with the reactivity of solids?

Chen (1999) answers the above questions by saying that the CPT, where the heat conduction diminishes at the centre of a symmetrical exothermically reactive solid, can be considerably different from the set oven temperature during a transient basket heating procedure for measuring exothermic reactivity. The CPT differs from the oven temperature by a larger amount for a greater oven temperature and depends on sample size and the nature of the materials concerned. Such differences can, under certain circumstances, lead to considerable variations in the estimation of the kinetic parameters for the two existing transient testing procedures. This is an important point of consideration for future work in the area of thermal ignition of particulate materials.

Barve & Mahadevan (1994) have shown the relationship of the inherent properties of coal to XPT as illustrated in Equation 2.2:

$$\mathrm{XPT} = 168.8 - 10.3\mathrm{M} + 0.12\mathrm{A} + 0.69\mathrm{M}^2 - 0.06\mathrm{MA} + 0.01\mathrm{A}^2 \qquad (2.2)$$

where M is the moisture content, A is the ash content.

The XPT and DTA of selected coal samples have been used jointly to obtain a consistent self-heating liability index, the Wits-Ehac Index (Onifade, 2018). The Wits-Ehac Index was developed in South Africa in the late 1980s to test the spontaneous combustion liability of coal (Eroglu, 1992). The apparatus consists of an oil bath, three coal and inert materials, an oil circular, a heater, a flowmeter, an air supply compressor and computers illustrated in Figure 2.1 (Wade, et al., 1987). When using the DTA, the difference in temperatures between the coal sample and an inert material sample is measured by a data logger, stored in a computer, and plotted against the temperature of the inert material sample. When the temperature difference between the inert material and the coal sample is plotted against the inert temperature, the part of the graph where the coal is heating faster than the inert sample is termed Stage II.

It is important to understand that during the DTA, three stages are obtainable. During Stage I, the temperature of an inert material sample is higher than the temperature of the coal sample. During Stage II, the coal sample begins to heat up at a higher rate than the heating rate of the inert material. High exothermicity is reached when the line crosses the zero-base line and is referred to as the XPT. The index makes use of the fact that coal highly prone to self-heating has a steeper Stage II slope and a lower XPT than coal not highly prone to self-heating. According to Wade et al. (1987), coal with a spontaneous combustion liability index below 3 is low risk, 3 to 5 medium risk, and coal with values greater than 5 are high risk. The index is calculated from the formula in Equation 2.3. The thermogram in Figure 2.2 illustrates the stages and the XPT for a given coal sample.

$$\text{Wits} - \text{Ehac Index} = \left(\frac{\text{Stage II slope}}{\text{XPT}}\right) * 500 \qquad (2.3)$$

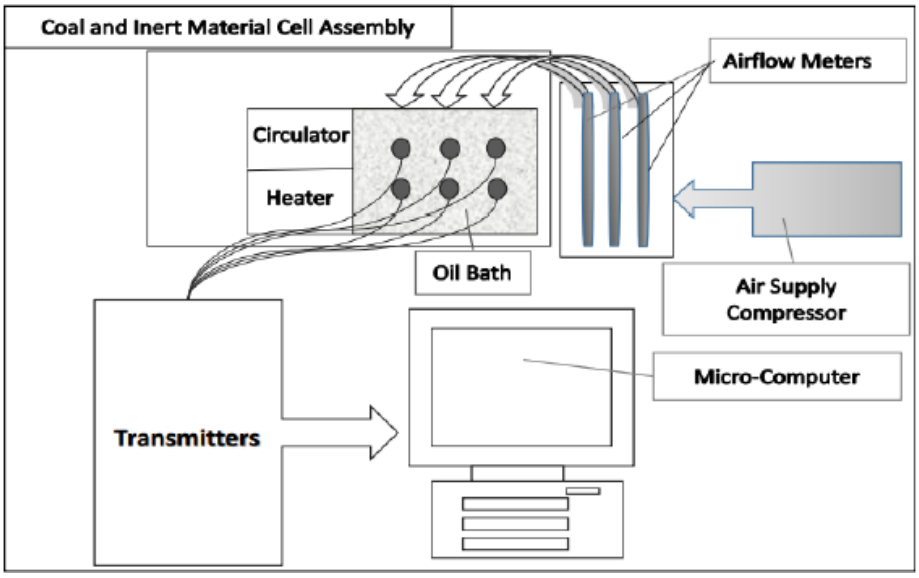

Figure 2.3: Schematic of the Wits-Ehac apparatus setup ***(Wade, et al., 1987)***

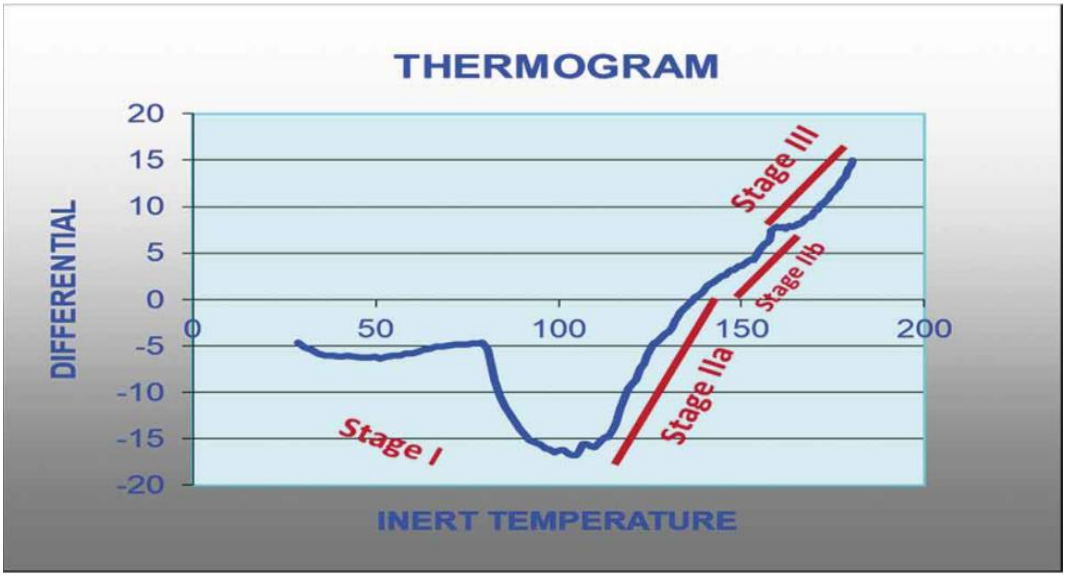

Figure 2.4: Differential analysis thermogram of coal sample ***(Wade, et al., 1987)***

2.5.6 Olpinski Index method

In this method, a pellet of powdered coal of 0.4g is heated at a constant rate in a Quinone steam bath with the flow of air through the pulverised coal. The time against the temperature curve is recorded until a temperature of 235^0C is reached. The temperature increase of the coal at this stage is used to provide a better definition of the spontaneous combustion liability index of Indian coal by establishing the

relationship between XPT, FT, WOP, proximate and ultimate analysis (Nimaje & Tripathy, 2016). This technique is generally used in Poland to categorize the spontaneous combustion liability of coal. The liability index is referred to as Szb Index.

2.5.7 Adiabatic calorimetry method

This technique involves placing a coal sample in a reaction vessel either in an adiabatic oven or oil bath such that the heat is not dissipated from the vessel. The coal temperature in a reaction vessel is controlled at intervals relative to the increase in the coal temperature. The reacting air or oxygen flows through the reaction vessel. This method is used in South Africa and New Zealand to reproduce the original condition of self-heating characteristics (Cliff, et al., 1996). The rate of temperature increases, and ignition temperature and the kinetic constant of coal are used to determine the proneness of coal to spontaneous combustion. Chen, et al. (2016) Use of adiabatic calorimetry to characterise thermal runaway of Li-ion cells is a crucial technique in battery safety testing. Various states of charge (SoC) of Li-ion cells were investigated to ascertain their thermal runaway features using a Vent Sizing Package 2 (VSP2) adiabatic calorimeter. To evaluate the thermal runaway characteristics, the temperature-pressure-time trajectories of commercial cylindrical cells were tested, and it was found that cells at a SoC of greater than 50% were subject to thermal explosion at elevated temperatures. Calorimetry data from various 18650 Li-ion cells with different SoC were used to calculate the thermal explosion energies and chemical kinetics; furthermore, a novel self-heating model based on a pseudo-zero-order reaction that follows the Arrhenius equation was found to be applicable for studying the exothermic reaction of a charged cell (Chen, et al., 2016). Having determined the various methods of predicting CSC, the various chemicals which have the potential to inhibit CSC are necessary to be investigated.

2.6 Chemical inhibitors on spontaneous combustion of coal

Many theories have been developed to explain the mechanism of CSC since the 17th century (Stach, et al., 1982). These theories include pyrite and phenolic action theories, coal-oxygen reaction theory, bacteria action theory, free radical theory, hydrogen atom theory and group action theory. Amongst all the proposed theories, the coal-oxygen reaction theory seems to have obtained the approval of most scholars (Li, et al., 2020). Experimental investigations confirm that coal adsorbs oxygen and an

oxidation reaction occurs between coal and oxygen. This interaction causes gradual heat accumulation, creating favourable conditions for spontaneous combustion (Xiao et al., 2018).

Physical-based materials for retarding CSC, such as chlorine salts ($MgCl_2$, KCl, CaCl2, and NaCl), have been used (Wang & Dou, 2014). These materials can retain water due to their hydrophobic properties. After they have absorbed water, a liquid membrane forms on the coal, preventing oxygen from coming into contact with the coal. The inhibition efficiency of 88% can be achieved using chlorine salts.

Sujiganti & Zhang (2000) analysed the effects of additives on the critical ambient temperature above which thermal runaway occurred and analysed the reaction rate of acid-washed coal. They explained that the effects of additives on CSC depended on the anion and cation in them. $CaCl_2$ and NaCl enhanced the critical ambient temperature and decreased the reaction rate, presenting an inhibition performance on the CSC. Zhang (2010) selected 20% $MgCl_2$ as an inhibitor to treat CSC and found that CO (Carbon Monoxide) production during oxidation was significantly suppressed.

Ammonium salts such as NH_4Cl, $NH_4H_2PO_4$, $(NH_4)2HPO_4$, and NH_4HCO_3 are commonly used CSC inhibitors. Ammonium salts exhibit a high water retention capacity (Li et al., 2020). These materials easily undergo thermal decomposition, which is an endothermic process, and the heat generated from coal oxidation is absorbed. Moreover, the pyrolysis products of ammonia (NH_3) and Carbon dioxide (CO_2) can dilute the concentration of oxygen (Zheng, 2010).

The acid products of ammonium salts such as H_3PO_4 can rupture hydroxyl groups of coal to limit spontaneous combustion (Liodakis, et al., 2002). Su, et al. (2014) reported that $NH_4H_2PO_4$, the main material used for developing ABC (mono ammonium phosphate-based) powders, underwent thermal decomposition when heated. This action may suppress heat accumulation in the process of CSC. Zeng, et al. (2010) used 20% NH_4HCO_3 and 20% $NH_4H_2PO_4$ as inhibitors to investigate their potential inhibition on CSC. Their studies reported a CSC inhibition rate of 74% to 80%. However, poor thermal stability limited the application of ammonium salts as a spontaneous combustion inhibitor. Moreover, the pyrolysis product of NH_3 is a toxic gas and is a health hazard for mine-workers.

The oxidation process causes an expansion for the volume of pyrite, thus promoting the development of coal pores. This exposes coal to oxygen, thereby promoting a coal-oxygen reaction. Yang (1996) simulated the oxidation process of coal by hydrogen peroxide and found that 10%-15% Ca $(OH)_2$ solution provides considerable performance in inhibiting high-sulphur coal oxidation. $Ca(OH)_2$ mainly inhibited spontaneous combustion in two ways. $Ca(OH)_2$ disrupted the self-oxidation cycle of pyrite, and the $CaSO_4$ generated in the reaction had low water solubility. This $CaSO_4$ settled on the surface of coal to form a hydrophilic membrane. Furthermore, the colloidal substance $Fe(OH)_3$ generated in the reaction encapsulated the coal by forming a protective coating that isolated oxygen from coal, thereby inhibiting the oxidation reaction. The inhibition performance of $Ca(OH)_2$ is relatively stable; however, low solubility can cause blockage in the device.

Inert gases and foams, mainly N_2 and CO_2, are generally used to forestall spontaneous combustion (Banerjee, 2000). When pumped into an enclosed area, the inert gases dilute the oxygen concentration in the space, thus inhibiting the coal oxidation (Shi & Zhou, 2014). Smith (1980) investigated the mechanism of CO_2 for the heat treatment of coal stockpiles and found that CO_2 reduced the rate of oxidation and inhibited spontaneous combustion. Ren, et al. (2019) also examined the effect of adding N_2 and CO_2 on spontaneous combustion and found that CO_2 has better inhibitory performance than N_2. Liquid N_2 and liquid CO_2 are potentially more efficient heat transfer mediums due to a considerable amount of heat being absorbed when liquid vaporises (Ray & Singh, 2007). This vaporization leads to an expansion in the volume of the cryogenic material, which results in an isotropic allocation of the heat-absorbing gas, thereby forcing the hot combustion gases out and displacing oxygen completely (Kim, 2004). Gases flow easily and cannot be trapped inside the danger area for a long period. Foam materials such as three-phase foam have been developed to restrict inert gases (Li, et al., 2020). Gypsum has not been tested on CSC, although it has promising application on the CSC.

2.7 Thermal decomposition of gypsum

Gypsum is used in building materials due to its excellent fire protection abilities (Wakili, 2007). The main property of gypsum to inhibit is due to its dehydration at elevated temperatures. Dehydration is an endothermic chemical reaction that absorbs energy

hence acting as a barrier to heat transfer. During the dehydration process, the water of crystallisation is transformed to vapour and released. This vapour is released by pressure through the pores of gypsum material, and the vapour is also released by pressure via molecular diffusion (Weber, 2011).

Numerous researches have been conducted on the behaviour of gypsum when exposed to high temperatures, which resulted in the development of simulation models. The easiest models of gypsum behaviour are based on pure heat conduction. In these models, the energy used during the dehydration process is introduced as a heat sink or by apparent heat capacity. Heat conduction models have been used for single boards (Belmiloudi, 2005) and assemblies of two boards with a cavity (Thomas, 2002). The heat conduction models are dependent on the properties of the material when exposed to high temperatures. These properties include the enthalpy of dehydration, density and thermal conductivity, which must be determined experimentally based on the reaction temperature. This reaction temperature is dependent on the partial vapour pressure and the heating rate. In most models, the reaction temperatures are chosen at fixed temperatures calibrated with fire tests and have been found to give reasonable results from standard engineering applications (Weber, 2011). This study used no fixed temperatures since the burning coal and coal shales were unknown.

2.7.1 Thermochemistry of gypsum

The most important mechanism of gypsum in the context of blast holes affected by spontaneous combustion is dehydration at elevated temperatures (Ghazi, 2007). The chemical reaction process occurs in two stages. The first stage transforms calcium sulphate dihydrate into hemihydrate. The enthalpy is in Equation 2.4:

$$\mathrm{h(T)} = \mathrm{h_{std}} + \int_{\mathrm{Tstd}}^{\mathrm{T}} \mathrm{Cp}(\theta)\mathrm{d}\theta \qquad (2.4)$$

where h (T) is the enthalpy, h_{std} is the standard enthalpy, T_{std} is the room temperature, T is temperature, and c_p is the specific isobaric heat capacity. Since the heat of reaction is the difference of the enthalpies, it is related to the difference in heat capacity by Equation 2.5:

$$\Delta h(T) = \Delta h_{std} + \int_{Tstd}^{T} \Delta Cp(\theta) d\theta \quad (2.5)$$

Where Δh is the specific enthalpy of phase change, Δh_{std} is the specific enthalpy of phase change at room temperature (Ghazi, 2007).

In both stages, part of the solid mass is transformed into water vapour. The corresponding loss of mass in each reaction can be calculated using stoichiometric calculations. The molecular mass of dihydrate is 17g/mol, and the molar mass of water is 18g/mol (Ghazi, 2007). The loss after the two reactions is 21% of the original mass, three quarters in the first reaction and one quarter in the second reaction. Commercial gypsum used for boards is not pure dihydrate, but it has certain amounts of non-reacting anhydrite and other components. The mass of hydration can be determined experimentally by using TGA (Ghazi, 2007).

2.7.2 Heat of dehydration

A graphical representation of the enthalpies for the *α*-varieties is plotted in Figure 2.3. The curves show the enthalpies calculated from the standard enthalpies at 25 °C by Eq. 2.4. The enthalpies of reaction are then the differences between the curves. The figure shows that the enthalpy of dehydration is almost independent of temperature. The heat of hydration increases with temperature, while the heat of evaporation decreases, resulting in an almost constant total heat of dehydration. The enthalpies of dehydration corresponding to the reaction temperatures used in the simulations are indicated by vertical lines in the figure. Figure 2.3 shows the enthalpies of gypsum when exposed to heat. The various stages are indicated with dotted lines, while the original gypsum is indicated with a solid line representing gypsum before exposure to heat.

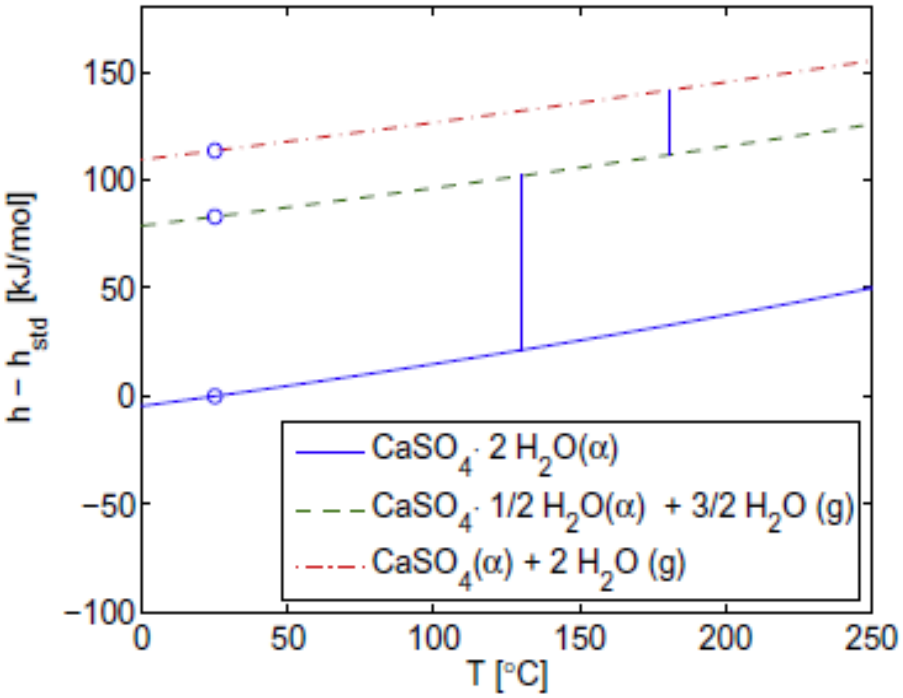

Figure 2.5: Enthalpies for gypsum products ***(Wakili, 2007)***

Taking a purity of 81% for gypsum, as determined from TGA, the heat of dehydration reaction relative to pure gypsum would be 650kJ/kg (Wakili, 2007). The heat of dehydration of gypsum is on standard tables between 642 and 663 kJ/kg (Wakili, 2007). The principal work source of thermodynamic data on gypsum in the literature is work done by Kelly, et al. (1941). The work provides a complete set of thermodynamic properties for several reactions. The dehydration due to fire produces a mixture of the two forms. Furthermore, the enthalpy of the different reactions depends on the temperature. Values in the literature are given in room temperature and atmospheric pressure conditions and must be adjusted to higher temperatures when used in models since the reactions will occur at a higher temperature.

Kontogeorgos & Founti, (2012) provided a framework that can facilitate the detailed simulation of gypsum board thermo-chemistry at ambient and elevated temperature conditions. The paper reviews gypsum board thermo-chemistry, presents a methodological approach for the calculation of composition and reaction energy, and focuses on methods calculating the ‘kinetic triplet’. The chemical kinetics of three main reactions that take place when a gypsum board is exposed at elevated temperatures: evaporation of free moisture content, dehydration of chemically bound water and

crystal mesh reorganization were investigated using Differential Scanning Calorimetry measurements under non isothermal conditions and in an inert atmosphere. Experiments using samples of deionized water and commercial gypsum board were carried out at temperatures up to 600 °C, with different heating rates. Mass and energy balance equations were considered in order to define the initial composition of a gypsum board and the energy that is absorbed/produced after the completion of the examined reactions. Model-free and model-fitting approaches were used for the definition of the kinetic parameters of the examined reactions. The approach minimizes the need for expensive and detailed experiments necessary for the determination of the gypsum board behaviour at elevated temperatures (Kontogeorgos & Founti, 2012).

2.8 Summary

The chapter defined spontaneous combustion and described in detail the factors that cause its occurrence. The influence of pyrite on the spontaneous combustion of coal was also discussed in light of the past and present literature. The methods of predicting spontaneous combustion liability of coal were mentioned and discussed, their applications and limitations indicated. The chemical inhibitors used to prevent CSC were discussed and their benefits stated. . Thermal decomposition, thermochemistry and heat of dehydration of gypsum were also discussed in detail.

3 RESEARCH METHODS

3.1 Introduction

This chapter discusses the various instruments which were used to collect and analyse data. It further describes in detail the geometry and nature of the holes and stockpiles used to collect data and how data was collected using various instruments.

3.2 Sources of data

3.2.1 Data from the hot-holes

Hot-hole data was acquired from three drilled holes. The holes were drilled on the interburden material overlying the No.2 seam coal. The drilled interburden consisted of shale, which was undergoing spontaneous combustion. The three holes were drilled 15m apart, and each hole was drilled 16m deep. Figure 3.1 illustrates the spraying machine and the hole sprayed with gypsum.

Figure 3.1 : Hot-hole with spraying machine

Data from the holes was acquired by using TEMPCO 305K hand-held digital thermometer. This is a hand-held portable digital thermometer designed to use type K-thermocouples with connection via industry-standard mini-plugs. This instrument's

measuring range is from -50^{0}C to 1300^{0}C. It has a resolution of 0.1^{0}C to 199.9^{0}C and 1^{0}C to 1300^{0}C with a reading rate of 2.5 times per second. The accuracy of this instrument is 0.3% + 1^{o}C from -50^{0}C to 1000^{0}C and accuracy of 0.5% + 1^{0}C from 1000^{0}C to 1300^{0}C (RS Thermocouple Selection Guide, 2020). Data from the holes was also acquired using the 64 channel NI CDAC (4 x NI9213) temperature card instrument. This instrument has 64 channel CMS software, and the probes are 32 x 20m type K-thermocouples with 30m extensions.

Both TEMCO 305K and 64-channel instruments were fitted with RS PRO type K-thermocouples. The thermocouple is a sensor used to measure temperature in different processes. It consists of two wire legs made from different metals joined together at their two ends to form two junctions (RS Mineral Insulated Thermocouples, 2020). The hot or measuring junction is connected to the body whose temperature is going to be measured. The cold junction or reference junction is connected to a body of known temperature. When the measuring junction is placed on something hot, a voltage or potential difference between this and the reference junction occurs. Using thermocouple reference tables, this voltage can then be converted into a temperature measurement (RS Thermocouple Selection Guide, 2020). This process is also known as the see beck effect. The thermocouples temperature probes have durable construction and feature a 310 stainless steel mineral insulated flexible sheath that can be bent and formed to suit a wide range of applications (RS Mineral Insulated Thermocouples, 2020). The thermocouple has a single element insulated junction for a reduction in electrical interference. One of the thermocouples is terminated with a miniature flat pin plug for a quick and easy connection, as illustrated in Figure 3.2.

Figure 3.2 Type K-Thermocouple. ***(RS Thermocouple Selection Guide, 2020)***

3.2.2 Data from stockpiles

An actual bituminous coal stockpile situated at the run of mine (ROM) pad was used. The geometry and parameters of the coal stockpile are typical of the Witbank Coalfields deposits. The geometry of the stockpile is of a truncated quadrangular pyramid. The height of the stockpile is 1.7m, and the width of 7m, corresponding to the haul truck used to tip the stockpiles. The length of the stockpiles was 10m each at the horizontal base. The slope angle of the stockpiles was 400. The fragmentation of the coal was mainly formed by coarse particles with a diameter of less than 15cm with an assumed particle size of 5cm.

A medium-scale test on two stockpiles of 60 tonnes each was carried out in this study. Stockpiles S1 was treated with gypsum, while Stockpile S2 was left untreated (control point) for 21 days at Khwezela Colliery in order to examine the inhibitory effects of the antioxidant on coal self-heating. Two 60T stockpiles from 2-Seam coal, which are known to be prone to spontaneous combustion, were used. At the beginning of testing, the temperatures of both the stockpiles were recorded, and they had similar temperatures. Both stockpiles were divided into six sections, namely; A1, A2, A3, A4, A5 and A6, as illustrated in Figure 3.3. The portions A1, A2 and A3 areas were sprayed with a single coat for 10 minutes using 3 kg powdered gypsum, while A4, A5, and A6 areas were sprayed twice using 6 kg of powdered gypsum (Onifade et al., 2021). Figure 3.3 shows a treated coal stockpile with corresponding sides.

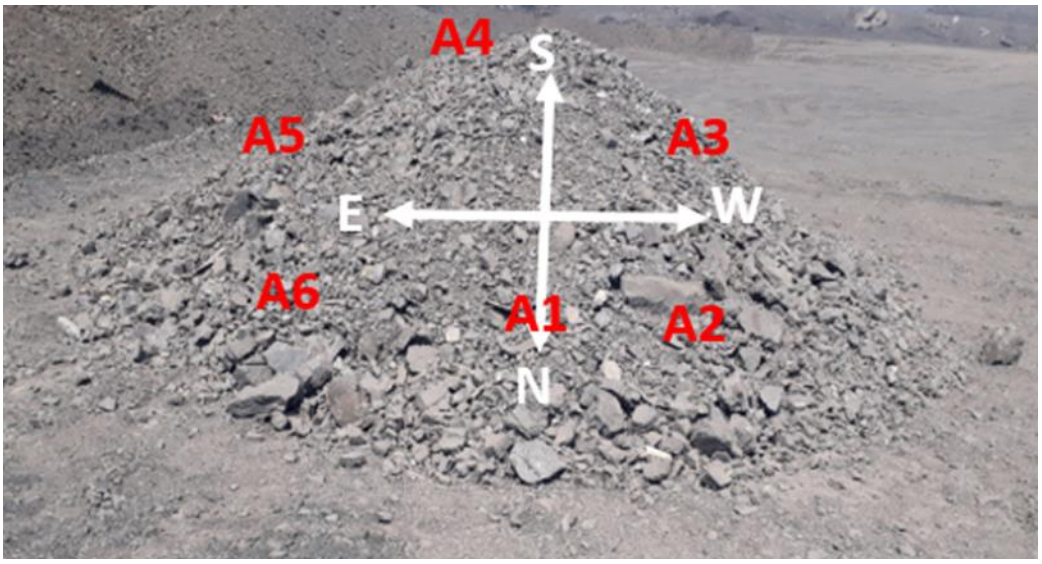

Figure 3.3 Treated coal stockpile with corresponding sides

The stockpiles were placed 15 m away from each other to minimise the influence of one stockpile on another due to weather conditions. Sections A1 was on the Northern part, A5 and A6 were on the Eastern part, A4 was on the Southern part, A2 and A3 were on the Western part. This was to ensure that an area to area comparison was reliable and consistent. Gypsum is a soft sulphate mineral composed of calcium sulphate dihydrate, with a chemical formula $CaSO_4 * 2H_2O$ (Dolezelova, et al., 2018). Gypsum was considered due to its wide availability and low cost.

Data from stockpiles was acquired using FLIR E85 advanced thermal imaging cameras for electrical and mechanical applications. The cameras offer the superior resolution and range performance needed to identify hot spots quickly. The camera has up to 161 472-pixel resolution and a larger, more vibrant liquid crystal display (LCD) screen. The camera is fitted with high-resolution infrared detectors up to 464 x 348 for crisp detailed images. It measures wide temperature ranges from -40^0C to 120^0C, 0^0C to 650^0C and 300^0C to 1500^0C (RS Thermocouple Selection Guide, 2020). Figure 3.4 illustrates a thermal image of the treated stockpile captured by the FLIR E85 camera.

Figure 3.4 FLIR E85 thermal image

3.3 Method of data collection

3.3.1 Data collection from hot-holes

TEMCO 305K was connected with a 20m long type K-thermocouple wire. One end of the thermocouple with two metal pins was connected to the TEMCO 305K instrument. The temperature sensor end was allowed to reach thermal equilibrium with the atmospheric temperature before being inserted into the hole. The sensor end was lowered 16m to the bottom of the hole to record the temperature. The measurement was recorded only after the instrument stopped reading the temperature. At this point, the temperature displayed on the instrument was the temperature measured by the sensor at the point where the sensor was suspended. The process was repeated at every 1m interval by pulling the type K-thermocouple 1m up the hole so that temperature readings are recorded every meter of the hole in order to cover all the lithological characteristic of the holes. This process was done from 06h00 to 16h00 every 2-hour interval for 21 days from 21 August 2020 to 10 September 2020. Sixty-four channel NI CDAC instrument was connected with 48 type K-thermocouples.

3.3.2 Data collection from stockpiles.

The testing equipment consisted of a compressor, powder mixer, spray gun, hose and spray assemble, as illustrated in Figure 3.1. While the compressor is used to spray the gypsum powder, the powder mixer makes the pulverised gypsum airborne to provide continuous spraying capabilities. The powder mixer also controls the whole process and has a lever to adjust the spraying speed.

3.4 Method of data analysis

3.4.1 Data analysis of holes and stockpiles

A *t*-test was used to determine if there is a significant difference between the means of the stockpiles and holes as it is freely available with MS Excel and easy to use. The Two-Sample *t*-test analysis tool tests for population equality means of each sample (Maree, 2014). The t-test tools employ different assumptions: that the population variances are equal, that the population variances are not equal, and that the two samples represent before-treatment and after-treatment observations on the same subjects.

A t-statistic value, t, is computed and shown as "t Stat" in the output tables for all three tools. Depending on the data, this value, t, can be negative or nonnegative. Under the assumption of equal underlying population means, if t < 0, "P (T <= t) one-tail" gives the probability that a value of the t-statistic would be observed that is more negative than t. If t >=0, "P(T <= t) one-tail" gives the probability that a value of the t-statistic would be observed that is more positive than t. t Critical one-tail gives the cut-off value so that the probability of observing a value of the t stat greater than or equal to t Critical one-tail is Alpha. P(T <= t) two-tail gives the probability that a value of the t-statistic would be observed larger in absolute value than t. P Critical two-tail gives the cut-off value so that the probability of an observed t-statistic larger in absolute value than P Critical two-tail is Alpha (Maree, 2014). Figure 3.1 indicates all variables which are measured using t-test

Table 3.1 *t*-test: Two samples assuming unequal variances

t-test: Two-samples assuming unequal variances		
	Stockpiles	
	S1W6	S2W6
Mean	50.2	95.0
Variance	167.1	3322.1
Observations	22.0	22.0
Degree of freedom(df)	23.0	
T stat	-3.6	
P(T<=t) two-tail	0.0	
T Critical two-tail	2.1	

Statistical analysis of data was used to assess the performance of gypsum on the hot-holes and coal stockpiles. A sample assuming unequal variances was used. Furthermore, the mean and variance of holes were determined and compared. A confidence level of 95% on a two-tailed test was chosen for the study. A 0.05 (5%) significance level resulted in critical values of 2.1, 2.0 and 2.0 for the same side of the stockpile, treated stockpile and holes, respectively. After the analysis, any value less than the critical value would imply that gypsum did not have a significant effect. However, any value greater than the critical value would imply that gypsum significantly affected the stockpile and holes temperature.

On the stockpiles, the temperature measurement per day was graphically represented and compared to atmospheric temperature. This was done to determine if atmospheric temperature influences the stockpile temperature and to extract any meaningful relationship between stockpile temperature and atmospheric temperature. This was done for every area measured on the stockpile for the duration of the experiment (A1 to A6 as per Figure 3.2). Each area of the treated stockpile was compared to a similar area on the stockpile that is not treated with gypsum in order to determine the effect of gypsum on the stockpile. The average temperature of each side of the stockpile was calculated, and corresponding sides were compared to determine the effectiveness of gypsum. On the treated stockpile, the average temperature of each side was

calculated and then compared to each other to determine the extent to which a higher concentration of gypsum affected the temperature of the stockpile. The overall temperature of the untreated and the treated stockpiles were calculated and compared to determine the extent to which gypsum inhibits the temperature of the stockpiles.

The temperature was measured on the three blast holes before treatment with gypsum to establish the initial temperature. The interburden above the No.2 seam coal consists mainly of sandstone and shale with a dark white colour. On an air-dried basis, the no.2 seam coal contains 31.59% ash, 26.73% volatile matter and 22.56 calorific value. The holes H1 and H2 were treated with gypsum while H3 was not treated. The temperature of each hole was measured at every 1m interval, where 0m is the collar of the hole. The average temperature of each hole per day was calculated and compared to the atmospheric temperature. This was to determine the influence of atmospheric conditions on the in-hole temperature. The average in-hole temperature of each hole was compared against one another in order to determine the extent to which different concentrations of gypsum affected the in-hole temperature of the two sprayed holes against the controlled hole.

3.5 Summary

This chapter discussed the sources of data. The use of a TEMCO 305K digital thermometer and 64-Channel thermocouple for in-hole temperature measurement, the FLIR E85 thermal camera used to collect stockpile data, and the characteristics and geometry of the stockpiles and hot-holes were discussed in detail. The holes were spaced 15m apart to minimize the thermal influence of each other. The composition of gypsum and its characteristics were also discussed, including how gypsum was sprayed to the two hot-holes and two coal stockpiles. The chapter concluded with a statistical analysis, which was used to assess the performance of gypsum on hot-holes and stockpiles.

4 RESULTS AND DISCUSSION OF COAL STOCKPILES

4.1 Introduction

The comparison between the atmospheric temperature and stockpiles is done for all 22 days of the study. Each side of the stockpile is compared to the atmospheric temperature. Further analysis is done by comparing similar sides of the stockpile to each other for 22 days. MS Excel was used to represent the findings graphically, and *t*-test analysis was done on a test statistic to assess the significance of gypsum on coal stockpile temperature. Lastly, the comparison of the two sides of the treated stockpile was done to determine the significance of a higher gypsum concentration on the spontaneous combustion of coal stockpiles. The graphical representation of measurements taken for 22 days is done together with statistical analysis using a t-test.

4.2 Stockpile temperature and atmospheric temperature

To easily interpret the results and observations from the two stockpiles, the following naming convention was adopted:

The measurement points A1, A2, and A3 are west side of the stockpile. When the measurements are on the treated stockpile, they are labelled S1W. S1 represents the treated stockpile. Similarly, when the same points are on the control stockpile, they are labelled S2W, where S2 represents the control stockpile. A4, A5 and A6 are on the east side of the stockpiles and follows the same naming convention for each stockpile. The measurements were taken at different hours as described in section 3.3.2. The numerals 6, 8, 10, 12, 14 and 16 are the exact hours at which measurements were taken. Thus, S1W6 represent the west side of the treated stockpile at 06h00. The same interpretation is valid for S2W6 and the other sides. The east side of the treated stockpile was sprayed twice, while the west side was treated once with gypsum. Below are the acronyms used to interpret the information:

- Treated stockpile = S1;
- Control stockpile = S2;
- A1, A2, A3 = West side(W);
- A4, A5, A6 = East side(E);
- 6, 8, 10, 12, 14, 16 = Hours at which measurements were taken.

4.3 Interpretation of results

4.3.1 Temperature measurement from the west side of the treated stockpile at 06h00

The stockpile temperature increased gradually from the initial temperature of 58^{0}C on day one to the peak temperature of 68^{0}C on day 5 of the experiment, as illustrated in Figure 4.1. A similar temperature pattern was observed on the weather temperature in Figure 4.1. The temperature dropped sharply to 54^0 C between day 5 and day 6. This would be attributed to the drop in weather temperature during the night. There was a sharp drop in temperature between day 11 and day 13, followed by a stable stockpile temperature. This pattern is also seen in the weather temperature. Between day 4 and day 15, there was a 44^{0}C rise in temperature, similar to a sharp rise in weather temperature. Then, the stockpile temperature stabilised at 65^{0}C until the last day of the experiment. This observation indicates that the change in temperature of the stockpile is affected by the temperature of the surrounding (Ozdeniz, et al., 2015), the wind direction and the wind speed of the environment.

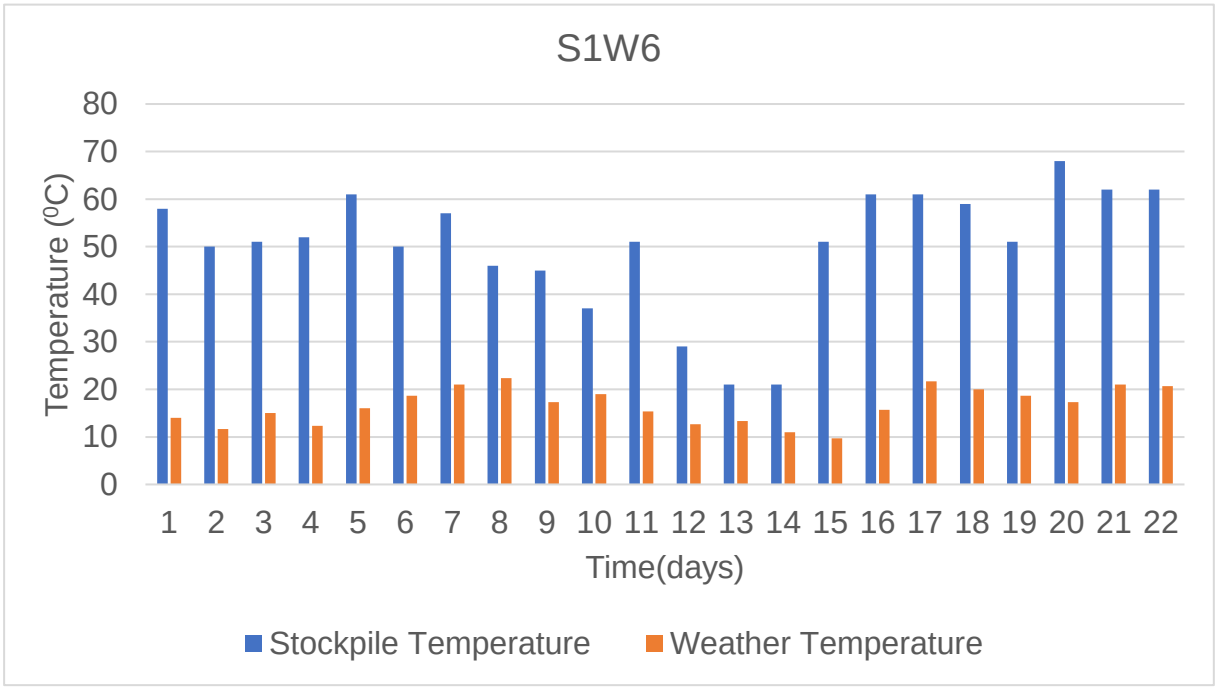

Figure 4.1 S1W6 temperature trend

4.3.2 Temperature measurements from the east side of the treated stockpile at 06h00

During the measurement of the treated stockpile on the east side, it was observed that the stockpile temperature decreased from day 4 to day 12 from 58^0C to 20^0C, respectively, as illustrated in Figure 4.2. It then increased sharply from day 14 to day 16 from a temperature of 20^0C for stockpile and 10^0C for the weather, and then it decreased to day 20 at 44^0C. The rise and fall of the temperature were similar to atmospheric temperature. The wind-driven forced convection and natural conduction could have also caused the changing pattern of the stockpile.

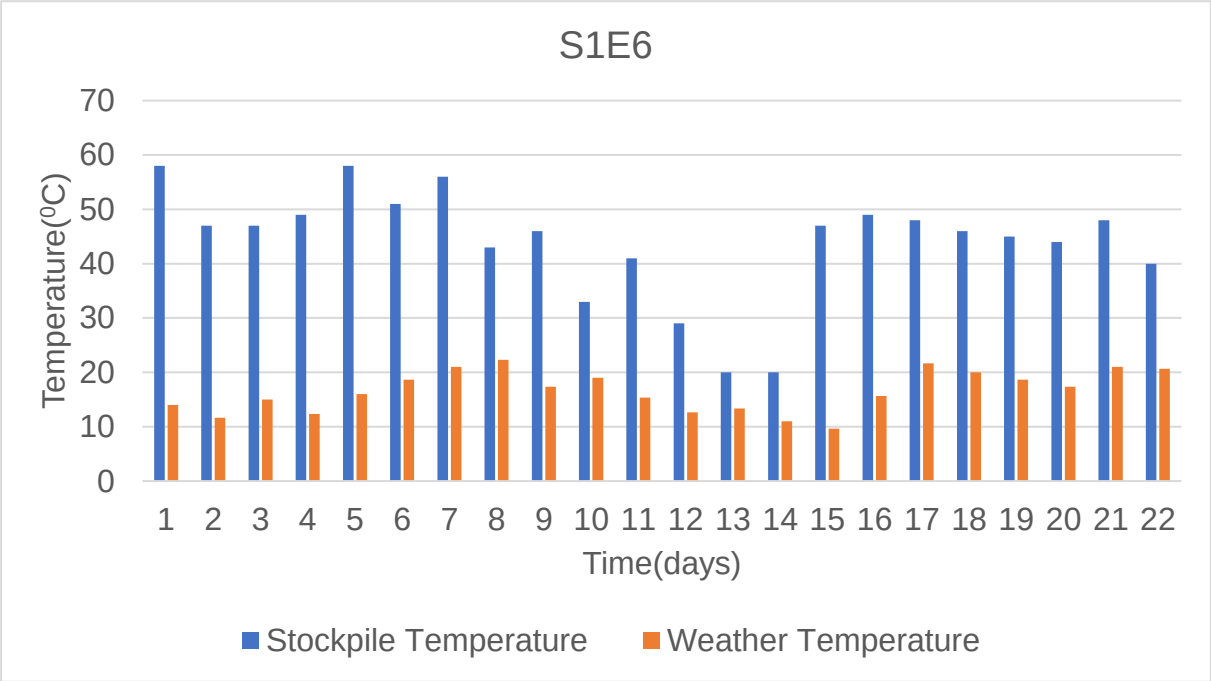

Figure 4.2 S1E6 temperature trend

4.3.3 Temperature measurements from the west side of the control stockpile at 06h00

Figure 4.3 temperature profile showed a similar trend from day one to day 8. There was a sharp increase in temperature from 45^0C to 242^0C on day 9 to day 11, and it dropped sharply until day 15 to a temperature of 61^0C. This was the day at which spontaneous combustion of the stockpile occurred on the untreated stockpile as

illustrated in Appendix B. The temperature increased gently until day 19 at 97^{0}C. It increased sharply for 24 hours to 221^{0}C then dropped suddenly and sharply to 77^{0}C on day 22, as illustrated in Appendix B. Based on the Mine's standard operating procedure, any stockpile temperature and blast hole with a temperature more than 80^{0}C is considered to be a spontaneous combustion hole or stockpile. Therefore, spontaneous combustion was observed from day 19 to day 22.

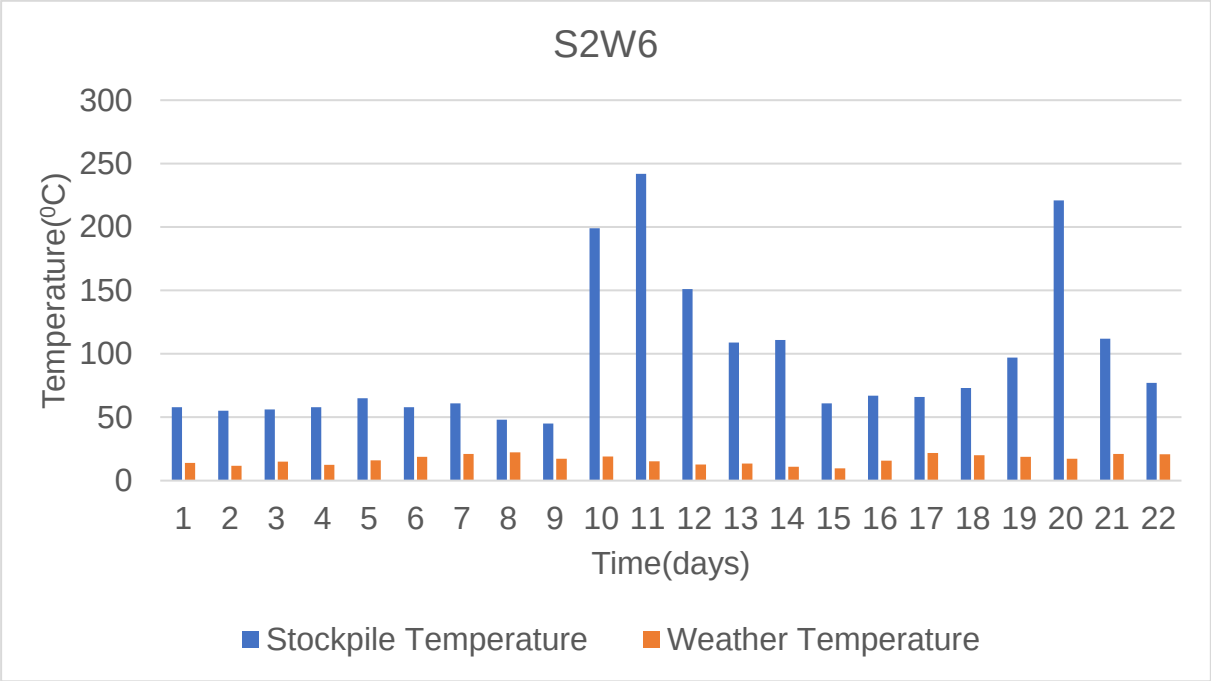

Figure 4.3 S2W6 temperature trend

4.3.4 Temperature measurements from the east side of the control stockpile at 06h00

In Figure 4.4, the temperature was similar to the weather temperature until day 9, when it increased sharply from 56^{0}C to the peak temperature of 241^{0}C on day 12. The temperature decreased to 65^{0}C on day 15, and it remained constant to day 18 at 65^{0}C. It then increased to 138^{0}C on day 20 and dropped to 77^{0}C until day 22. The stockpile experienced thermal runaway and intense spontaneous combustion on the day 9 at this area. S2E6 and S2W6 have similar temperature profiles, as illustrated in Appendix B. This could be attributed to both points having the same coal quality and being close to each other, as illustrated in Figure 3.4.

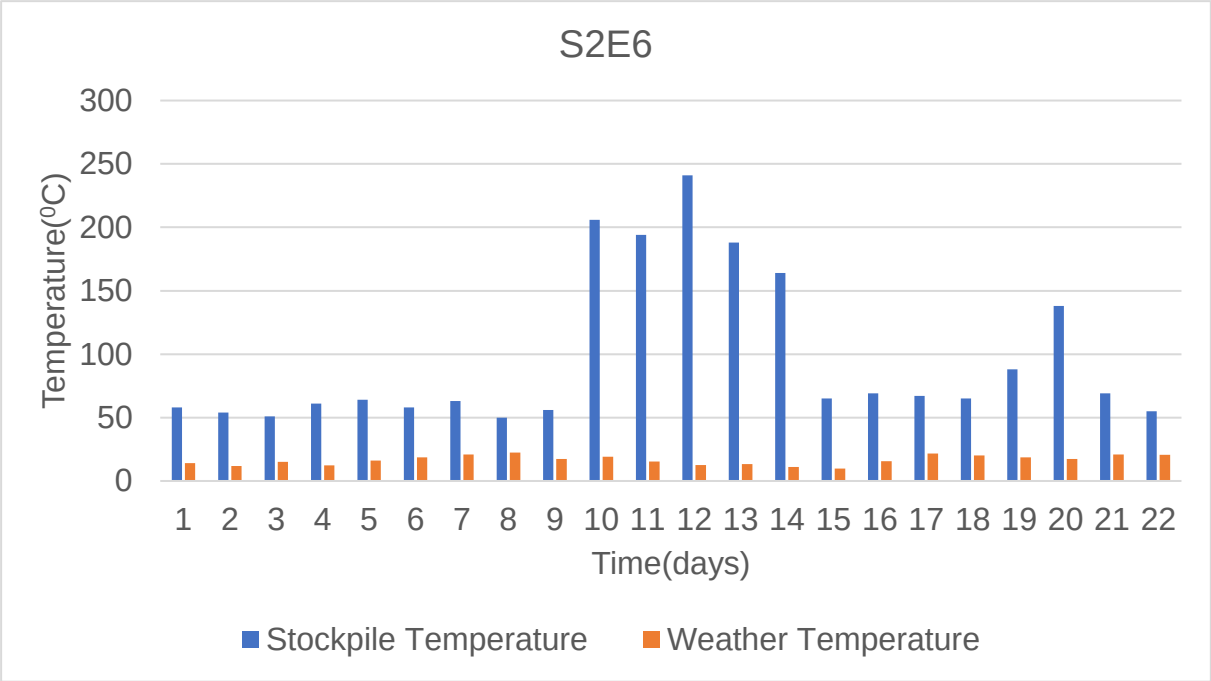

Figure 4.4 S2E6 temperature trend

4.3.5 Temperature measurement from the west side of the treated stockpile at 08h00

Figure 4.5 illustrates that the stockpile and atmosphere temperatures were consistent from day 1, with the temperature of the stockpile and atmosphere at 58^0C and 14^0C, respectively. The temperature of the stockpile started to decrease, on average, from day 5 to day 14 from 63^0C to 13^0C, respectively. However, there was an erratic change in temperature between those days. The stockpile temperature increased sharply from day 14 to day 17 from 21^0C to 62^0C, respectively. It then stabilised until the last day.

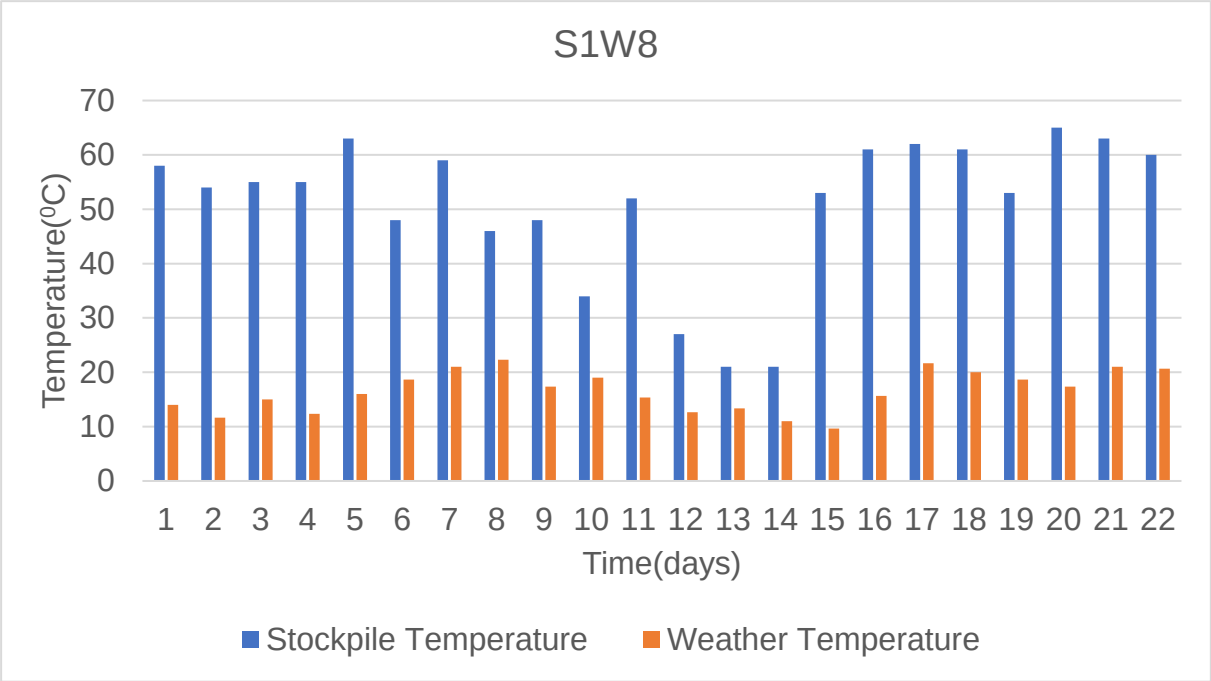

Figure 4.5 S1W8 temperature trend

4.3.6 Temperature measurements from the west side of the treated stockpile at 08h00

The temperatures of the stockpile and the atmosphere temperature have shown a similar trend by decreasing from day 1 to day 2, as illustrated in Figure 4.6. Stockpile temperature decreased from 58^0C to 47^0C. From day 4, the stockpile temperature increased from 12^0C to 22^0C from day 4 to day 8, respectively. The temperature then decreased from 56^0C to 20^0C on day 14. The atmospheric temperature decreased similar to stockpile from day 8 to day 15 from 22^0C to 10^0C respectively. A sharp temperature rise of the stockpile was observed from day 14 to day 16 when temperature increased from 20^0C to 50^0C respectively and then stabilised. Similarly, the atmosphere's temperature increased sharply from day 15 to day 17 from 10^0C to 22^0C, then stabilised. The high temperature of the stockpile on days that the atmospheric temperature was low could be attributed to the wind-driven forced convection.

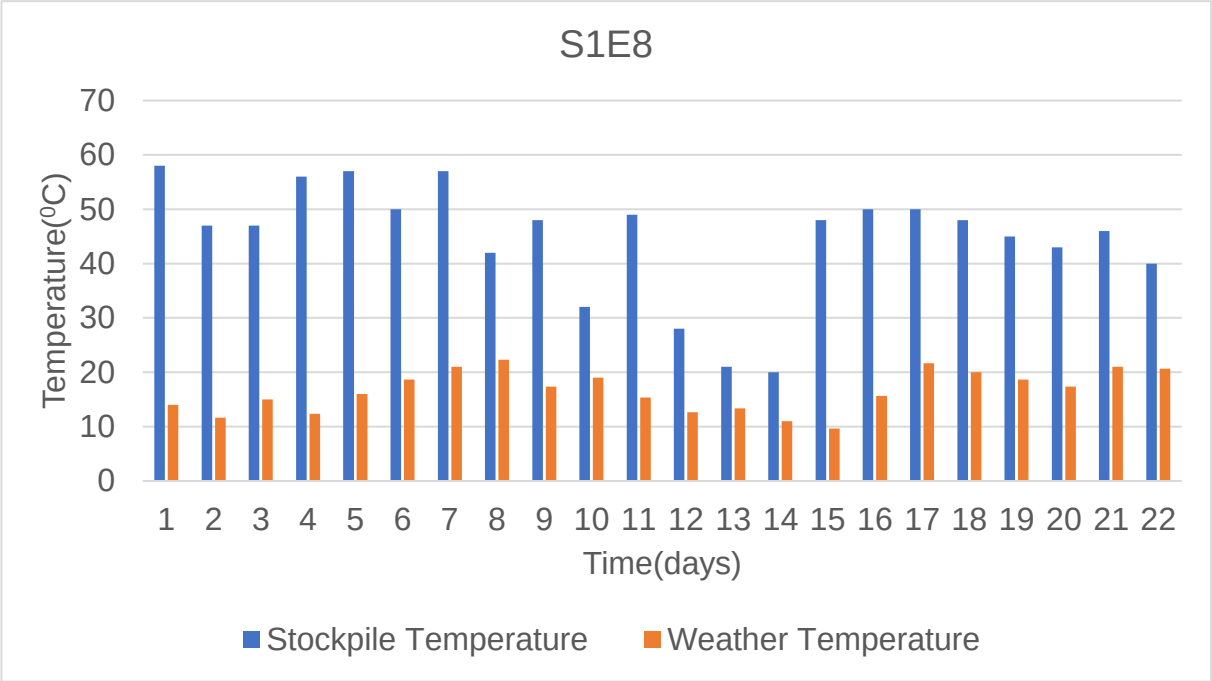

Figure 4.6 S1E8 temperature trend

4.3.7 Temperature measurements from the east side of the control stockpile at 08h00

The temperature of the control stockpile and the atmosphere were constant from day 1 to day 9, as illustrated in Figure 4.7. The temperature of the stockpile increased sharply from day 9 to day 11 from 50^0C to 229^0C, this could be attributed to wind-driven forced convection. The stockpile temperature decreased sharply from day 11 to day 15 from 229^0C to 63^0C. This could be attributed to the coal having partially burned out. The atmosphere's temperature remained constant with slight changes while the temperature of the stockpile increased sharply from day 19 to day 20, then decreased sharply from day 20 to day 22. The related temperature measurements were 96^0C to 219^0C then dropped to 77^0C, respectively. Intensive spontaneous combustion of the stockpile was observed from day 9, where the stockpile was burning with red-hot spots.

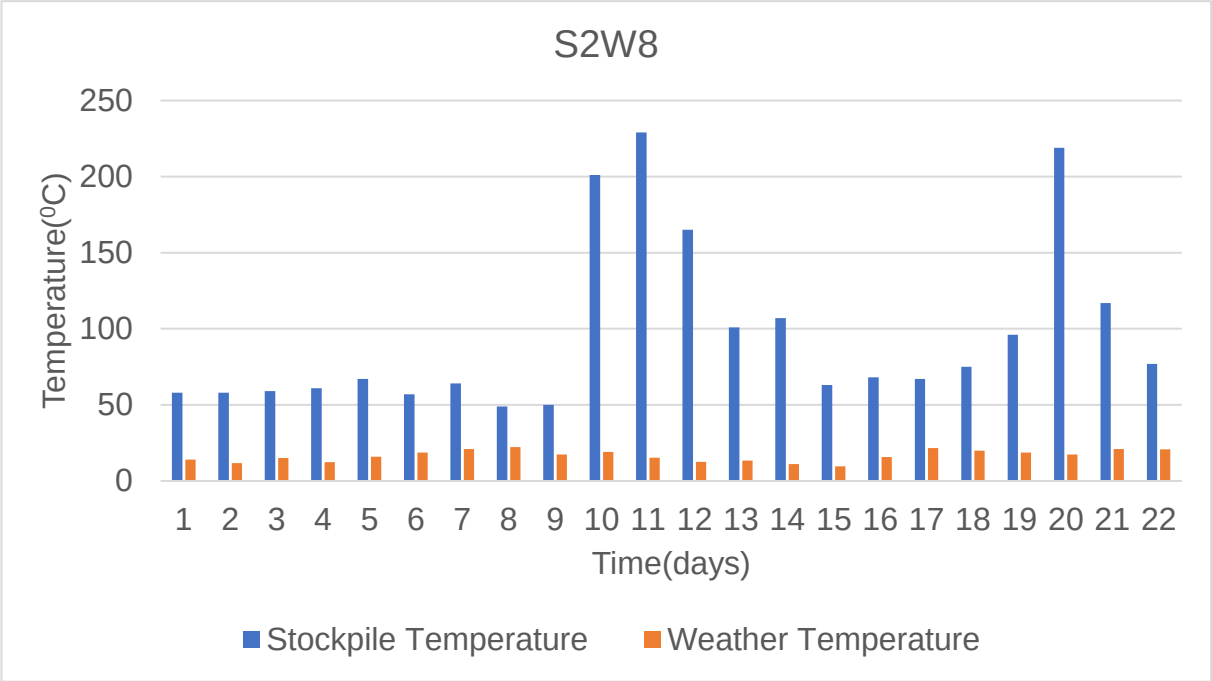

Figure 4.7 S2W8 temperature trend

4.3.8 Temperature measurements from the west side of the control stockpile at 08h00

The stockpile temperature increased sharply from 57^{0}C on day 9 to 202^{0}C on day 10 while the atmosphere's temperature remained constant, as illustrated in Figure 4.8. The coal was partially burned out. The stockpile temperature decreased gently from 10^{0}C to 162^{0}C on day 14, then decreased sharply to 67^{0}C on day 15. It remained constant until it increased gently to 140^{0}C on day 20, then dropped sharply to 56^{0}C on day 22.

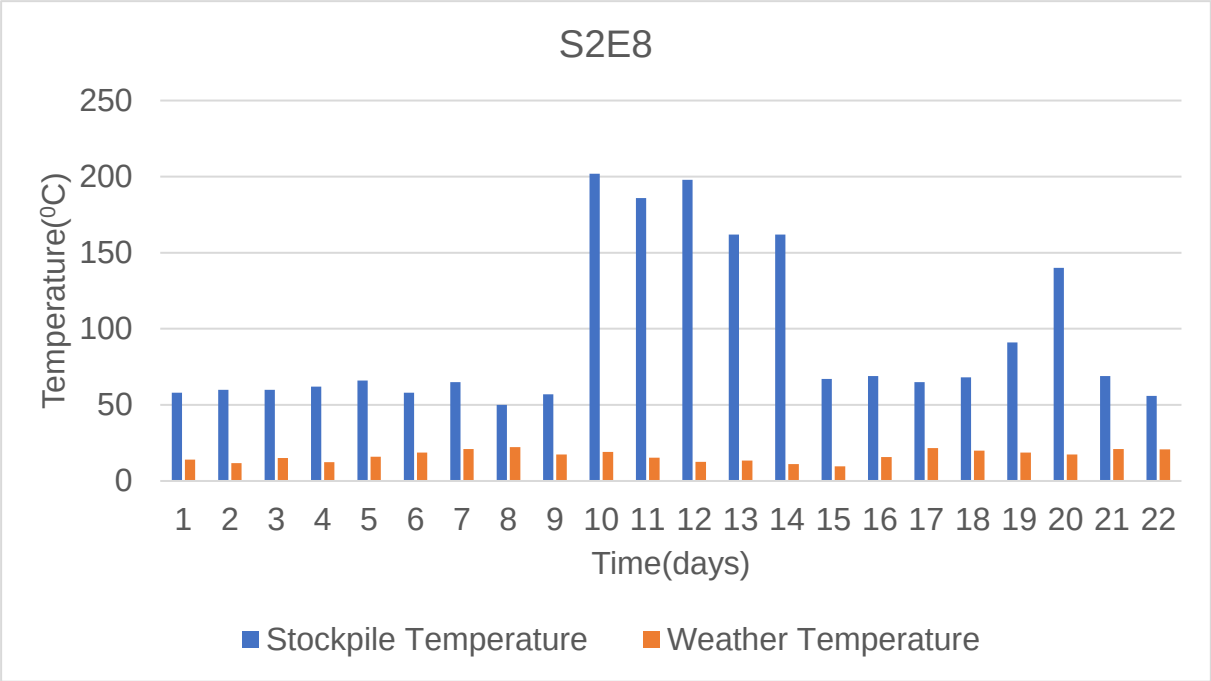

Figure 4.8 S2E8 temperature trend

4.3.9 Temperature measurements from the east side of the treated stockpile at 10h00

In Figure 4.9, the temperatures of the stockpile and atmosphere decreased consistently from day 1 to day 2. The stockpile temperature increased gently from 51^{0}C on day 2 to a peak temperature of 64^{0}C on day 5, and then it decreased to 33^{0}C on day 10. The stockpile temperature increased sharply from 33^{0}C on day 10 to 56^{0}C on day 11. It then decreased sharply to 20^{0}C on day 14. Both the stockpile and atmospheric temperatures increased; however, the stockpile had the sharpest increase to a maximum temperature of 62^{0}C then remained constant until day 22. The atmospheric temperature increased to 22^{0}C then remained constant until day 22.

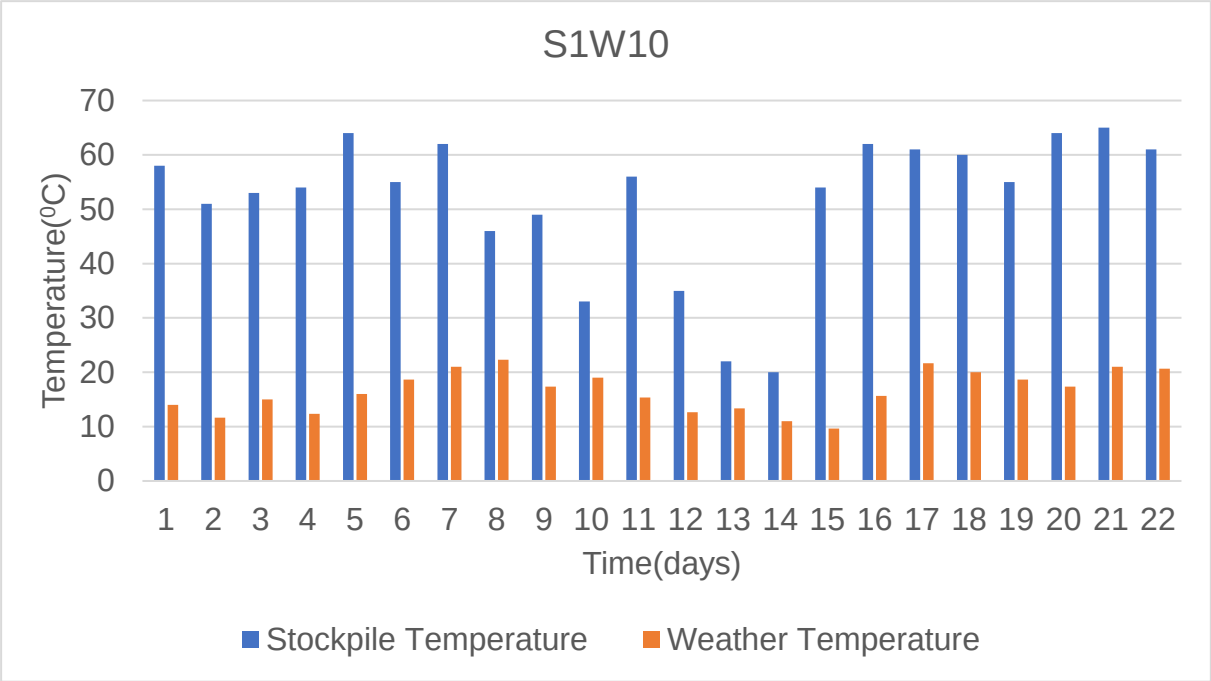

Figure 4.9 S1W10 temperature trend

4.3.10 Temperature measurements from the west side of the treated stockpile at 10h00

In Figure 4.10, the stockpile temperature decreased from 58^{0}C to 49^{0}C from day 1 to day 2, respectively, while the atmospheric temperature decreased from 14^{0}C to 12^{0}C. The stockpile temperature increased gently from day 2 to a maximum temperature of 57^{0}C on day 5, while the atmosphere temperature gently increased from day 2 to a maximum temperature of 22^{0}C on day 8. The stockpile temperature decreased erratically to 29^{0}C on day 10, then increased sharply to 53^{0}C on day 11 and sharply decreased from day 11 to day 14 to 20^{0}C. The stockpile temperature increased sharply from day 14 to 49^{0}C on day 15, then stabilised until day 22, in which a slight drop of temperature to 42^{0}C was observed.

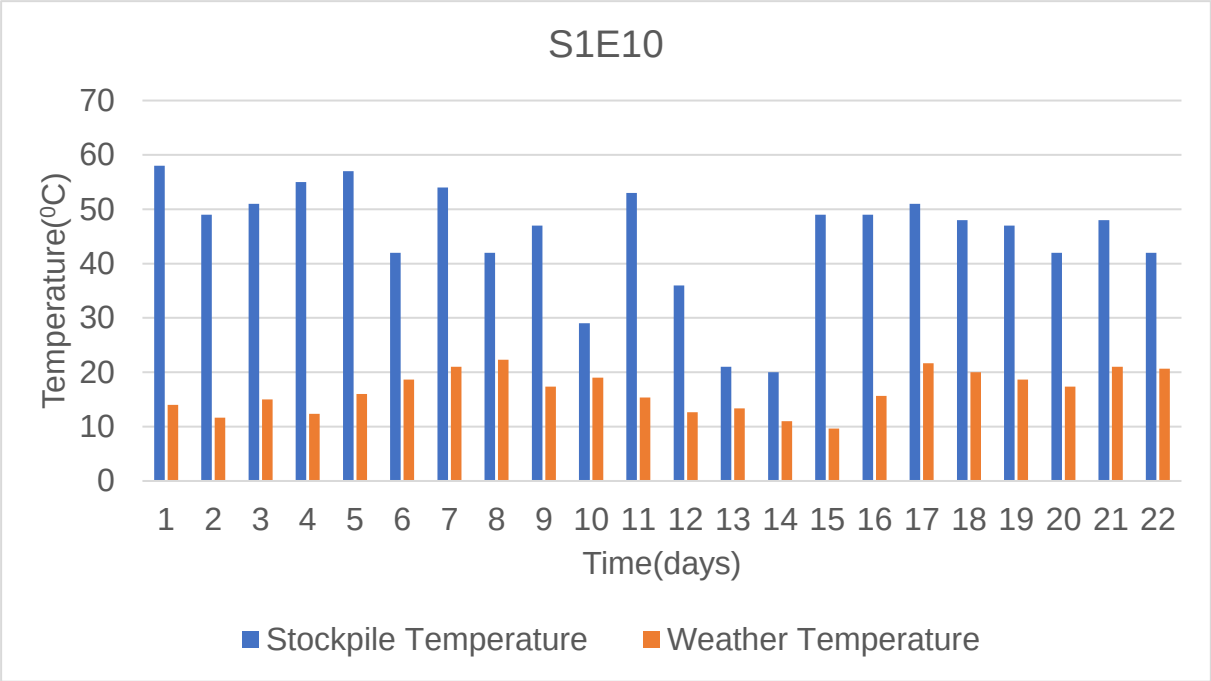

Figure 4.10 S1E10 temperature trend

4.3.11 Temperature measurements from the east side of the control stockpile at 10h00

In Figure 4.11, the stockpile temperature decreased gently from 58^{0}C on day 1 to 49^{0}C on day 9, while the temperature of the atmosphere increased from 14^{0}C on day 1 to a maximum temperature of 22^{0}C on day 8. The stockpile temperature increased sharply from day 9 to a maximum temperature of 239^{0}C on day 11; it then decreased sharply to 64^{0}C on day 15. The sharp increase could be due to wind-driven forced convection. The stockpile temperature increased gently from day 15 to 218^{0}C on day 20, then dropped sharply to 79^{0}C on day 22. On the other hand, the atmospheric temperature increased sharply from day 15 to 22^{0}C on day 17 then stabilised until day 22.

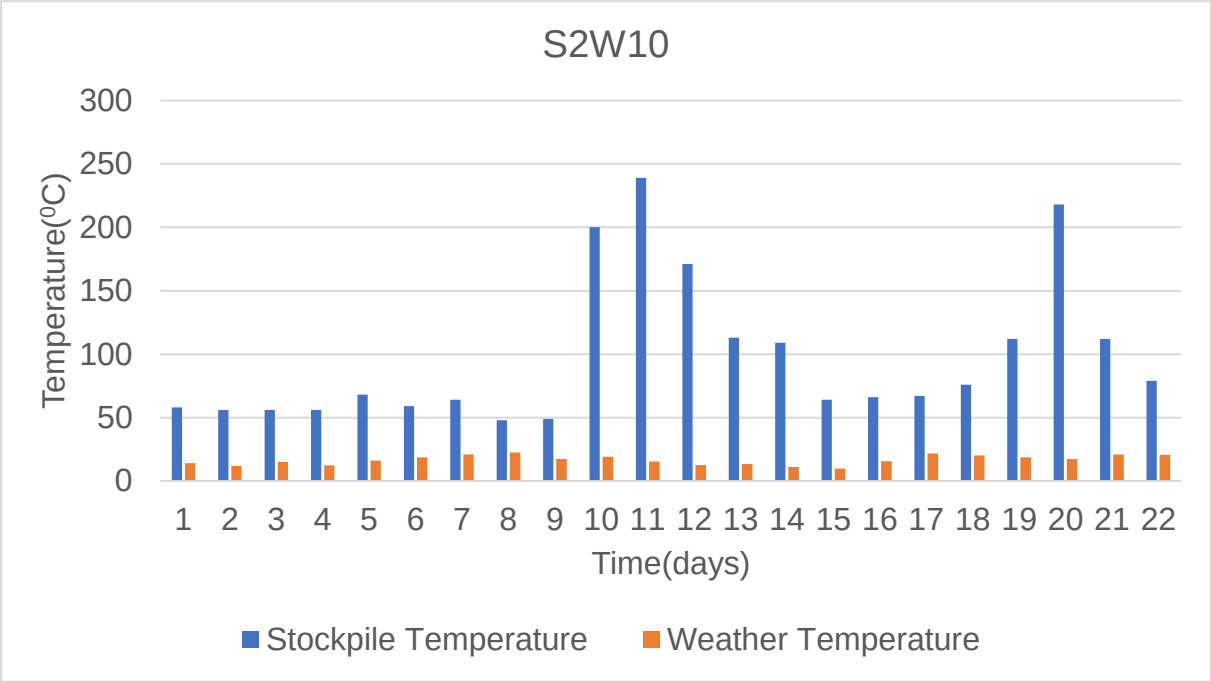

Figure 4.11 S2W10 temperature trend

4.3.12 Temperature measurements from the west side of the control stockpile at 10h00

Figure 4.12 illustrates the temperature of the stockpile, which decreased from 58^{0}C on day 1 to the lowest temperature of 49^{0}C on day 8. The temperature then increased sharply to a maximum of 205^{0}C on day 11. It decreased sharply to a lower temperature of 66^{0}C on day 15. The temperature constantly stabilised to day 18 at a temperature of 69^{0}C. The stockpile temperature then increased sharply to 135^{0}C on day 20 then decreased to 57^{0}C on day 22.

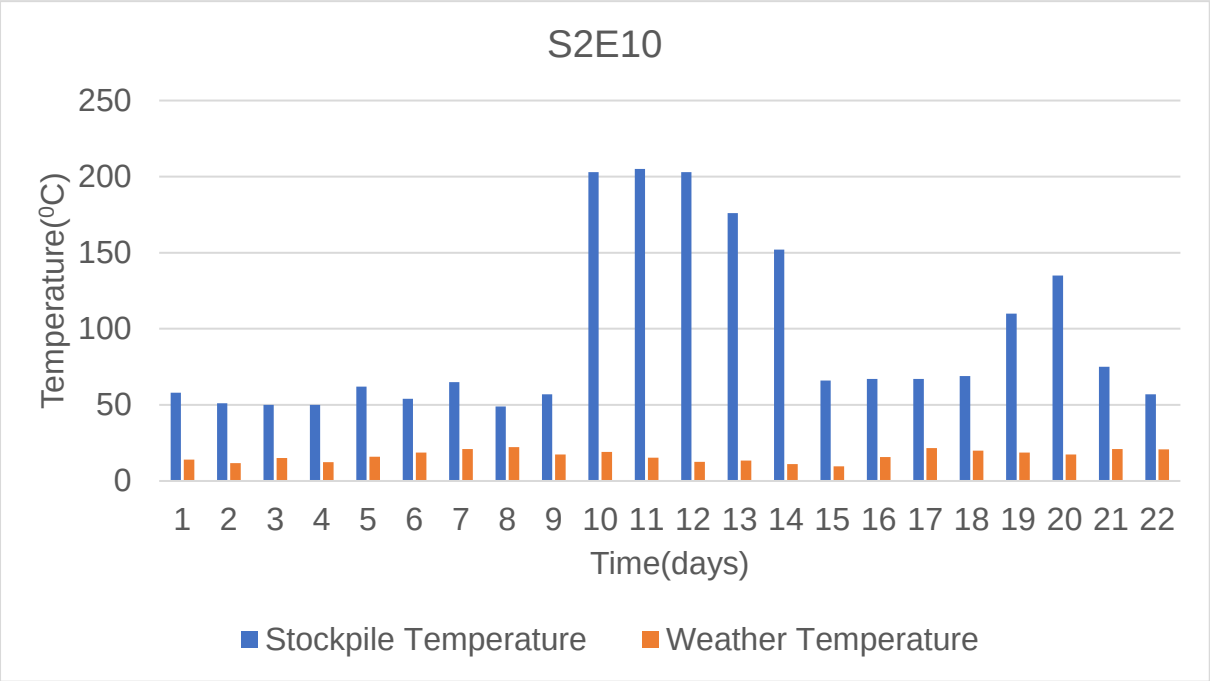

Figure 4.12 S2E10 temperature trend

4.3.13 Temperature measurements from the east side of the treated stockpile at 12h00

In Figure 4.13, the stockpile temperature decreased from 58^{0}C on day 1 to 48^{0}C on day 2. It then increased gently to 63^{0}C on day 5. The stockpile temperature decreased sharply from day five to 32^{0}C on day 10, and it increased to 57^{0}C on day 11. The lowest temperature of 20^{0}C was observed on day 14. The stockpile temperature increased sharply to 59^{0}C on day 15. It gently increased from day 15 to a maximum temperature of 66^{0}C on day 21, dropping slightly to the final temperature of 61^{0}C.

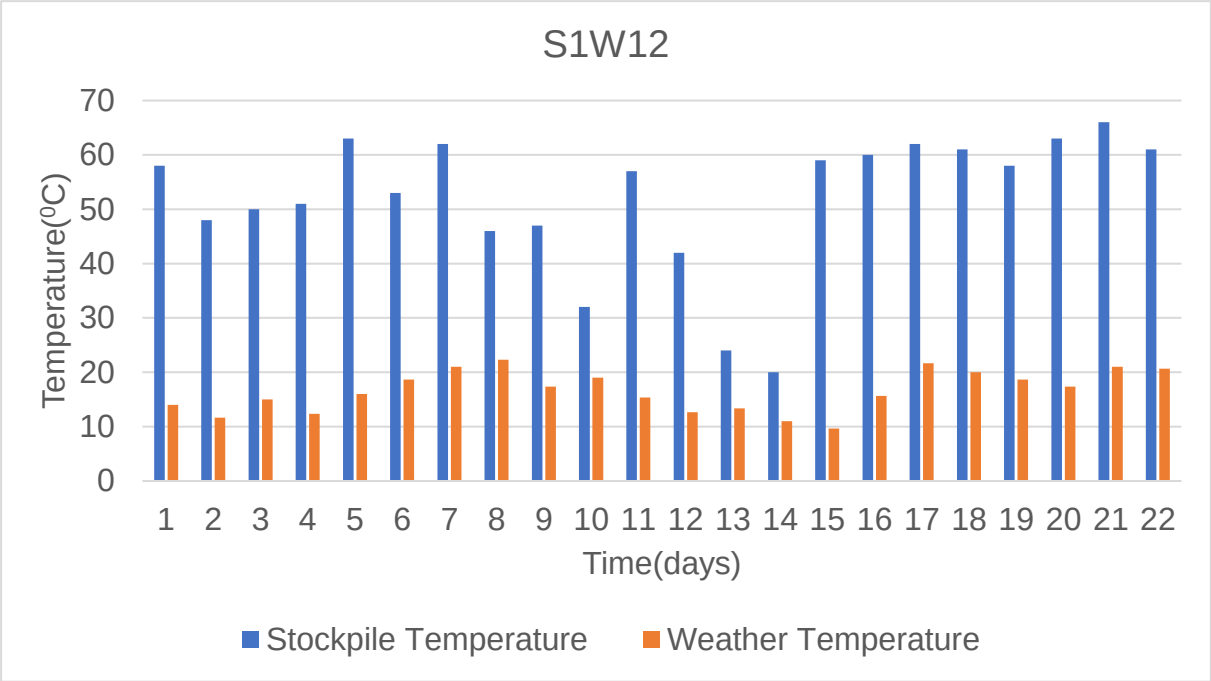

Figure 4.13 S1W12 temperature trend

4.3.14 Temperature measurements from the west side of the treated stockpile at 12h00

In Figure 4.14, the stockpile temperature decreased sharply from 58^{0}C to 41^{0}C from day 1 to day 2, respectively. It then increased to 42^{0}C on day 4 and then increased sharply to a maximum temperature of 55^{0}C on day 5. The stockpile temperature decreased erratically to 29^{0}C on day 10. It then increased sharply to 52^{0}C on day 11. Then it decreased to a minimum temperature of 20^{0}C on day 14. This drop was followed by a sharp rise to 48^{0}C on day 15, then increasing slightly to 50^{0}C on day 19 and dropping erratically to a final temperature of 42^{0}C on day 22.

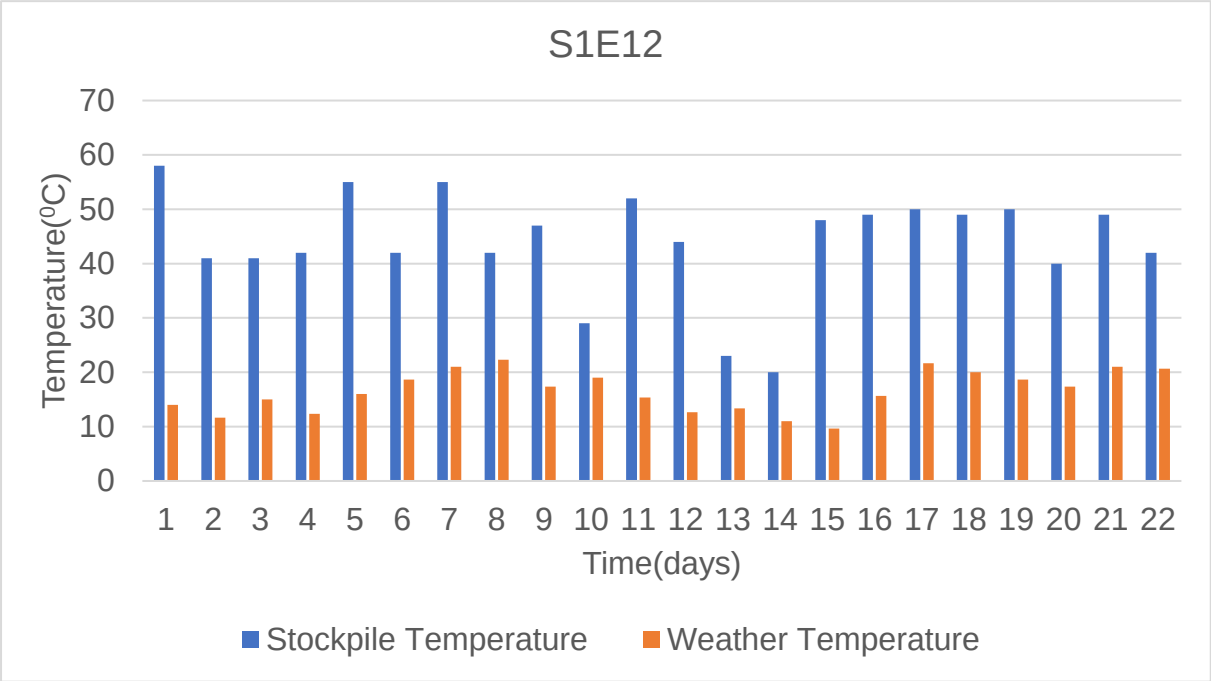

Figure 4.14 S1E12 temperature trend

4.3.15 Temperature measurements from the east side of the control stockpile at 12h00

In Figure 4.15, the stockpile temperature decreased gently from 58^{0}C on day 1 to 50^{0}C on day 9. There was a sharp increase from day 9 to a maximum temperature of 232^{0}C on day 11, followed by a sharp decrease to 65^{0}C on day 15. The stockpile temperature increased gently to 77^{0}C on day 18, then increased sharply to 215^{0}C on day 20. The stockpiled coal started burning due to spontaneous combustion on day nine.

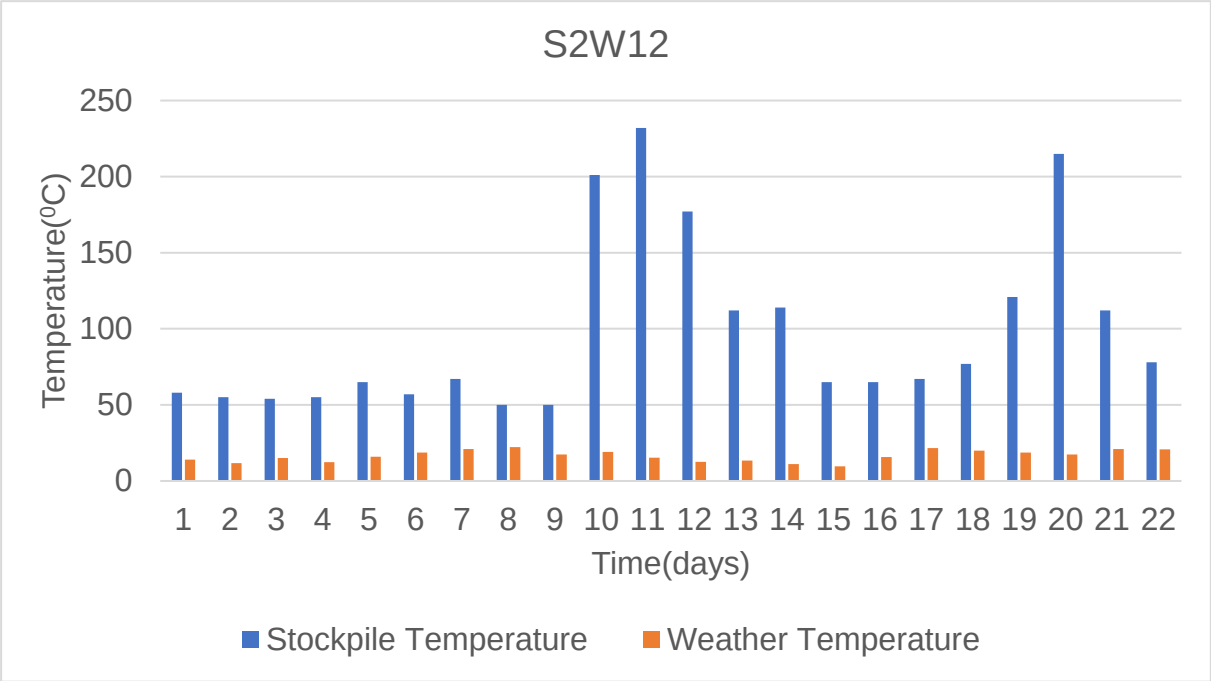

Figure 4.15 S2W12 temperature trend

4.3.16 Temperature measurement from the west side of control stockpile at 12h00

In Figure 4.16, the stockpile temperature decreased gently from 58^{0}C on day 1 to 46^{0}C on day 3 and then increased gently to 58^{0}C on day 9. The stockpile temperature increased sharply to a maximum of 219^{0}C on day 12. The temperature then decreased sharply to 67^{0}C on day 15 and then increased gently to a temperature of 70^{0}C on day 18. The stockpile temperature increased sharply from day 18 to 122^{0}C on day 20, dropping sharply to a final temperature of 57^{0}C on day 22.

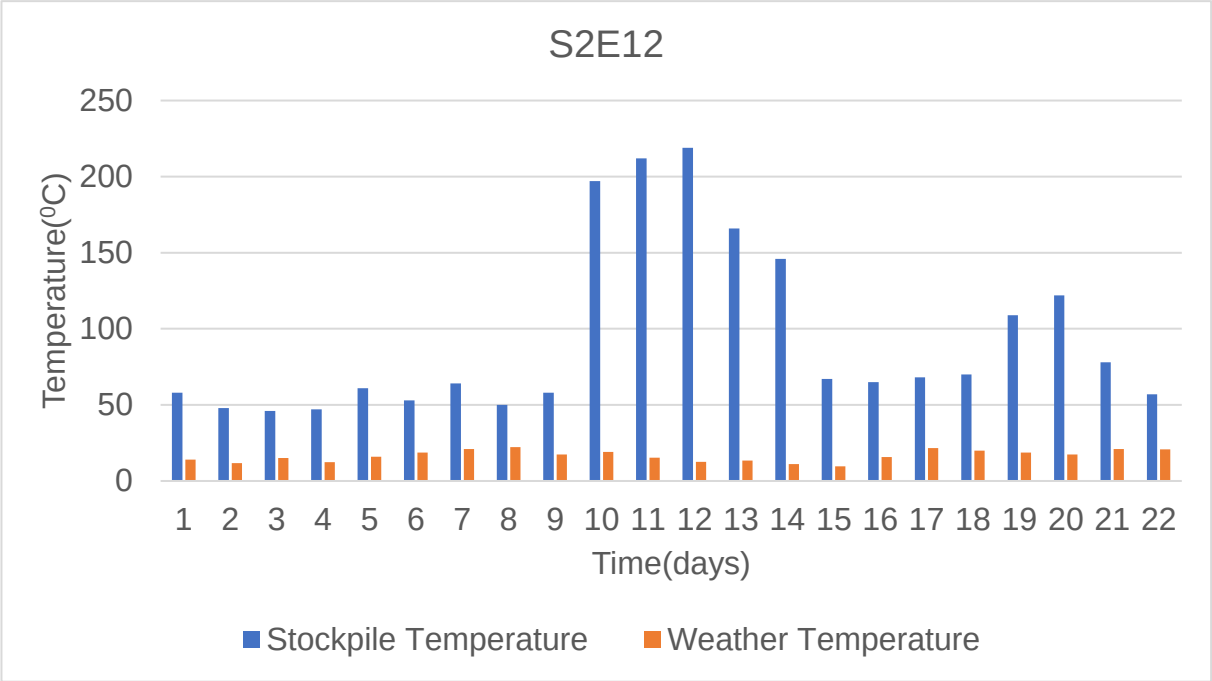

Figure 4.16 S2E12 temperature trend

4.3.17 Temperature measurements from the west side of the treated stockpile at 14h00

In Figure 4.17, the temperature increased gently from 58^{0}C on day 1 to a maximum temperature of 64^{0}C on day 5. The stockpile temperature started to decrease sharply from day 5 to a lower temperature of 27^{0}C on day 10. It then increased sharply to 49^{0}C on day 11. The stockpile temperature decreased sharply from day 11 to the lowest temperature of 19^{0}C on day 14, after which it increased sharply to a temperature of 62^{0}C and remained constant to the final temperature of 60^{0}C on day 22.

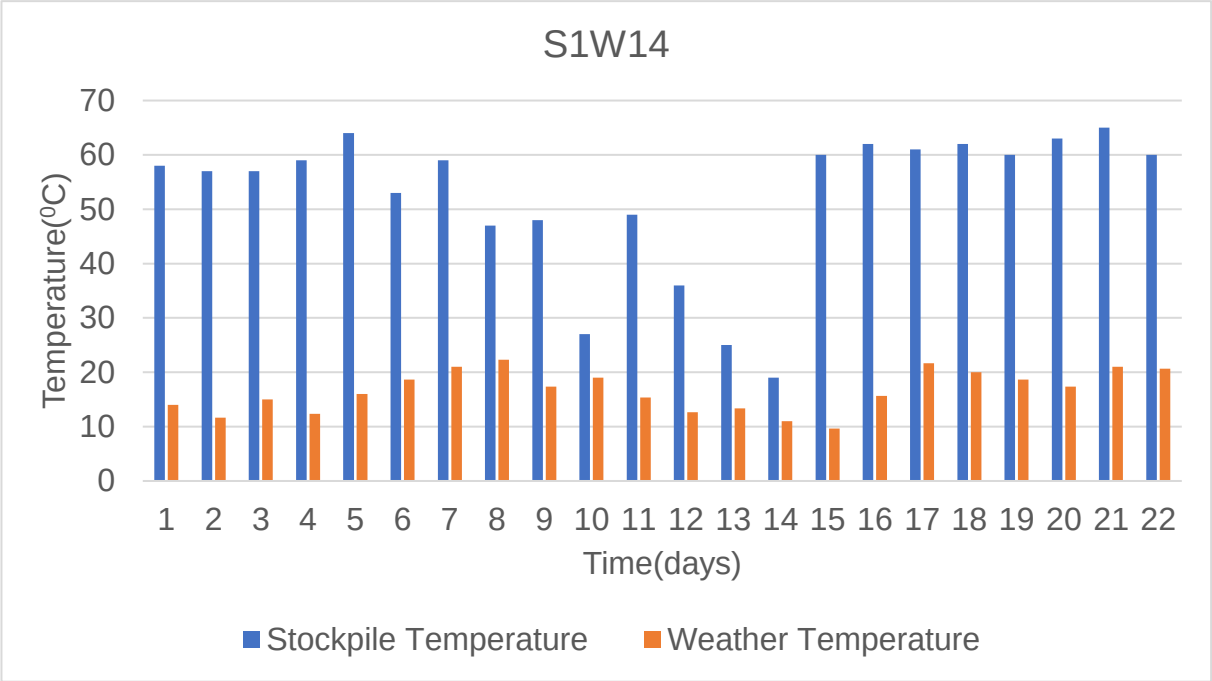

Figure 4.17 S1W14 temperature trend

4.3.18 Temperature measurements from the west side of the control stockpile at 14h00

In Figure 4.18, the stockpile temperature dropped gently from 58^0C to 53^0C from day 1 to day 2 respectively, it then increased gently to a temperature of 56^0C on day 5. The stockpile temperature decreased erratically to 24^0C on day 10, and then it increased sharply to 47^0C on day 11. The temperature decreased to 19^0C on day 14, then it increased sharply to 51^0C, dropping to the final temperature of 41^0C on day 22.

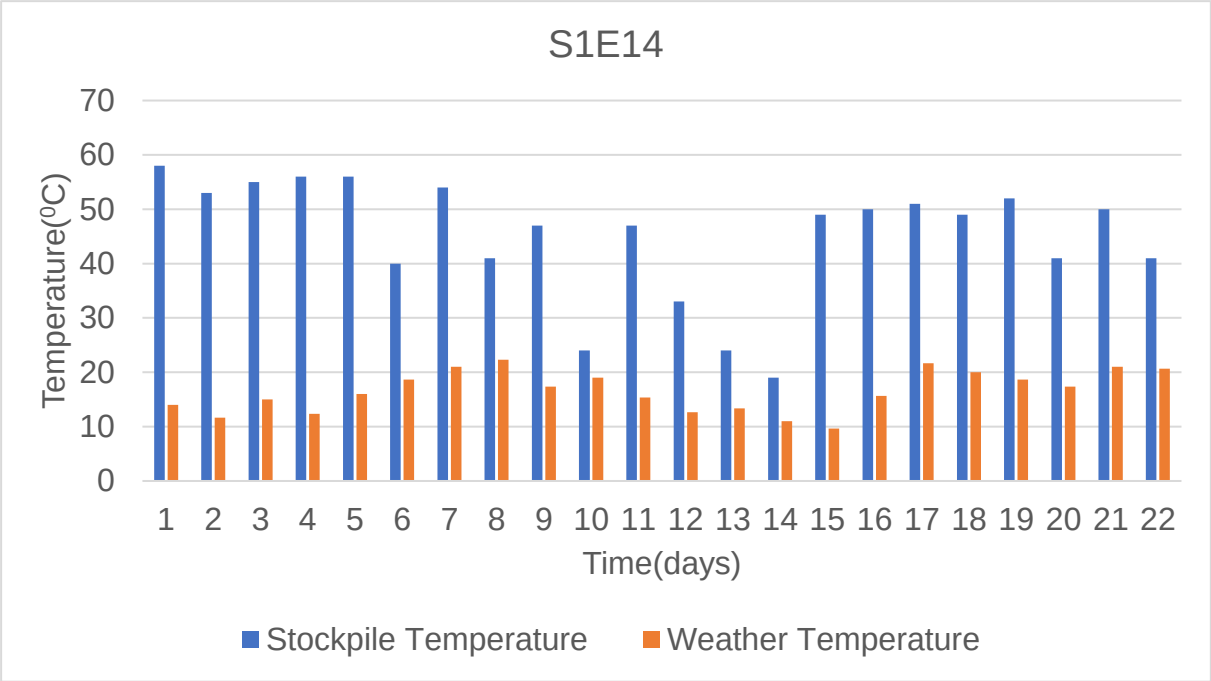

Figure 4.18 S1E14 temperature trend

4.3.19 Temperature measurements from the west side of the control stockpile at 14h00

In Figure 4.19, the stockpile temperature increased slightly from 58^{0}C on day 1 to 65^{0}C on day 5 before decreasing to the lowest temperature of 50^{0}C on day 9. The stockpile temperature increased sharply to a maximum temperature of 235^{0}C on day 11, followed by a sharp decrease to 64^{0}C on day 15. The stockpile temperature increased gently from day 15 to 72^{0}C on day 18, then it increased sharply to 208^{0}C, dropping sharply to the final temperature of 78^{0}C on day 22.

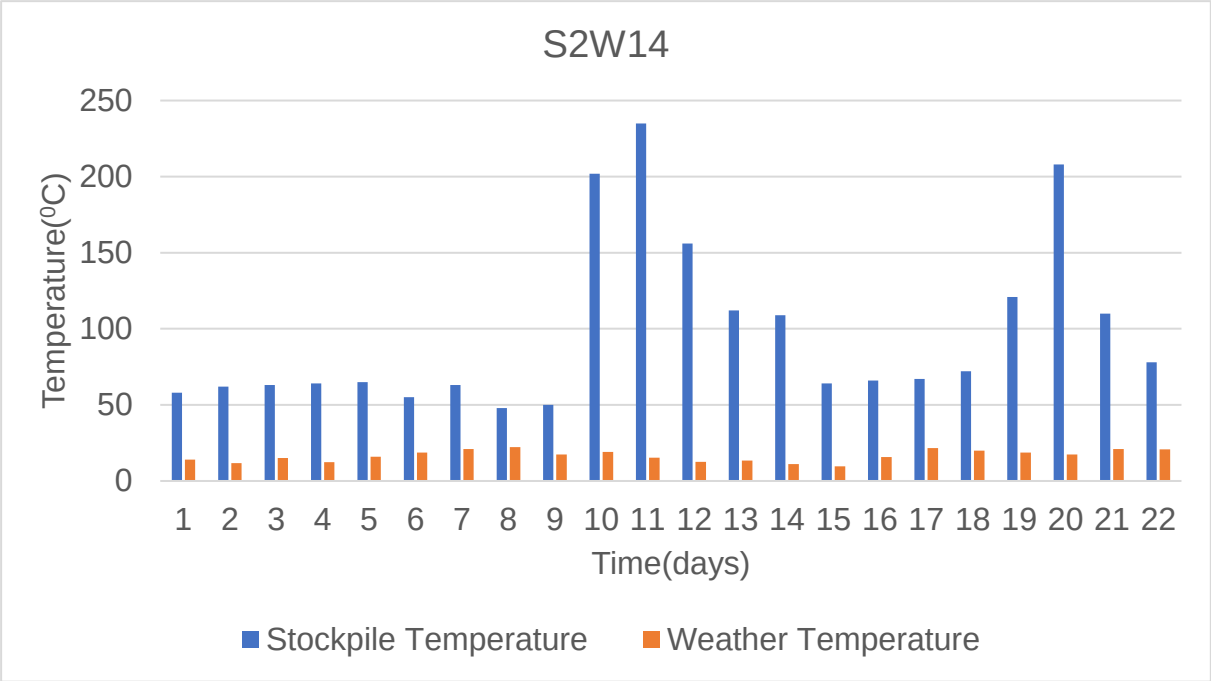

Figure 4.19 S2W14 temperature trend

4.3.20 Temperature measurements from the east side of the control stockpile at 14h00

In Figure 4.20, the stockpile temperature increased gently from 58^{0}C on day 1 to 64^{0}C on day 4, decreasing gently to the lowest temperature of 50^{0}C. The stockpile temperature increased sharply to the highest temperature of 249^{0}C on day 12. It then decreased sharply to 68^{0}C and then maintained a gentle decrease to 64^{0}C on day 18. The stockpile temperature increased sharply from day 18 to 136^{0}C on day 20, dropping sharply to the final temperature of 57^{0}C on day 22.

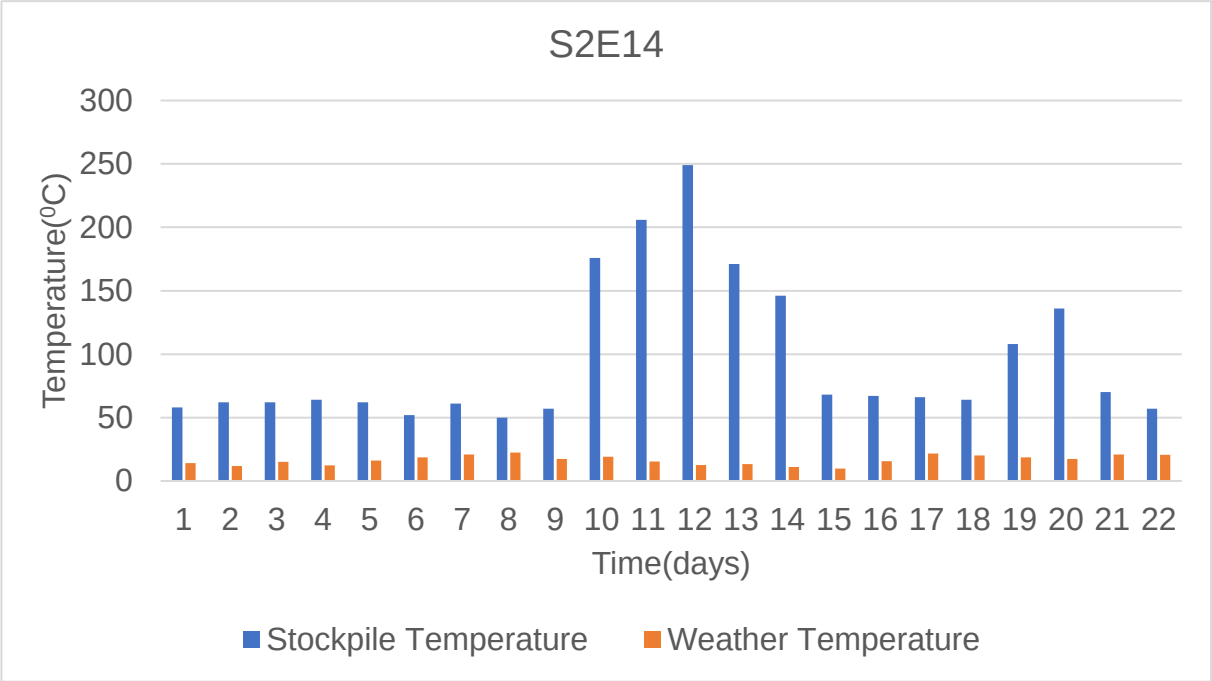

Figure 4.20 S2E14 temperature trend

4.3.21 Temperature measurements from the west side of the treated stockpile at 16h00

In Figure 4.21, the stockpile temperature decreased by 1^0C from 58^0C on day 1 to 57^0C on day 2. It then increased gently from day 2 to 61^0C on day 4. The stockpile temperature decreased erratically from day 4 to a minimum temperature of 19^0C on day 14. The stockpile temperature increased sharply from day 14 to 61^0C on day 15, increasing slightly to 65^0C on day 21, followed by a slight decrease to 59^0C on day 22.

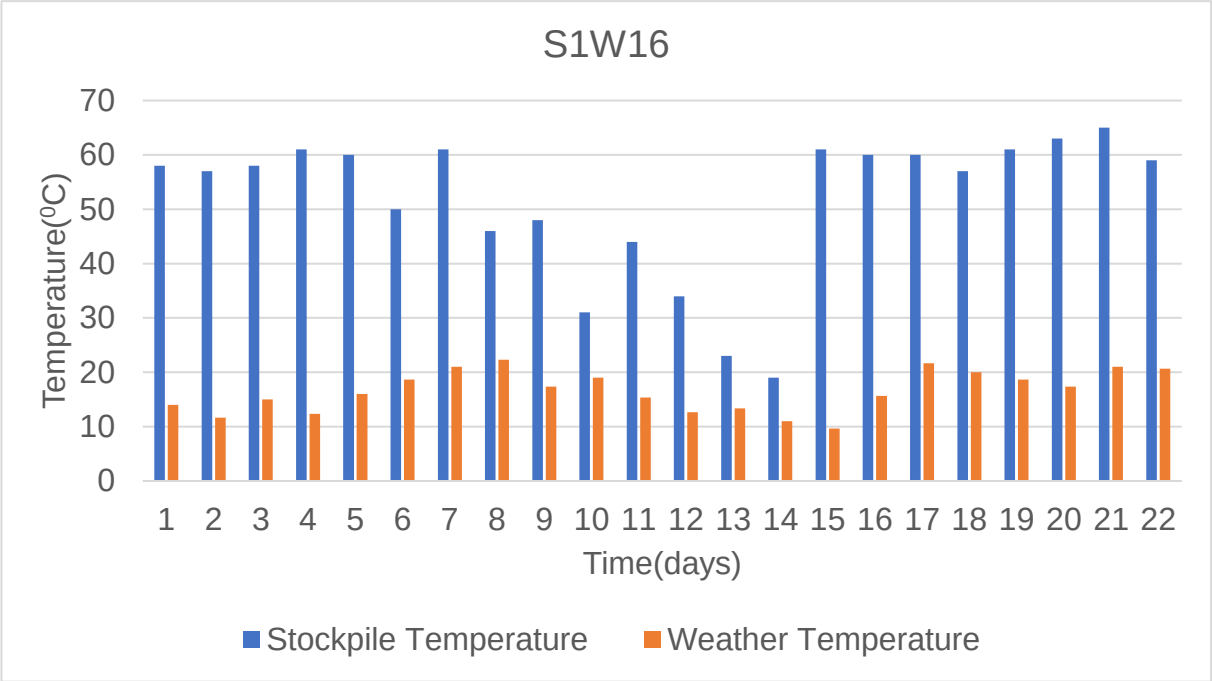

Figure 4.21 S1W16 temperature trend

4.3.22 Temperature measurements from the east side of the treated stockpile at 16h00

In Figure 4.22, the stockpile temperature decreased slightly from 58^{0}C on day 1 to 56^{0}C on day 2, increasing slightly to 58^{0}C on day 4. The stockpile temperature decreased sharply from day 4 to a temperature of 28^{0}C on day 10. The temperature then increased to 39^{0}C before it decreased sharply to the lowest temperature of 18^{0}C on day 14. The stockpile temperature increased sharply from day 14 to 49^{0}C on day 15, decreasing to 45^{0}C on day 18. The stockpile temperature increased erratically then dropped to a final temperature of 40^{0}C on day 22.

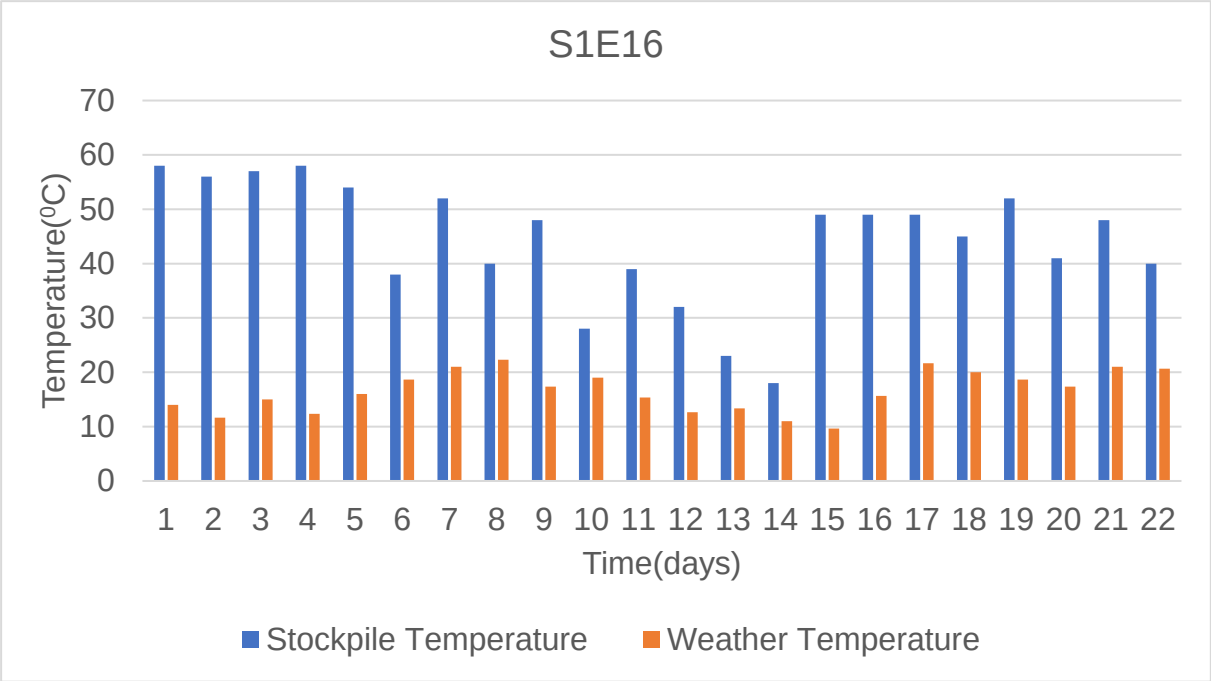

Figure 4.22 S1E16 temperature trend

4.3.23 Temperature measurements from the west side of the control stockpile at 16h00

In Figure 4.23, the stockpile temperature increased slightly from 58^{0}C on day 1 to 67^{0}C on day 5, decreasing to the lowest temperature of 50^{0}C on day 9. The stockpile temperature increased sharply from day 9 to a maximum temperature of 235^{0}C on day 11, followed by a sharp decrease to 65^{0}C on day 16. The temperature increased gently to 71^{0}C on day 18, followed by a sharp rise to 213^{0}C on day 20. The stockpile then decreased sharply from day 20 to a final temperature of 77^{0}C on day 22.

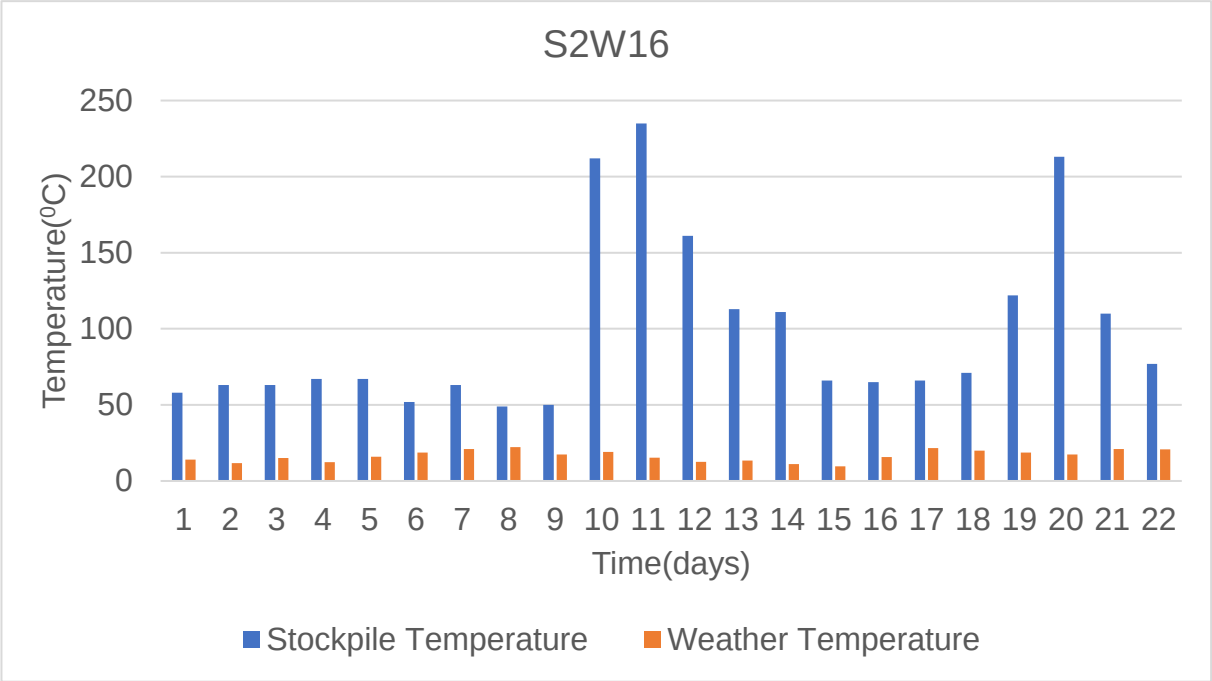

Figure 4.23 S2W16 temperature trend

4.3.24 Temperature measurements from the east side of the control stockpile at 16h00

In Figure 4.24, the stockpile temperature increased gently from 58^{0}C on day 1 to 66^{0}C on day 4 before decreasing gently to 48^{0}C on day 6. The stockpile temperature increased gently from day 6 to 59^{0}C on day 9 before it increased sharply to a maximum temperature of 246^{0}C on day 12. The stockpile temperature decreased sharply from day 12 to 70^{0}C on day 15, gently decreasing to 57^{0}C on day 19. It then increased sharply from day 19 to 139^{0}C on day 20. Finally, the stockpile temperature decreased sharply from day 20 to 57^{0}C on day 22.

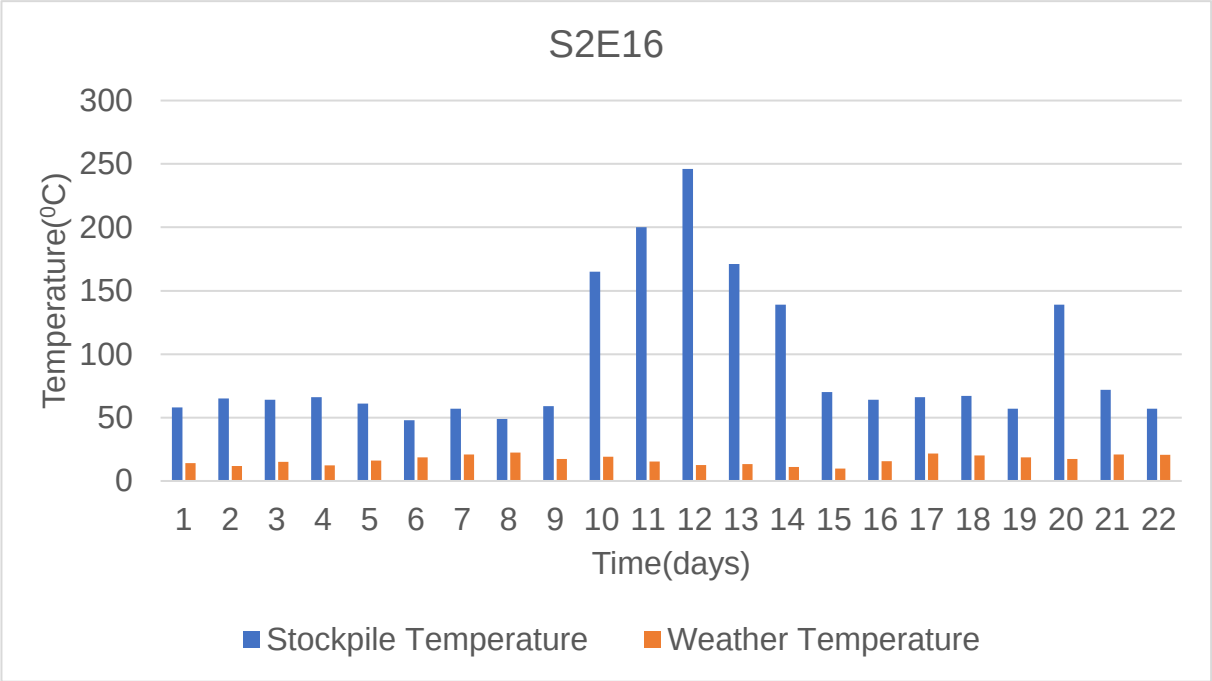

Figure 4.24 S2E16 temperature trend

4.4 Comparison of same sides of the treated and control stockpiles

4.4.1 West side temperature of the treated and control stockpiles variations at 06h00

Figure 4.25 shows the temperature comparison of the west side of the treated stockpile (S1W) and the west side of the control stockpile (S2W) at 06h00. Both stockpiles experienced a similar temperature trend from day 1 to day 9. On day 1, they both had the same temperature of 58^{0}C, and from day 2, there were minor differences, with the control stockpile being 6^{0}C above the treated stockpile. On day 8, both stockpiles had the same temperature of 45^{0}C. From day 9, the control stockpile temperature increased sharply from 45^{0}C to a maximum of 242^{0}C, dropping sharply to 61^{0}C on day 15. During the same period, treated stockpile temperature decreased to a minimum of 21^{0}C on day 13, then increasing to 51^{0}C on day 15. Both stockpiles maintained a constant temperature trend from day 16 until day 17. From day 17, the control stockpile temperature increased from 66^{0}C to 221^{0}C on day 20, then decreased to a minimum temperature of 77^{0}C. During the same period, the treated stockpile temperature decreased from 61^{0}C on day 17 to 51^{0}C on day 19 before increasing to 62^{0}C on day 22. The control stockpile experienced burning due to spontaneous combustion from

day 9, while the treated stockpile did not experience burning due to spontaneous combustion.

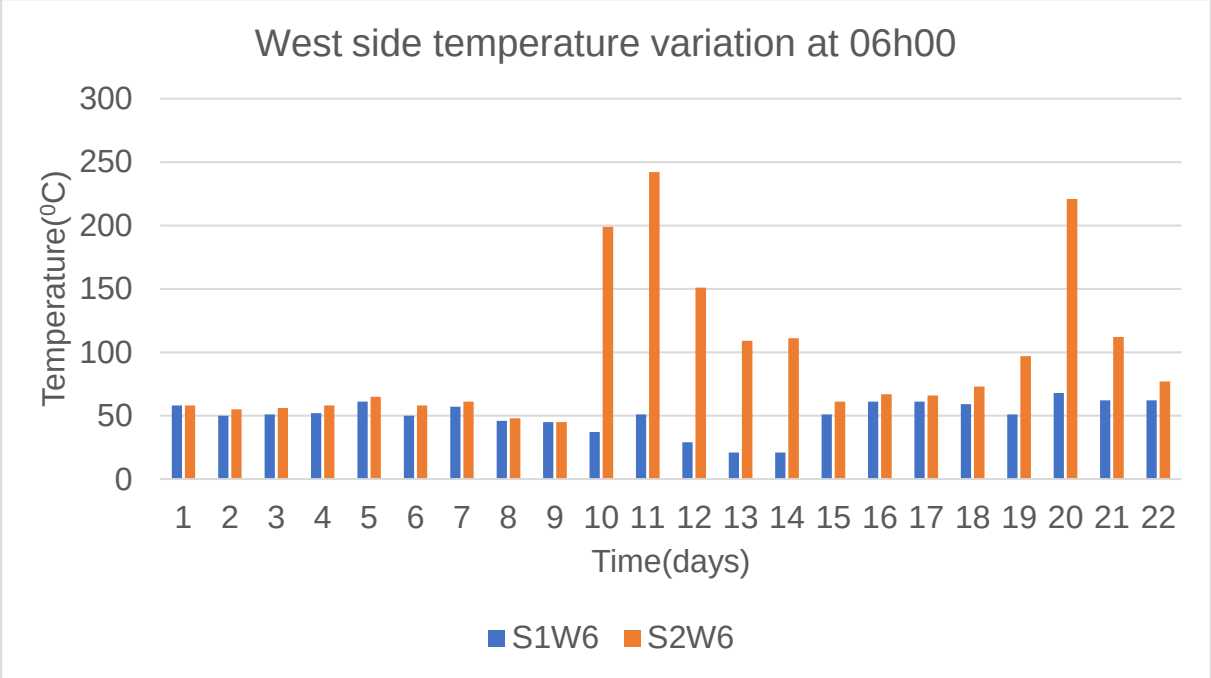

Figure 4.25 west side temperature variation at 06h00

Table 4.1 *t*-test for west side at 06h00

t-test: Two-samples assuming unequal variances		
	Stockpiles	
	S1W6	S2W6
Mean	50.2	95.0
Variance	167.1	3322.1
Observations	22.0	22.0
Degree of freedom(df)	23.0	
T Stat	-3.6	
P(T<=t) two-tail	0.0	
T Critical two-tail	2.1	

Table 4.1 illustrates the statistical analysis of the west side of the treated stockpile (S1W6) and the control stockpile (S2W6). The *t*-test of a sample assuming unequal variances was used to assess the significance of gypsum on the treated stockpile compared to the control stockpile. S1W6 stockpile has a mean of 50.2, while S2W6 has a mean of 95. The means of the two stockpiles have a difference of 44.8. Similarly, the variances of S1W6 and S2W6 are 167.1 and 3322.10, respectively. The huge variance difference of 3154.99 indicates that the two stockpiles have different responses to heat. The treated stockpile shows a lower variability than the control stockpile. It is deduced that gypsum affected the treated stockpile by ensuring that the temperature fluctuations were reduced while the control stockpile does not exhibit the same trend as observed on the treated stockpile.

The significance level of 0.05 on a two-tailed test resulted in the test statistic critical value of 2.1, a test statistic outcome whose absolute value is greater than the critical value would result in rejection of the assumption that gypsum did not affect the stockpile temperature. The absolute value of the test statistic obtained is 3.6, which is greater than the critical value of 2.1. Therefore, gypsum affected the temperature of the treated stockpile.

4.4.2 East side temperature variations of the treated and control stockpiles at 06h00

Figure 4.26 illustrates the east side temperature variations of the treated stockpile (S1E6) and the control stockpile (S2E6). The temperature of both stockpiles on day 1 is 58^0C. After day 1, both stockpiles had a similar temperature trend, with the control stockpile having a slightly higher temperature of 6^0C. This trend continued until day 9 where the temperature of the control stockpile increased sharply to a maximum of 241^0C, then decreased to a temperature of 65^0C on day 15. The temperature of the treated stockpile decreased from 46^0C on day 9 to the lowest temperature of 20^0C on day 14, increasing to 47^0C on day 15. From day 15, the treated stockpile temperature decreased to 40^0C on day 22.

On the other hand, the control stockpile maintained the same temperature of 65^0C from day 15 until day 18. The temperature then increased to 138^0C on day 20 before it decreased to 55^0C on day 22. Similar to the west side, the east side of the control

stockpile started burning due to spontaneous combustion on day nine, while the treated stockpile did not experience burning due to spontaneous combustion.

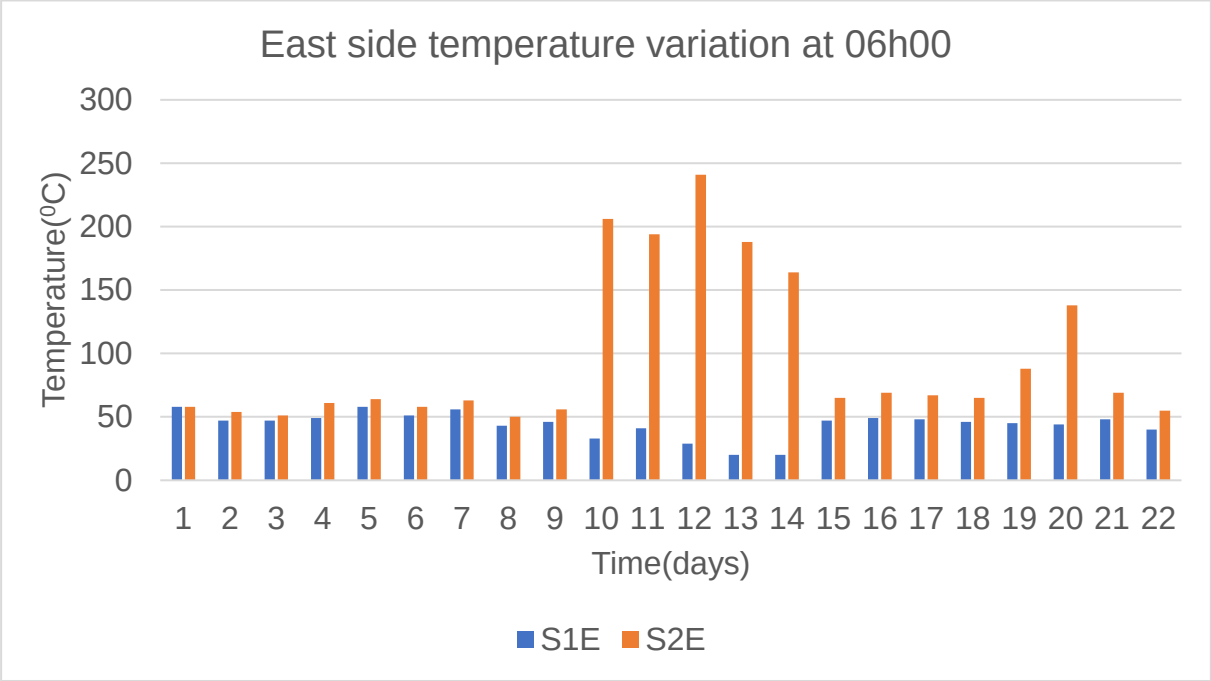

Figure 4.26 East side temperature variation at 06h00

Table 4.1 *t*-test for east side at 06h00

t-test: Two-samples assuming unequal variances		
	Stockpiles	
	S1E6	S2E6
Mean	43.9	96.5
Variance	106.0	3679.6
Observations	22.0	22.0
Degree of freedom(df)	22.0	
T Stat	-4.0	
P(T<=t) two-tail	0.0	
T Critical two-tail	2.1	

Table 4.2 represent the statistical analysis of the east side of the treated stockpile (S1E6) and the east side of the control stockpile (S2E6). S1E6 stockpile has a mean of 43.9 while S2E6 was 96.5. The variance of S1E6 and S2E6 are 106.0 and 3679.6, respectively. The huge difference of 3573.26 between the variances of the two stockpiles indicates the significant differences between the temperatures of the stockpiles. S1E6 had a lower variability of temperature compared to S2E6. This indicates that gypsum had a significant effect on the temperature of the treated stockpile. The test statistic absolute value of 4.016 was obtained from the analysis. Since the test statistic value is greater than the critical value, the treatment results occur due to gypsum. Hence, it is concluded that gypsum treatment affected the temperature of the treated stockpile.

4.4.3 West side temperature variations of the treated and control stockpiles at 08h00

In Figure 4.27, the temperature of both stockpiles on day one was 58^0C; from day 2, the temperature of the control stockpile increased slightly more than the temperature of the treated stockpile. The temperature difference between the two stockpiles was 6^0C until day 9. The temperature of the control stockpile increased sharply at day 9 from 50^0C to a maximum temperature of 229^0C on day 11. It then decreased to 63^0C on day 15. During the same period, the temperature of the treated stockpile decreased from 50^0C on day 9 to the lowest temperature of 21^0C on day 14, increasing slightly to a maximum temperature of 67^0C on day 17. The temperature of the control stockpile started to increase sharply from 67^0C on day 17 to a temperature of 219^0C on day 20, dropping to a final temperature of 77^0C. On the other hand, the temperature of the treated stockpile decreased from 62^0C on day 17 to 60^0C on day 22. It is evident from Figure 4.27 that the treated stockpile was not affected by spontaneous combustion, while the control stockpile was affected by spontaneous combustion from day nine when a thermal runaway was observed.

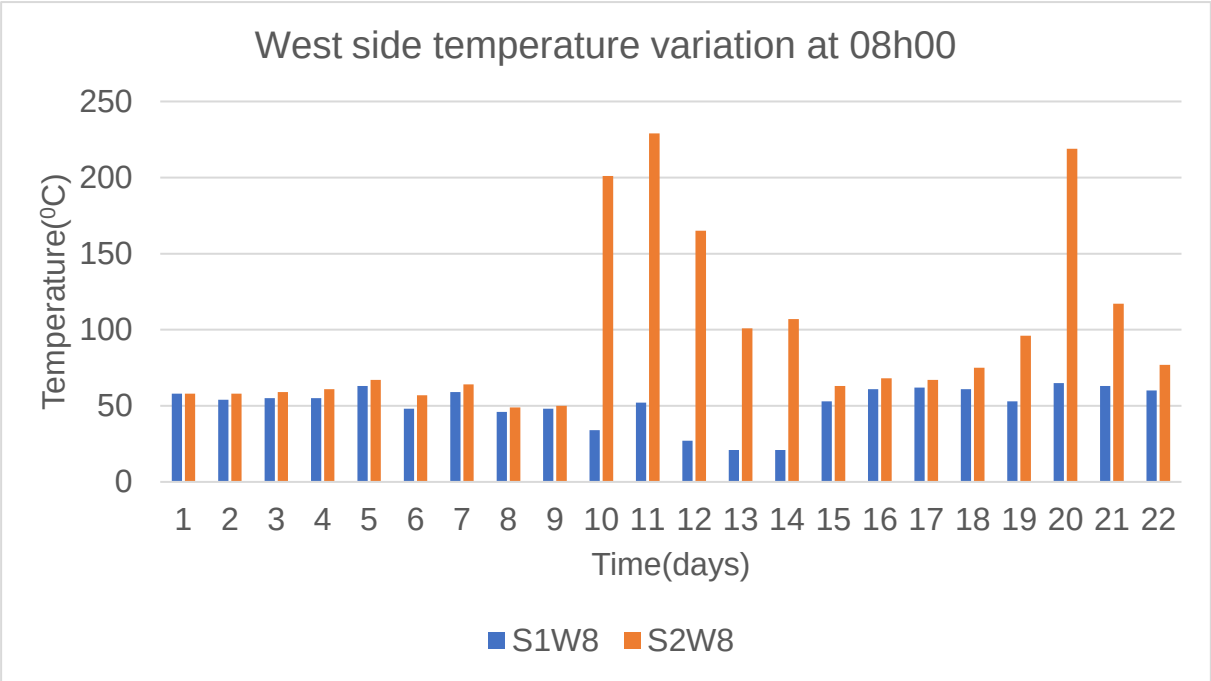

Figure 4.27 West side temperature variation at 08h00

Table 4.2 *t*-test for west side at 08h00

t-test: Two-samples assuming unequal variances		
	Stockpiles	
	S1W8	S2W8
Mean	50.9	95.8
Variance	178.9	3138.1
Observations	22.0	22.0
Degree of freedom(df)	23.0	
T Stat	-3.7	
P(T<=t) two-tail	0.0	
T Critical two-tail	2.1	

Table 4.3 represent the statistical analysis of the west side of the treated stockpile (S1W8) and control stockpile (S2W8). S1W8 has a mean of 50.9, while S2W8 has a mean of 95.8. The two stockpiles have a mean difference of 44.1. Furthermore, the temperature of S2W8 was significantly higher than S1W8. The variance of S1W8 is

178.9, while the variance of the S2W8 is 3138.1, with a difference between variances of 2959.2. The temperature of S2W8 was significantly higher than the S1W8 each day of the data collection, and every hour, it was also significantly variable due to the onset of spontaneous combustion on day 9. The lower variability obtained from S1W8 indicates that gypsum affected the stockpile's temperature compared to the control stockpile. The test statistic absolute value of 3.661 was obtained from the analysis. Since the test statistic value is greater than the critical value, then the outcome of the treatment occurred due to gypsum. Hence it is concluded that gypsum treatment affected the temperature of the treated stockpile.

4.4.4 East side temperate variations of the treated and control stockpiles at 08h00

In Figure 4.28, both stockpiles started with the same temperature of 58^0C on day 1. The temperature of the treated stockpile decreased to 47^0C on day 3, while the temperature of the control stockpile increased to 66^0C on day 5, decreasing to 50^0C on day 8. The temperature of the treated stockpile increased to 57^0C from day 4 to day 7, then decreased to the lowest temperature of 20^0C on day 14. The control stockpile temperature increased substantially from 50^0C on day 8 to a maximum temperature of 202^0C on day 10, fluctuating with a downward trend to 162^0C on day 14 before decreasing sharply to 67^0C on day 15. From day 15, both treated and control stockpiles maintained a similar trend from 48^0C and 67^0C, respectively, to day 17. The temperature of the control stockpile increased from 65^0C on day 17 to 140^0C on day 20, then decreased to a final temperature of 56^0C on day 22. The treated stockpile decreased from 50^0C on day 17 to a final temperature of 40^0C on day 22. It is evident from the observation that the treated stockpile did not experience spontaneous combustion while the control stockpile experienced spontaneous combustion from day eight.

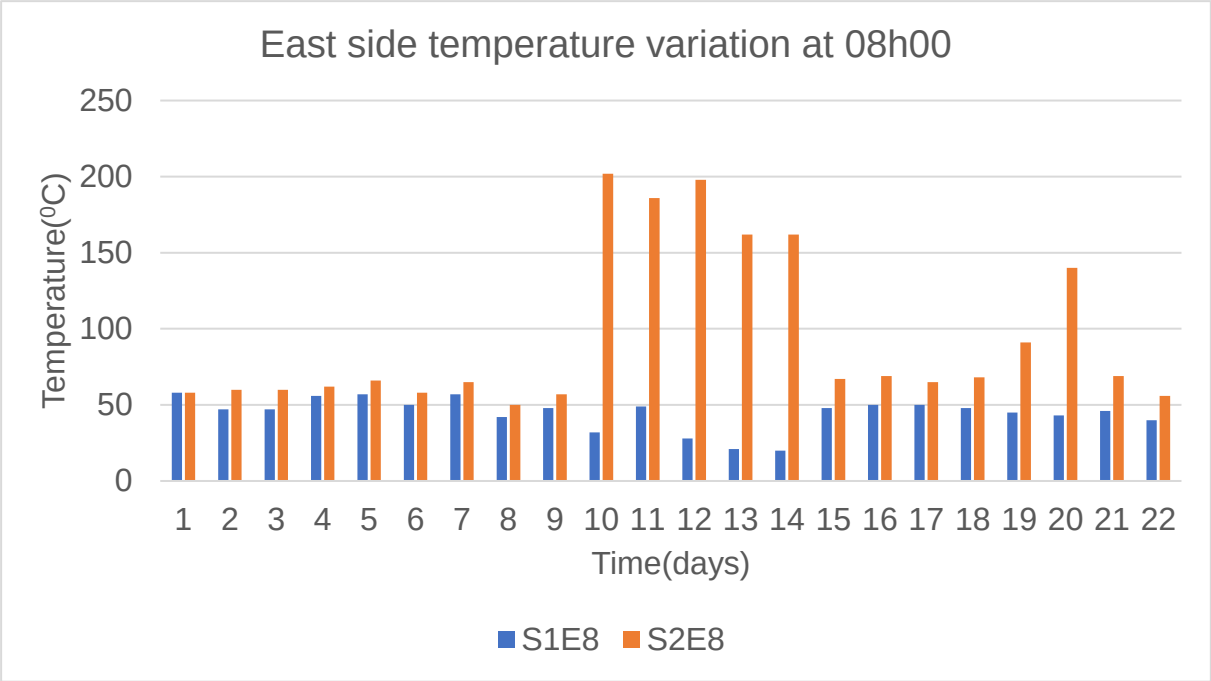

Figure 4.28 East side temperature variation at 08h00

Table 4.4 represent the statistical analysis of the east side of the treated stockpile (S1E8) and the control stockpile (S2E8). S1E8 has a mean of 44.6, while S2E8 has a mean of 94.1, with a mean difference of 49.5. S2E8 had a higher temperature measurement on both daily and hourly measurements, as confirmed by the high mean. S1E8 had lower temperatures daily and hourly, as confirmed by the lower mean. Similarly, S2E8 had significantly higher variable daily and hourly temperature as confirmed by a variance of 2767.4 compared to lower S1E8 variance of 114.2. The low mean and variance of S1E8 affirm that the outcome occurred due to the application of gypsum. The test statistic absolute value of 4.3 was obtained from the analysis. Hence, it is concluded that gypsum treatment affected the temperature of the treated stockpile.

Table 4.3 *t*-test for east side at 08h00

t-test: Two-samples assuming unequal variances		
	Stockpiles	
	S1E8	S2E8
Mean	44.6	94.1
Variance	114.2	2767.4
Observations	22.0	22.0
Degree of freedom(df)	23.0	
T Stat	-4.3	
P(T<=t) two-tail	0.0	
T Critical two-tail	2.1	

4.4.5 West side temperature variations of the treated and control stockpiles at 12h00

In Figure 4.29, both stockpiles started on day one with the same temperature of 58^0C. They maintained a slight difference in temperature of 2^0C, although the trend was the same until they were both at 49^0C on day 9. The temperature of the control stockpile increased from 49^0C on day 9 to a maximum temperature of 239^0C on day 11, decreasing to 64^0C on day 15. The treated stockpile temperature decreased from day 9 to the lowest 20^0C on day 14, increasing to a maximum temperature of 66^0C on day 16. From day 16, the treated stockpile temperature decreased to 61^0C on day 22. The temperature of the control stockpile increased from 67^0C on day 17 to 218^0C on day 20, then decreased to 79^0C on day 22. It is evident from these graphs that the treated stockpile was not affected by spontaneous combustion, whereas the control stockpile was affected by spontaneous combustion from day 9.

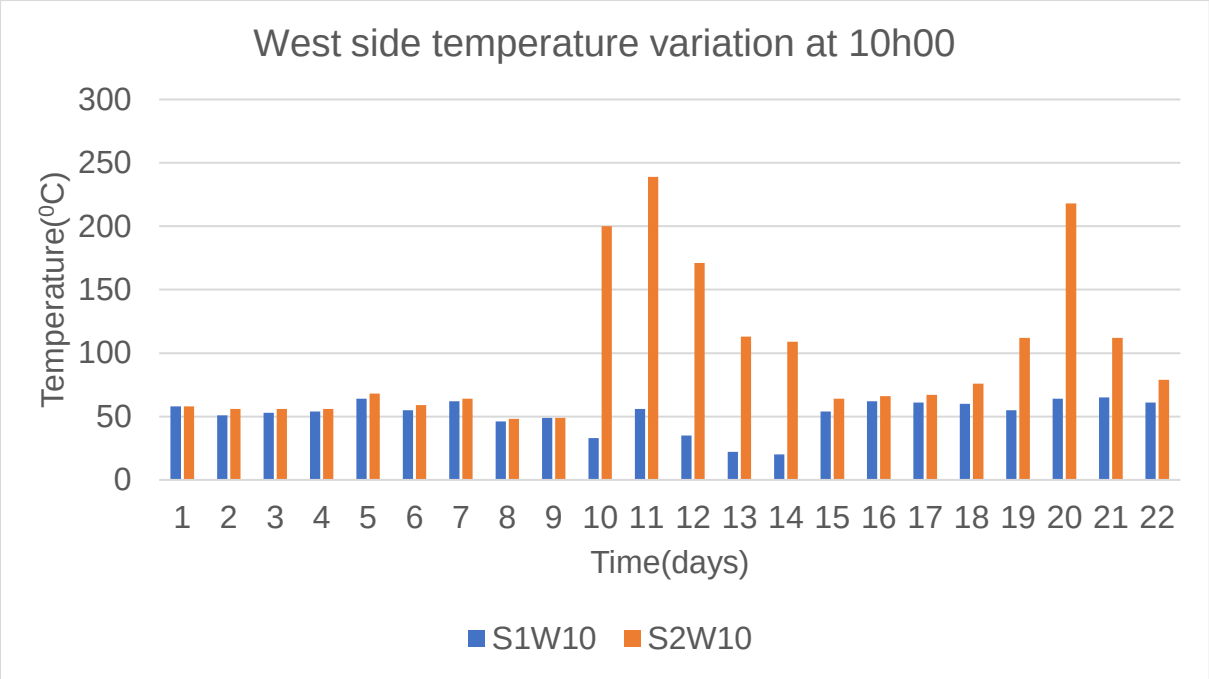

Figure 4.29 West side temperature variation at 10h00

Table 4.4 *t*-test for west side at 10h00

t-test: Two-samples assuming unequal variances		
	Stockpiles	
	S1W10	S2W10
Mean	51.8	97.3
Variance	170.5	3337.9
Observations	22.0	22.0
Degree of freedom(df)	23.0	
T Stat	-3.6	
P(T<=t) two-tail	0.0	
T Critical two-tail	2.1	

Table 4.5 represent the statistical analysis of the west side of the treated stockpile (S1W10) and the west side of the control stockpile (S2W10). The S1W10 has a mean of 51.8, while S2W10 has a mean of 97.3. The mean difference between the stockpiles is 45.5. The S1W10 has exhibited a higher temperature on a daily and hourly basis

than the S2W10. This is confirmed by the high mean of the control stockpile compared to the treated stockpile. S1W10 has a variance of 170.5, while S2W12 has a variance of 3337.9, with the difference between variances of the two stockpiles of 3167.4. The low variability of the treated stockpile compared to the control stockpile signifies the gypsum's effectiveness to control the stockpile's temperature. The test statistic absolute value of 3.6 was obtained from the analysis. Since the test statistic value is greater than the critical value, then the outcome of the treatment results did occur due to gypsum. Hence, it is concluded that gypsum treatment affected the temperature of the treated stockpile.

4.4.6 East side temperature variations of the treated and control stockpiles at 10h00

In Figure 4.30, both stockpiles had the same temperature of 58^0C on day 1 of the study. The temperature of both stockpiles decreased simultaneously to the same temperature of 51^0C on day 2. From day 2 to day 5, the treated stockpile experienced a higher increase in temperature than the control stockpile until day 5, when they both had the same temperature of 62^0C due to a rapid increase in control stockpile temperature from day 4. From day five, both stockpiles had a similar temperature trend until day 8, when the control stockpile increased sharply to a maximum of 205^0C then decreased to 66^0C on day 15. During the same period, the treated stockpile temperature decreased from 47^0C on day 9 to the lowest 20^0C, then increased to 49^0C on day 15. From day 15, they both had the same trend until day 17, when the temperature of the treated stockpile decreased from 51^0C to a final temperature of 42^0C on day 22. The control stockpile temperature increased sharply from 69^0C on day 18 to 135^0C on day 20 and decreased to 57^0C on day 22. It is evident from the observation that the treated stockpile was not affected by spontaneous combustion, while the control stockpile was affected by spontaneous combustion from day 9.

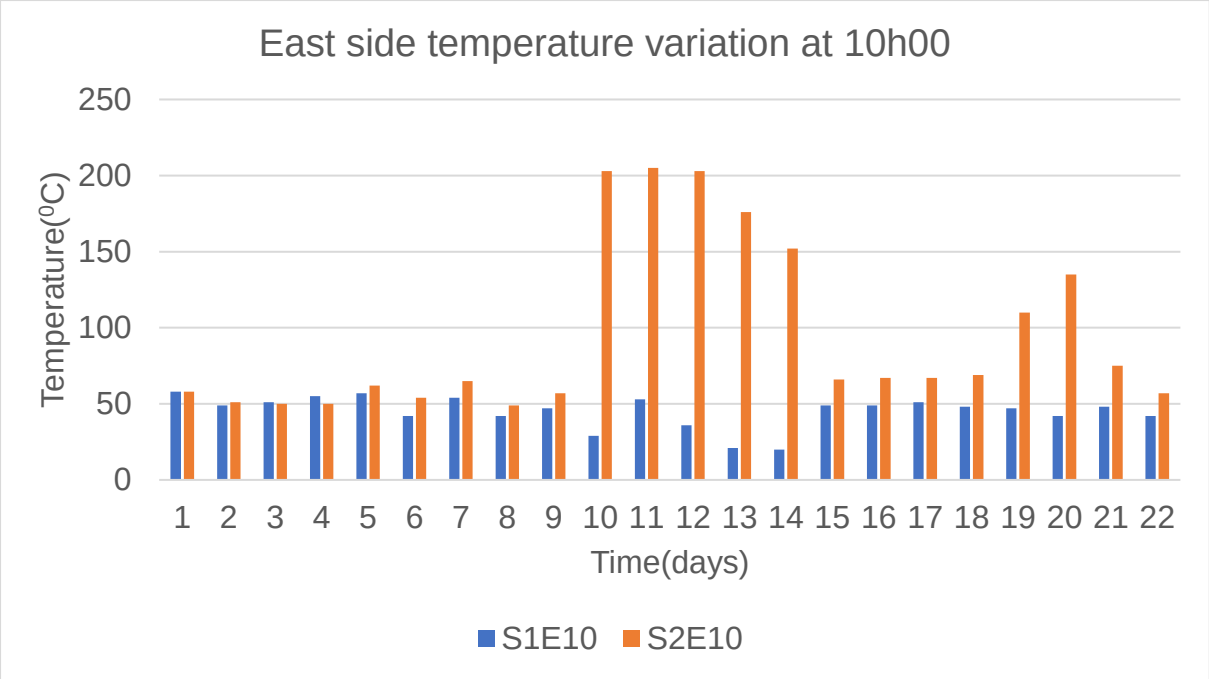

Figure 4.30 East side temperature variation at 10h00

Table 4.5 *t*-test for east side at 10h00

t-test: Two-samples assuming unequal variances		
	Stockpiles	
	S1E10	S2E10
Mean	45.0	94.6
Variance	108.5	3170.2
Observations	22.0	22.0
Degree of freedom(df)	22.0	
T Stat	-4.1	
P(T<=t) two-tail	0.0	
T Critical two-tail	2.1	

Table 4.6 represent the statistical analysis of the east sides of the treated stockpile (S1E10) and control stockpile (S2E10). S1E10 had a mean of 45 while S2W10 had a mean of 94.6, with a mean difference of 49.6. The high mean of S2W10 indicates the higher temperatures measured daily and hourly compared to the lower temperatures

of S1E10 measured simultaneously with the S2W10. The lower temperatures of S1E10 could be attributed to the effectiveness of gypsum application. S1E10 has a variance of 108.5, while S2E10 has a variance of 3170.2, with a variance difference of 3061.7. The low variance of the treated stockpile affirms the effectiveness of gypsum application compared to the control stockpile, which has high temperature measurements daily and hourly. The test statistic absolute value of 4.1 was obtained from the analysis. Since the test statistic value is greater than the critical value, then the outcome of the treatment results did not occur by chance. Hence, it is concluded that gypsum treatment affected the temperature of the treated stockpile.

4.4.7 West side temperature variations of the treated and control stockpiles at 12h00

In Figure 4.31, both stockpiles started at the same temperature of 58^0C on day 1. The temperature of the treated stockpile decreased to 48^0C on day 2, while the control stockpile decreased to 55^0C. They both experienced an increase in temperature with minor variations until day 9. From day 9, the control stockpile temperature increased from 50^0C to a maximum temperature of 232^0C, then decreased to 112^0C, increasing slightly to 114^0C on day 14. The control stockpile temperature decreased to 65^0C on day 15 from day 14. During the same period, the treated stockpile temperature decreased with minor fluctuations to a minimum temperature of 20^0C on day 14, then increased to 59^0C on day 15. The temperature of the treated stockpile increased gently from 59^0C on day 15 to a final temperature of 61^0C on day 22. The control stockpile increased from 65^0C on day 15 to 215^0C on day 20, dropping to a final temperature of 78^0C on day 22. The observation indicates that spontaneous combustion did not affect the treated stockpile, while the control stockpile was affected by spontaneous combustion from day nine.

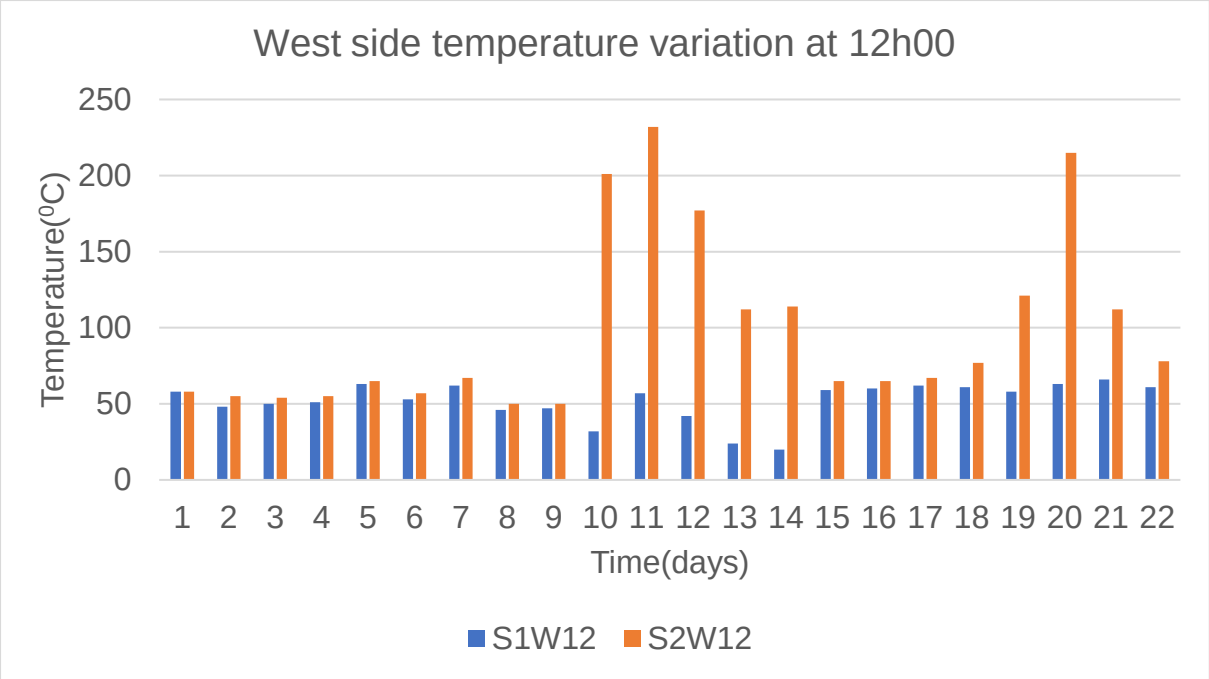

Figure 4.31 West side temperature variation at 12h00

Table 4.6 *t*-test for west side at 12h00

t-test: Two-samples assuming unequal variances		
	Stockpiles	
	S1W12	S2W12
Mean	52.0	97.6
Variance	162.0	3296.3
Observations	22.0	22.0
Degree of freedom(df)	23.0	
T Stat	-3.6	
P(T<=t) two-tail	0.0	
T Critical two-tail	2.1	

Table 4.7 represent the statistical analysis of the west side of the treated stockpile (S1W12) and the control stockpile (S2W12). S1W12 has a mean of 52.0, while S2W12 has a mean of 97.6. The difference between the means is 45.6. The low mean of the S1W12 indicates that the temperature measurements were lower on a daily and hourly

basis, while the high mean of the S2W12 indicates the high-temperature measurements on a daily and hourly basis. The lower mean of S1W12 also indicates the effectiveness of the applied gypsum on managing the temperature. S1W12 had a variance of 162.0 while S2W12 had a variance of 3296.3, with a difference between the variances of 3134.3.

Similarly, the low variance of the treated stockpile indicates that the temperature fluctuation in the stockpile was very low compared to the high fluctuations of the control stockpile. This further indicates the effectiveness of gypsum to manage the temperature of the coal stockpiles. The test statistic absolute value of 3.6 was obtained from the analysis. Since the test statistic value is greater than the critical value, the outcome of the treatment results occurred due to gypsum. Hence, it is concluded that gypsum treatment affected the temperature of the treated stockpile.

4.4.8 East side temperature variations of the treated and control stockpiles at 12h00

In Figure 4.32, both stockpiles have the same temperature of 58^0C on day 1. Their temperature decreased to 41^0C for the treated stockpile and 48^0C for the control stockpile on day 2. They exhibited a similar increase in temperature trends with fluctuations until day 8. The temperature of the control stockpile increased from 50^0C on day 8 to a maximum temperature of 219^0C on day 12, then decreased from day 12 to 67^0C on day 15. During the same period, the temperature of the treated stockpile decreased from 42^0C on day 8 to the lowest temperature of 20^0C on day 14, then increased to 48^0C on day 15. While the temperature of the treated stockpile increased from 48^0C on day 15 to 50^0c on day 17, the temperature of the control stockpile decreased from 67^0C on day 15 to 65^0C on day 16. The temperature of the control stockpile increased from day 16 to 122^0C on day 20, then decreased to 57^0C on day 22. The temperature of the treated stockpile decreased from 50^0C on day 17 to a final temperature of 42^0C on day 22. The treated stockpile was not affected by spontaneous combustion, while the control stockpile was affected by spontaneous combustion from day 8.

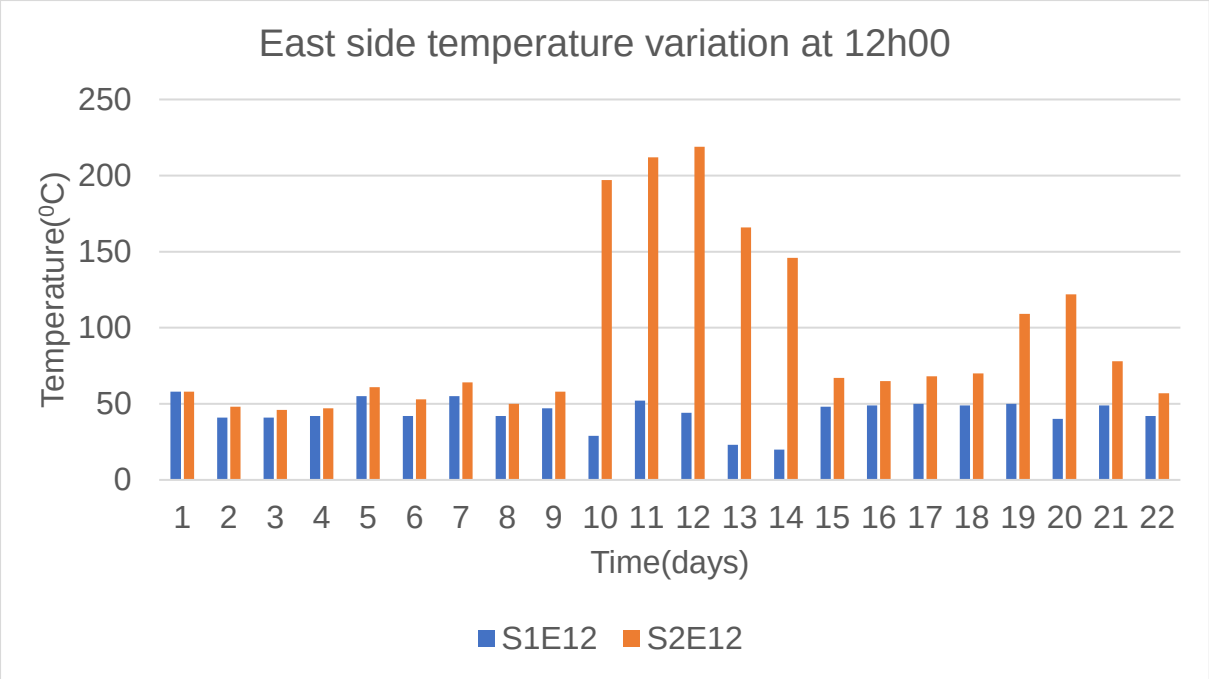

Figure 4.32 East side temperature variation at 12h00

Table 4.7 *t*-test for east side at 12h00

t-test: Two-samples assuming unequal variances		
	Stockpiles	
	S1E12	S2E12
Mean	44.0	93.7
Variance	93.6	3253.7
Observations	22.0	22.0
Degree of freedom(df)	22.0	
T Stat	-4.0	
P(T<=t) two-tail	0.0	
T Critical two-tail	2.1	

Table 4.8 represent the statistical analysis of the east side of the treated stockpile (S1E12) and the control stockpile (S2E12). S1E12 has a mean of 44 while S2E12 has a mean of 93.7, with a mean difference of 49.7. The low mean of the S1E12 indicates that the temperature measurements made daily and hourly for the study's duration

were lower than the higher temperature measurements of the S2E12. It further affirms that gypsum application on the treated stockpile was effective to manage the temperature. S1E12 has a variance of 93.6, while S2E12 has a variance of 3253.7, with a difference between the variances of 3160.0. The low variance of the treated stockpile indicates that the application of gypsum effectively managed the temperature fluctuation in the stockpile. The test statistic absolute value of 4.0 was obtained from the statistical analysis. Since the test statistic value is greater than the critical value, the outcome of the treatment results occurred due to gypsum. Hence, it is concluded that gypsum treatment affected the temperature of the treated stockpile.

4.4.9 West side temperature variations of the treated and control stockpiles at 14H00

In Figure 4.33, both stockpiles have the same temperature of 58^0C on day 1. The temperature of the control stockpile increased slightly to 65^0C on day 5, while the temperature of the treated stockpile decreased to 57^0C on day 3, increasing to 65^0C on day 5. On day 5, both stockpiles have the same temperature of 65^0C, and they maintain a similar trend with the control stockpile at 2^0C higher than the treated stockpile until day 9. The control stockpile increased from 50^0C on day 9 to a maximum temperature of 235^0C on day 11, then decreased to 64^0C on day 15. On the other hand, the treated stockpile decreased from 50^0C on day 9 to the lowest 19^0C before increasing to 60^0C on day 15. The treated stockpile maintained 60^0C from day 15 with slight fluctuation to the final day 22 at 60^0C. The control stockpile increased gently from 64^0C on day 15 to 72^0C on day 18, then it increased sharply to 208^0C on day 20, dropping to a final temperature of 78^0C on day 22. The observation shows that the treated stockpile did not experience spontaneous combustion while the control stockpile experienced spontaneous combustion from day nine.

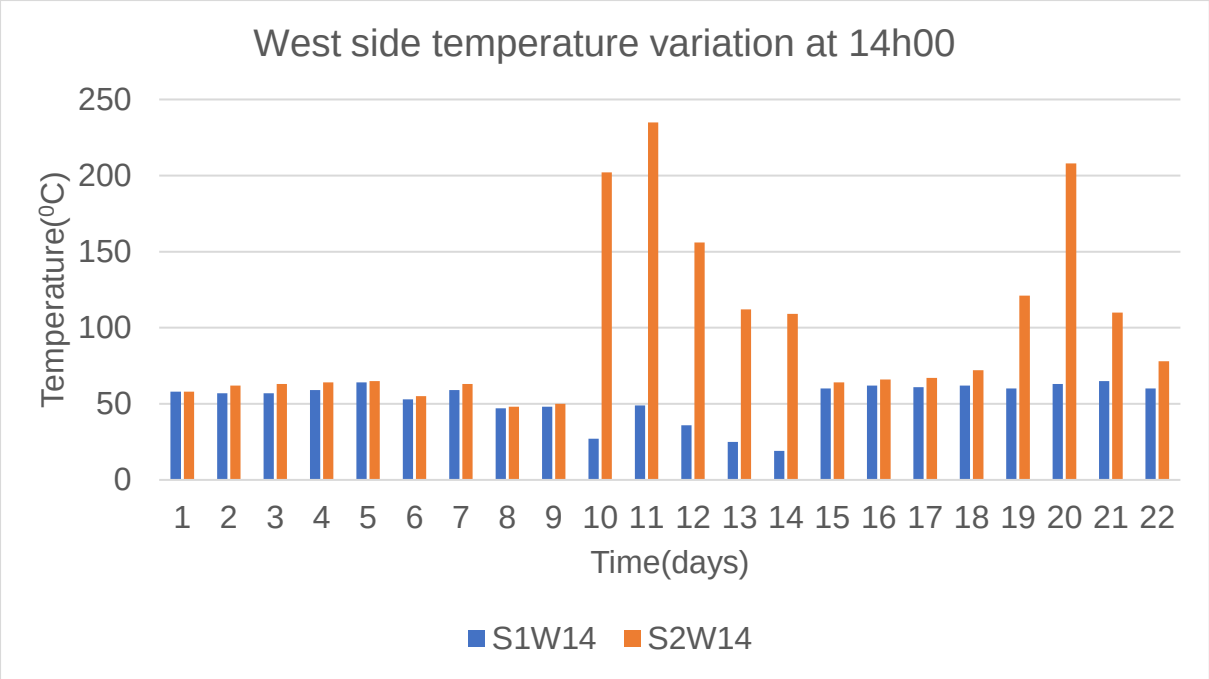

Figure 4.33 West side temperature variation at 14h00

Table 4.8 *t*-test for west side at 14h00

t-test: Two-samples assuming unequal variances		
	Stockpiles	
	S1W14	S2W14
Mean	52.3	96.7
Variance	182.8	3069.7
Observations	22.0	22.0
Degree of freedom(df)	23.0	
T Stat	-3.7	
P(T<=t) two-tail	0.0	
T Critical two-tail	2.1	

Table 4.9 represent the statistical analysis of the west side of the treated stockpile (S1W14) and the control stockpile (S2W14). S1W14 has a mean of 52.3, while S2W14 has a mean of 96.7, with a mean difference of 44.4. The lower mean of the S1W14 indicates that the daily and hourly temperature measurements were lower than the S2W14 measured taken simultaneously. These lower temperature measurements are attributed to the effectiveness of gypsum application in managing the temperature of coal stockpiles. S1W14 has a variance of 182.8, while S2W14 has a variance of 3069.7, with a difference between the variances of 2886.9. The low-temperature variance on the treated stockpile indicates the effectiveness of gypsum in managing the spontaneous combustion of coal stockpiles. The test statistic absolute value of 3.7 was obtained from the statistical analysis. Since the test statistic value is greater than the critical value, the outcome of the treatment results occurred due to gypsum. Hence, it is concluded that gypsum treatment affected the temperature of the treated stockpile.

4.4.10 East side temperature variation of the treated and control stockpiles at 14h00

Figure 4.34 represents the east side temperature variations of the treated stockpile (S1E18) and control stockpile (S2E18). The stockpiles started at the same temperature of 58^0C on day 1, and the treated stockpile decreased to 53^0C while the control temperature increased to 62^0C on day 2. The control stockpile maintained the same temperature until day 5. The temperature decreased from 62^0C to 50^0C on day 8, while the treated stockpile increased from 53^0C to 56^0C on day 5, decreasing to the lowest 19^0C on day 14 with fluctuation between the days. The treated stockpile increased from 14^0C to 49^0C on day 15, while the control stockpile increased sharply from 50^0C to 249^0C on day 12. The control stockpile decreased from 249^0C on day 12 to 68^0C on day 15, decreasing gently to 64^0C on day 18. The treated stockpile decreased gently from 49^0C on day 15 to the final temperature of 41^0C on day 22. The control stockpile increased sharply from 64^0C on day 18 to 136^0C on day 20, dropping to a final temperature of 57^0C on day 22. The observation indicates that spontaneous combustion did not affect the treated stockpile, while the control stockpile was affected by spontaneous combustion from day nine.

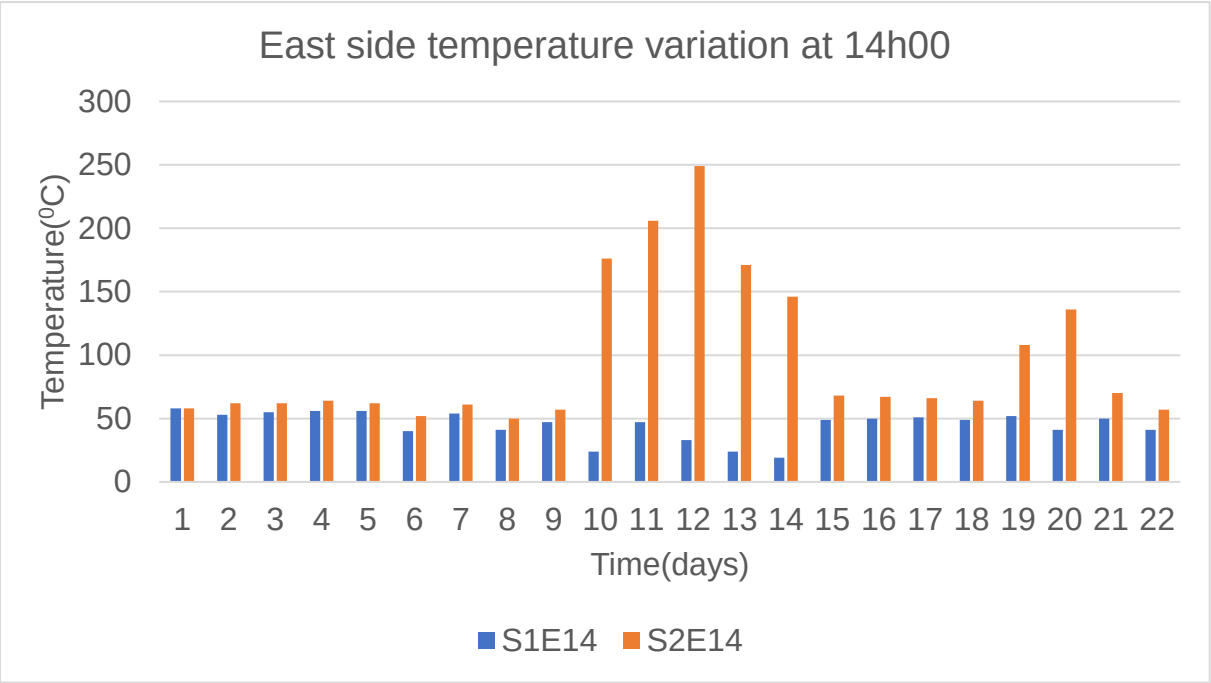

Figure 4.34 East side temperature variation at 14h00

Table 4.9 *t*-test for east side at 14h00

t-test: Two-samples assuming unequal variances		
	Stockpiles	
	S1E14	S2E14
Mean	45.0	96.0
Variance	124.1	3345.6
Observations	22.0	22.0
Degree of freedom(df)	23.0	
T Stat	-4.1	
P(T<=t) two-tail	0.0	
T Critical two-tail	2.1	

Table 4.10 represents the statistical analysis of the east side of the treated stockpile (S1E14) and the control stockpile (S2E14). S1E14 has a mean of 45.0, while S2E14 has a mean of 96.0, with a mean difference of 51.0. The lower mean on S1E14 indicates that the temperature measurements taken daily and hourly were lower than

the temperatures of the control stockpile taken simultaneously. This indicates that the application of gypsum on the treated stockpile was effective in managing the temperature. S1E14 has a variance of 124.1, while S2E14 has a variance of 3345.7, with a variance difference of 3221.5. The lower variance of the treated stockpile indicates that the application of gypsum effectively managed the daily and hourly temperature fluctuation of the treated stockpile compared to the control stockpile. The test statistic absolute value of 4.1 was obtained from statistical analysis. Since the test statistic value is greater than the critical value, the outcome of the treatment results occurred due to gypsum. Hence, it is concluded that gypsum treatment affected the temperature of the treated stockpile.

4.4.11 West side temperature variations of the treated and control stockpiles at 16h00

Figure 4.35 represents the west side temperature variations of the treated stockpile (S1W16) and control stockpile (S2W16). The temperature of both stockpiles on day 1 of the study was 58^0C. The control stockpile increased gently from day 1 to 67^0C on day 5, while the treated stockpile increased to 60^0C on day 5. Both stockpiles decreased from day 5 to 50^0C on day 9. The control stockpile increased sharply from day 9 to a maximum temperature of 235^0C on day 11, decreasing sharply to 113^0C on day 13. It then gently decreased to 111^0C on day 14, decreasing sharply to 66^0C on day 15. The treated stockpile decreased from 50^0C on day 9 to the lowest temperature of 19^0C on day 14 with minor fluctuations in between, and then it increased to 61^0C on day 15. The treated stockpile decreased from 61^0C on day 15 to 59^0C on day 22. The control stockpile increased sharply from 66^0C on day 17 to 213^0C on day 20, then decreased sharply to a final temperature of 77^0C on day 22. The treated stockpile was not affected by spontaneous combustion, while the control stockpile was affected by spontaneous combustion from day nine.

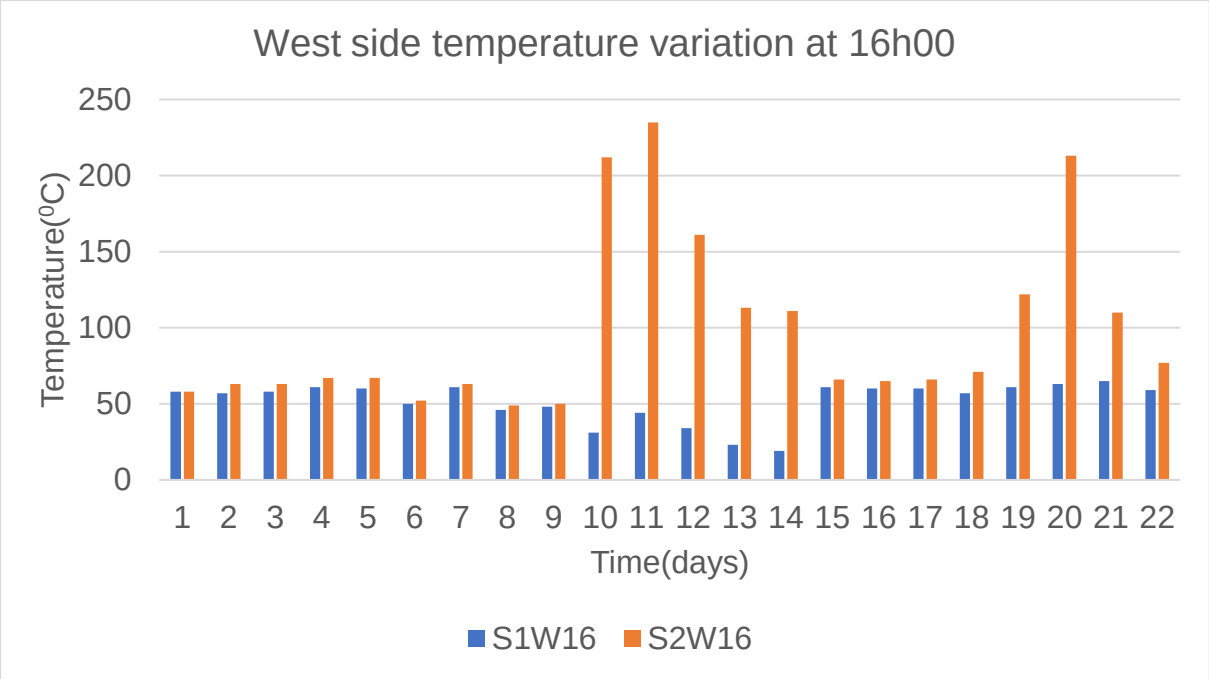

Figure 4.35 West side temperature variation at 16h00

Table 4.10 *t*-test for west side at 16h00

t-test: Two-samples assuming unequal variances		
	Stockpiles	
	S1W16	S2W16
Mean	51.6	97.9
Variance	180.4	3257.0
Observations	22.0	22.0
Degree of freedom(df)	23.0	
T Stat	-3.7	
P(T<=t) two-tail	0.0	
T Critical two-tail	2.1	

Table 4.11 represent the statistical analysis of the west side of the treated stockpile (S1W16) and the control stockpile (S2W16). S1W16 has a mean of 51.6, while S2W16 has a mean of 97.9, with a mean difference of 46.3. The lower mean of the S1W16 indicates that the daily and hourly temperature measurements were lower than the

S2W16, which has a higher mean. It also affirms that the application of gypsum on the coal stockpile effectively managed the coal stockpile's temperature. S1W16 has a variance of 180.4, while S2W16 has a variance of 3257.0, with a difference between the variances of 3076.6. The lower variance of the treated stockpile indicates that the application of gypsum was effective in managing the temperature fluctuations on the treated stockpile. The test statistic absolute value of 3.7 was obtained from the statistical analysis. Since the test statistic value is greater than the critical value, then the outcome of the treatment occurred due to gypsum. Hence, it is concluded that gypsum treatment affected the temperature of the treated stockpile.

4.4.12 East side temperature variations of the treated and control stockpiles at 16h00

Figure 4.36 represents the east side temperature variations of the treated stockpile (S1E16) and control stockpile (S2E16). Both stockpiles started with the same temperature of 58^0C on day 1. The control stockpile increased to 65^0C on day 2, while the treated stockpile decreased to 56^0C on day 2. From day 2, the control stockpile increased by 1^0C to 66^0C on day 4, decreasing to 49^0C on day 8. The treated stockpile increased from 56^0C on day 2 to 58^0C on day 4, from which it decreased to the lowest 18^0C after some fluctuations. It then increased sharply to 49^0C on day 15. The control stockpile decreased after fluctuations to 49^0C on day 8, increased sharply to a maximum temperature of 246^0C on day 12, and decreased sharply to 70^0C on day 15. The control stockpile decreased gently from 70^0C on day 15 to 57^0C on day 19 before it increased sharply to 139^0C, dropping to the final temperature of 57^0C on the last day of the study. The treated stockpile decreased gently from 49^0C on day 15 to the final temperature of 40^0C on day 22. The treated stockpile was not affected by spontaneous combustion, while the control stockpile was affected by spontaneous combustion from day nine.

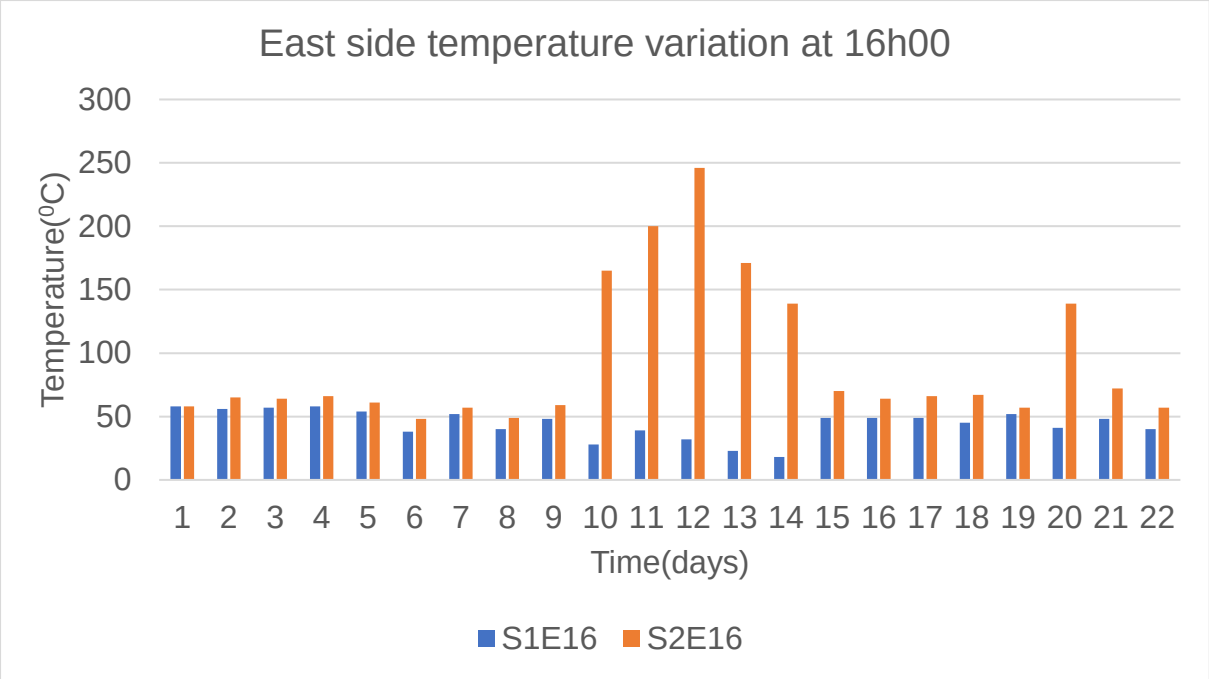

Figure 4.36 East side temperature variation at 16h00

Table 4.11 *t*-test for east side at 16h00

t-test: Two-samples assuming unequal variances		
	Stockpiles	
	S1E16	S2E16
Mean	44.3	92.7
Variance	126.6	3199.1
Observations	22.0	22.0
Degree of freedom(df)	23.0	
T Stat	-3.9	
P(T<=t) two-tail	0.0	
T Critical two-tail	2.1	

Table 4.12 represent the statistical analysis of the east side of the treated stockpile (S1E16) and the control stockpile (S2E16). S1E16 has a mean of 44.3, while S2E16 has a mean of 92.7, with a mean difference of 48.5. The lower mean of the S1E16 indicates that the daily and hourly temperature measurements were lower than the

S2E16. It also affirms that the application of gypsum on coal stockpiles was effective in managing the temperature. S1E16 has a variance of 126.6, while S2E16 has a variance of 3199.1. S1E16 and S2E16 have the difference between the variances of 3072.5. The lower variance of the treated stockpile indicates that the application of gypsum was effective in preventing high-temperature fluctuations compared to the control stockpile. The test statistic absolute value of 3.9 was obtained from statistical analysis. Since the test statistic value is greater than the critical value, the outcome of the treatment results occurred due to gypsum. Hence, it is concluded that gypsum treatment affected the temperature of the treated stockpile.

4.5 Temperature variations of the treated stockpile.

Figure 4.37 represent the temperature variations of a treated stockpile. The side treated two times is indicated by S1E and is on the east side of the stockpile, while the side treated once is indicated by S1W, and it was on the West side of the stockpile. Both sides of the stockpile started at the same temperature of 58^0C on day 1 of monitoring. The east side decreased to 49^0C, while the west side decreased to 53^0C on day 2. The temperature of both sides increased from day 2, with the west side at a higher temperature than the east side. On day 5, the east side increased from 49^0C to 56^0C, while the west side increased from 53^0C to 63^0C. Both stockpiles experienced fluctuations in temperature from day 5. The west side decreased from 63^0C on day 5 to the lowest temperature of 20^0C on day 14.

Similarly, the east side decreased from 56^0C on day 5 to the lowest temperature of 20^0C on day 14. On day 14, both sides had the same temperature of 20^0C. Both sides experienced a sharp rise in temperature from 20^0C on day 14, with the west side attaining a 61^0C on day 16 while the east side attained a maximum temperature of 50^0C on day 17. The temperature of the east side decreased from 50^0C on day 17 to the final temperature of 41^0C on day 22, with fluctuation between the days. The west side maintained 61^0C from day 16 to day 22 with major fluctuations. The west side attained a maximum temperature of 64^0C, while the east side attained a maximum temperature of 56^0C. The side treated two times with gypsum experienced the lowest temperature compared to the side treated once and the control stockpile.

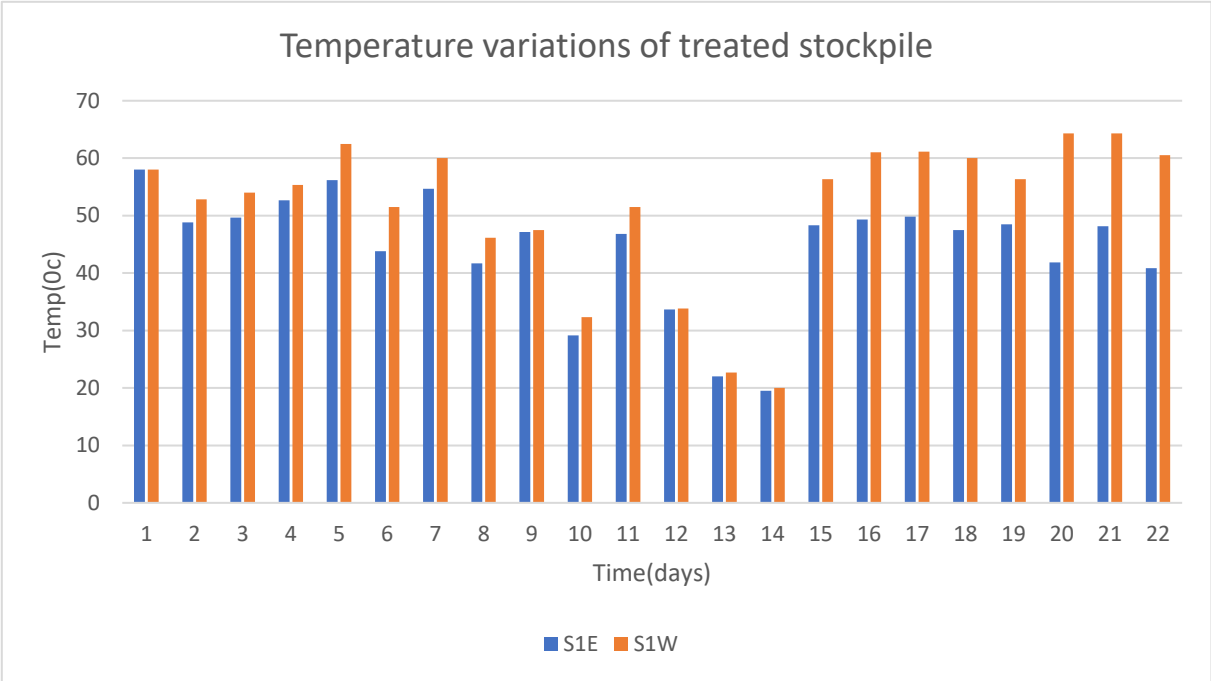

Figure 4.37 Temperature variations of treated stockpile

Table 4.12 *t*-test for treated stockpile

t-test: Two-samples assuming unequal variances		
	Stockpiles	
	S1E	S1W
Mean	44.5	51.5
Variance	103.1	167.6
Observations	22.0	22.0
Degree of freedom(df)	40.0	
T Stat	-2.0	
P(T<=t) two-tail	0.0	
T Critical two-tail	2.0	

Table 4.13 represent the statistical analysis of the east side of the treated stockpile (S1E) and the west side of the treated stockpile (S1W). S1E has a mean of 44.5, while S1W has a mean of 51.5, with a mean difference of 7.0. The lower mean of S1E

indicates that the daily and hourly temperature measurements on that side were lower than S1W measurements. It also indicates that as the concentration of gypsum increases, the spontaneous combustion of coal stockpiles decreases. S1E has a variance of 103.1, while S1W has a variance of 167.6, with the difference of the variance of 64.5. The lower variance of the S1E indicates that the temperature fluctuations were lower compared to S1W. This indicates that the higher the concentration of gypsum, the lower the temperature fluctuations. The significance level of 0.05 on a two-tailed test resulted in the test statistic critical value of 2.0. The test statistic absolute value of 2.0 was obtained from the statistical analysis. This indicates that the higher concentration of gypsum reduces the spontaneous combustion of coal stockpiles. Pure gypsum is known to have high resistance to elevated temperatures, and it retains its original strength at 400^0C (Dolezelova, et al., 2018). This could explain the low temperature observed on the treated stockpile.

4.6 Description of the highest temperature on the control stockpile

Figure 4.38 illustrates the highest temperatures measured on points A1 and A6 of the control stockpile. Point A1 was on the west side, while point A6 was on the east side of the control stockpile. The control stockpile started burning on day 9 at a temperature of 554^0C, as illustrated in Figure 4.38, while the treated stockpile did not burn throughout the entire study. The highest temperature at 660^0C was recorded on day 11 of the study.

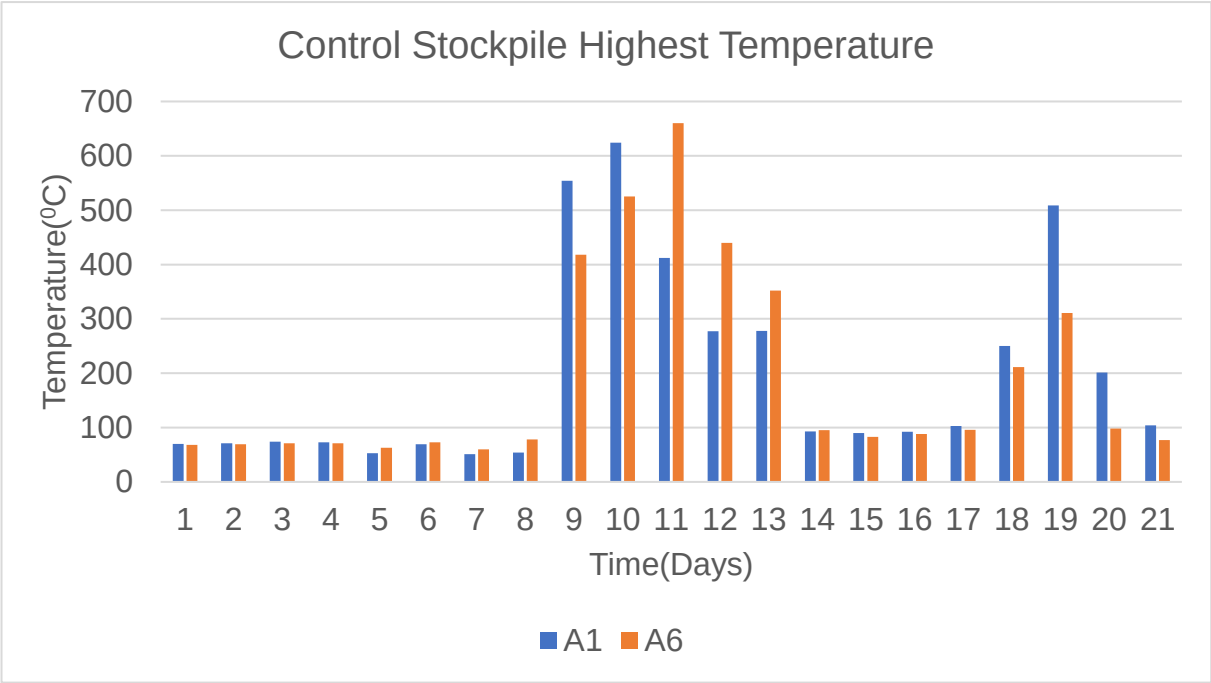

Figure 4.38 Control stockpile highest temperatures

4.7 Summary

This chapter discussed the results obtained from the treatment of stockpiles with gypsum. The graphical representation of temperature trends for each day of recorded measurements as illustrated from Figure 4.1 to Figure 4.38 was discussed, including an explanation of the observations. The t-test table for the holes and stockpile sides, as illustrated in Table 4.1 to Table 4.13, was also discussed. The temperature of the stockpiles and the atmospheric temperature have shown similar trends for the first nine days of the experiment. The stockpile temperature on day 1 was 58^0C, while the atmospheric temperature on day 1 was 14^0C. After day 9 of the study, a rapid increase in temperature was observed on the west side of the control stockpile, while the treated stockpile showed a slight decrease in temperature. The rapid temperature rise could be attributed to the thermal runaway and wind-driven forced convection of coal stockpiles since spontaneous combustion occurred

The statistical analysis was conducted on the same sides of the stockpiles to determine the significance of gypsum on managing the spontaneous combustion of coal stockpiles. Gypsum had a significant effect on the spontaneous combustion of coal stockpiles. A similar comparison was made on the different sides of the treated

stockpile. It was found that as the concentration of gypsum is increased, the temperature variability is decreased significantly. The variance of the same side of the stockpiles between treated and control stockpiles differed by more than 3000 while the mean differences were more than 40^0C. This indicated that gypsum is effective in managing the spontaneous combustion of coal.

5 RESULTS AND DISCUSSION OF IN-HOLE TEMPERATURE

5.1 Introduction

This chapter deals with the analysis of the in-hole temperature before and after treatment with gypsum.

- Hole H1 was treated twice with a higher concentration of gypsum;
- Hole H2 was treated once with a lower concentration of gypsum;
- Hole H3 was not sprayed with gypsum for it to serve as a control hole against which the other two holes are compared.

A 64-channel thermocouple and TEMCO thermometer were used to collect data on all the holes daily for 22 days, on which day 1 data was collected before the application of gypsum. The *t*-test statistical analysis of data is discussed to highlight the significance of gypsum in managing spontaneous combustion of hot-holes. A graphical representation of results is also shown for all the measurements taken.

5.2 In-hole temperature variations

Figure 5.1 represent the temperature changes of the holes observed over 22 days. The holes are 16m deep measurements were taken down the hole at 1m intervals. The temperature reflected on the graph represents the average temperatures measured daily from 06h00 in the morning to 16h00 in the evening from the 21st August 2020 to the 10th September 2020.

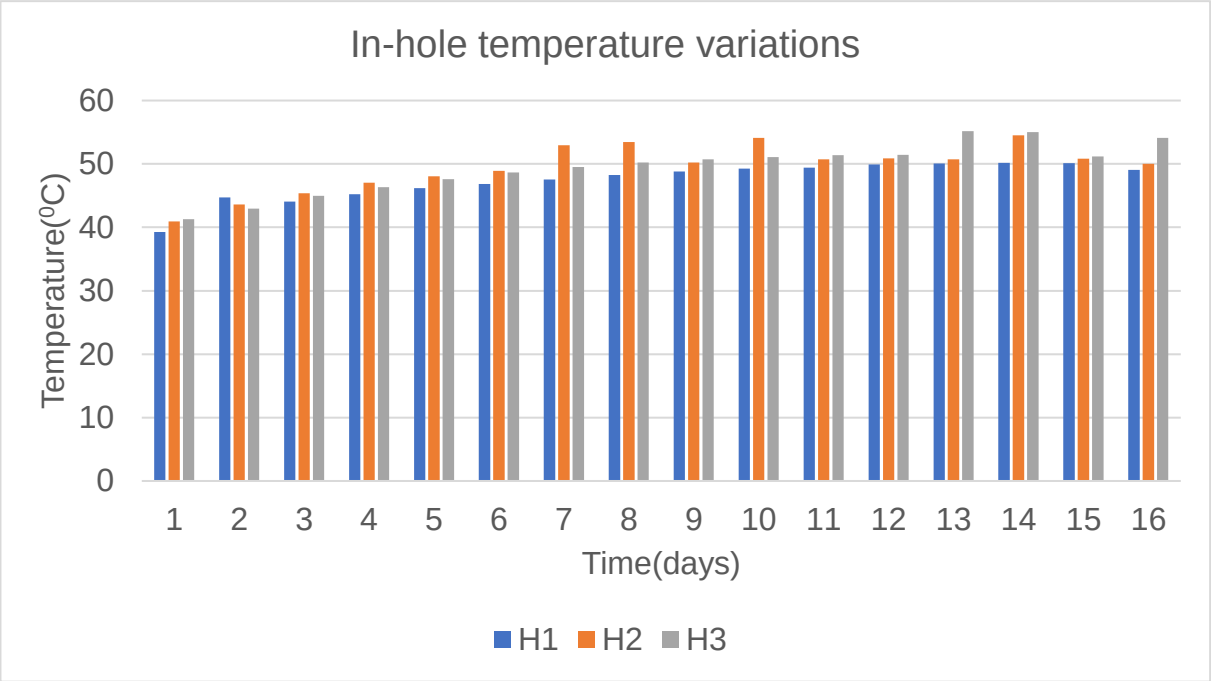

Figure 5.1 In-hole temperature variations

On day 1, all holes were measured to establish the initial temperature. H1 measured 39^{0}C, H2 measured 41^{0}C after the treatment with gypsum and H3 measured 41^{0}C. The temperature of H1 was the lowest at 1m below the collar, and it increased rapidly to 45^{0}C at 2m below the collar. The H2 temperature at 1m depth was slightly lower than the control hole; however, H2 experienced a rapid increase in temperature and exceeded the temperature of the control hole at a depth of 1.5m. At 2m depth, all treated holes had a higher temperature than the control hole. H1 measured 45^{0}C, H2 measured 44^{0}C, and H3 measured 43^{0}C. H1 temperature decreased beyond the temperature of H2 and H3 at 3m depth in which H1 measured 44^{0}C, H2 measured 45^{0}C, and H3 measured 45^{0}C. The temperature of H2 remained slightly above the control hole H3.

All holes had a similar increase in temperature from 3m depth to 6m depth. From 6m depth, the temperature of H2 increased sharply from 49^{0}C at 6m to 53^{0}C at 7m. The temperature of H3 increased from 49^{0}C at 6m to 50^{0}C at 7m depth, and the H1 temperature increased from 47^{0}C at 6m to 48^{0}C at 7m depth. The temperature of the control hole increased at a higher rate than the treated holes from 4m to 12m depth. From 7m depth, the temperature of H2 increased slightly from 53^{0}C at 7m to 53.4^{0}C at

8m depth. The temperature of H1 increased from 48^0C at 7m depth to 48^0C at 8m depth, while H3 increased from 49^0C at 7m to 50^0C at 8m depth.

The temperature of H2 decreased sharply from 53^0C at 8m depth to 50^0C at 9m depth while the temperature of H1 increased from 48^0C at 8m to 49^0C at 9m depth, and the temperature of H3 increased from 50^0C at 8m to 51^0C at 9m depth. Although the temperature of H2 decreased to a lower temperature than the control hole, the temperature of the control hole and H1 increased between 8m and 9m depths. From 9m depth, the temperature of H2 increased sharply from 50^0C to 54^0C at 10m depth. During the same depth increment, H1 and H3 maintained the same temperature of 49^0C and 51^0C, respectively. The temperature of H2 decreased from 54^0C at 10m depth to 51^0C at 11m depth while H1 maintained the same temperature of 49^0C and H3 maintained the same temperature of 51^0C. At 11m depth, H1 and H2 had temperatures below the control hole H3.

The temperature of H1 increased from 49^0C at 11m to 50^0C at 12m, while the temperature of H2 remained the same at 51^0C. The temperature of H3 remained the same at 51^0C, although it was higher than the temperature of the treated holes. The temperature of H3 increased sharply from 12m depth to a maximum temperature of 55^0C at 13m depth. On the other hand, H1 and H2 maintained the same previous temperatures of 50^0C and 51^0C, respectively. The temperature of H2 increased sharply from 51^0C at 13m to the maximum temperature of 55^0C, while H3 maintained the same previous temperature of 55^0C and H1 maintained the temperature of 50^0C.

From 14m depth, H2 and H3 decreased from the same temperature of 55^0C to 51^0C, while H1 maintained the previous temperature of 50^0C. From 15m depth, the control hole temperature increased to 54^0C while H2 decreased from 51^0C to 50^0C. The temperature of H1 decreased from 50^0C at 15m to 49^0C at 16m. Throughout the temperature at each 1m interval, the temperature of the holes increased, with H1 treated twice exhibiting a slow constant rise in temperature than H2 and H3.

Table 5.1 *t*-test for H1 and H3

t-test: Two-samples assuming unequal variances		
	Stockpiles	
	H1	H3
Mean	47.4	49.8
Variance	8.8	16.3
Observations	16.0	16.0
Degree of freedom(df)	28.0	
T Stat	-1.6	
P(T<=t) two-tail	0.0	
T Critical two-tail	2.0	

Table 5.1 represents the t-test statistical analysis of holes H1 and H3. The test statistic of samples assuming unequal variance was used to assess the significance of gypsum in managing in-hole temperature. H1 has a mean of 47.4, while H3 has a mean of 49.5, with a difference of 2.1. The lower mean of the treated hole indicates that the temperature measurements of the treated hole were lower than the measurements of the control hole. This difference could be attributed to the application of gypsum in the hole. H1 has a variance of 8.8, while H3 has a variance of 16.3, with a difference between variances of 7.4. The lower temperature variance of the treated hole indicates that the in-hole temperature fluctuations of H1 were lower than H3. Since H1 was treated twice with gypsum, it is concluded that gypsum reduced the in-hole temperature. The test statistic absolute value of 1.6 was obtained from the statistical analysis. It is concluded that although the higher concentration of gypsum reduced the in-hole temperature fluctuations, it was not significant in managing the temperature of the hole.

Table 5.2 *t*-test for H2 and H3

t-test: Two-samples assuming unequal variances		
	Stockpiles	
	H2	H3
Mean	49.5	49.5
Variance	14.4	16.3
Observations	16.0	16.0
Degree of freedom(df)	30.0	
T Stat	0.0	
P(T<=t) two-tail	1.0	
T Critical two-tail	2.0	

Table 5.2 represents the statistical analysis of the temperature of the treated hole H2 and the control hole H3. Hole H2 has a mean of 49.5, while H3 has a mean of 49.5, with a mean difference of 0.0. H2 has a variance of 14.4, while H3 has a variance of 16.3, with a difference between the variances of 1.9. The lower variance of H2 can be attributed to gypsum application. The test statistic absolute value of 0.0 was obtained from the statistical analysis. It is concluded that a lower concentration of gypsum was not effective in managing the in-hole temperature of H2.

Table 5.3 *t*-test for H1 and H2

t-test: Two-samples assuming unequal variances		
	Stockpiles	
	H1	H2
Mean	47.4	49.5
Variance	8.8	14.4
Observations	16.0	16.0
Degree of freedom(df)	28.0	
T Stat	-1.7	
P(T<=t) two-tail	0.1	
T Critical two-tail	2.0	

Table 5.3 represent the statistical analysis of the in-hole temperature of hole H1, which was treated twice with gypsum, and hole H2, which was treated once with gypsum. H1 has a mean of 47.4, while H2 has a mean of 49.5, with a mean difference of 2.1. The lower mean of H1 indicates that the in-hole temperature was lower as compared to H2. H1 has a variance of 8.8, while H2 has a variance of 14.4, with a variance difference of 5.6. The lower variance on H1 indicates that the in-hole temperature fluctuations were lower compared to H2. It is concluded that the higher the gypsum concentration in the hot-hole, the lower the temperature fluctuations. The test statistic absolute value of 1.7 was obtained from the statistical analysis. Although the test statistic value obtained is smaller than the critical value, gypsum's overall effectiveness in managing the in-hole temperature was low, gypsum was effective in managing the in-hole temperature fluctuation.

5.3 Summary

This chapter indicated the graphical representation of measured temperature on each day for 22 days, on which day one represented the temperature measurements before the treatment of the holes with gypsum. A statistical analysis of the measurements was also done to assess the significance of gypsum in managing the in-hole temperature and spontaneous combustion. Although the 1.7 test statistic value is lower than the critical value, gypsum was still effective in managing the in-hole temperature variations.

6 CONCLUSIONS AND RECOMMENDATIONS

6.1 Conclusion

Coal mining in the Witbank area of Mpumalanga Province in South Africa is heavily affected by the self-heating of coal and coal shales. During drilling, charging, blasting, loading, transportation, stockpiling, and coal processing, these problems are encountered. Khwezela Colliery has experienced a loss of coal due to spontaneous combustion. In order to manage these incidents caused by spontaneous combustion, a solution to use gypsum in managing in-hole temperature and coal stockpiles was evaluated.

On coal stockpiles, test statistic assuming sample of unequal variances was used to assess the significance of gypsum on the coal stockpiles and a significance level of 0.05 was chosen and found that:

- The significance level of 0.05 resulted in the test statistic critical value of 2.1 for comparisons of the same sides of the stockpiles.
- The significance level of 0.05 resulted in the test statistic's critical value of 2.0 when comparing the east and west sides of the treated stockpile.
- Gypsum was effective in managing the spontaneous combustion of coal stockpiles.
- The absolute value of test statistics for comparisons of the same sides of the stockpiles ranged from 3.6 to 4.3.
- The test statistic critical value for comparing the sides of the treated stockpile was 2.0 when a confidence level of 0.05 was used. The treated stockpile produced an absolute value of test statistic of 2.0.
- The control stockpile started burning on day nine at a temperature of 554^0C. However, the highest temperature of the stockpile was 660^0C during day 11. The sharp rise in temperature of the control stockpile could be attributed to the thermal runaway point of the coal stockpile being reached such that uncontrollable spontaneous combustion occurred.
- The statistical analysis and graphical representation have shown that the temperature of the treated stockpile was lower than the temperature of the control stockpile.

- The statistical analysis and graphical representation show that the treated stockpile had a lower temperature than the control stockpile on the west side.
- The east side of the treated stockpile had a lower temperature than the west side of the treated stockpile. This affirms that a higher concentration of gypsum on the stockpile has a higher spontaneous combustion management ability.
- Based on the statistical analysis performed on the data, gypsum had a significant effect on the spontaneous combustion of stockpiles.
- The control stockpile experienced spontaneous combustion, while the treated stockpile did not experience spontaneous combustion throughout the study.
- A higher concentration of gypsum was found to reduce the temperature fluctuations of the stockpile significantly.

On hot-holes, the following observations were noted:

- The absolute value of test statistics obtained from comparing the holes ranged from 0.0 to 1.7. These absolute values of the test statistic are lower than the test statistic critical value of 2.0.
- The higher concentration hole produced a higher absolute value of test statistic.
- Therefore, it is concluded that a higher concentration of gypsum used on H1 reduced the in-hole temperature fluctuations.

6.2 Recommendation

The study was based on a 60T stockpile. It is recommended that a larger stockpile be used to evaluate the effectiveness of gypsum. In addition, the characterization of coal and gypsum must be determined.

Three holes were drilled on a relatively small area of the mine which would be drilled and blasted within six months as per the production schedule. It is recommended that the study be done on a larger area after characterization of coal with more holes and allowed for a longer duration.

6.3 Limitation of study and future research work

The duration of the experimentation was limited because of the costs and production requirements. The experiment had to be completed before production machinery started to work on the experimental area. The study was also limited by the imposition of the covid-19 lockdown in March 2020. The imposition resulted in a delay to deliver the spray machine from the University of the Witwatersrand, while at the same time production at the mine was ongoing.

7 REFERENCES

Akgun, F. & Essenhigh, R., 2001. Self-ignition characteristics of coal stockpile : theoretical prediction from a two-dimestional unsteady-state model. *Fuel,* Volume 80, pp. 409-415.

Arisoy, A. & Beamish, B., 2015. Reaction kinetics of coal oxidation at low temperatures. *Fuel,* Volume 159, pp. 412-417.

Banerjee, S., 2000. *Prevention and Combating Mine Fires,*: IBH Publishing.

Barve, S. & Mahadevan, V., 1994. *Prediction of spontaneous heating liability of Indian coals based on proximate constituents.* Poland, In Proceedings of 12th International Coal Preparation Congress. 23-27 May 1994.

Beamish, B. & Hamilton, G., 2005. Effects of moisture content on the R70 self-heating rate of callide coal. *Internation Journal of Coal Geology,* Volume 64, pp. 133-138.

Beamish, B., Lin, Z., Beamish, R., 2012. Investigating the influence of reactive pyrite on coal self-heating, in Naj Aziz and Bob Kininmonth (eds.), Proceedings of the 2012 Coal Operators' Conference, Mining Engineering, University of Wollongong, 18-20 February 2019.

Belmiloudi, A., 2005. Mathematical and numerical analysis of dehydration of gypsum plasterboards exposed to fire. *Applied Mathematical Computing,* Volume 163(3), pp. 1023-1041.

Bhattacharyya, K., 1971. The role of absorption of water vapour in the spontaneous heating of coal. *Fuel,* Volume 50, pp. 367-380.

Carras, J., 1994. Self heating of coal and related materials:models,application and tests. *Program Energy and Computer Science,* Volume 20(1), pp. 1-15.

Carras,J. & Young,B., 1994. Self-heating of coal and related materials:Models,application and test methods. *Progress in Energy and Combustion Sciecne,* Volume 20(1), pp. 1-15.

Choudhury, N., Boral, P., Mitra, T. & Adak, A., 2007. Assessment of nature and distribution of inertinite in Indian coals for burning characteristics. *International Journal of Coal Geology,* Volume 72(2), pp. 141-152.

Cliff, D., Rowlands, D. & Sleeman, J., 1996. *In spontaneous combustion in Australian underground coal mines..* Brisbane, Safety in Mines Testing and Research Station. New Edition.

Deng, J., Huang, H. & Jin, Y., 2013. Experiment on low temperature oxidation characteristics of high-sulphur coal in high humidity environment. *Coal Mine Safety,* Volume 44, pp. 32-35.

Department of Mineral Resources, 2009. *dmr.gov.za.* [Online] Available at: https://www.dmr.gov.za/LinkClick.aspx?fileticket=kpgLoOGqGDs%3D&portalid=0[Accessed 6 December 2020].

Dullien, F., 1979. Porous media fluid transport and pore structure. *Series E : applied Sciences,* Volume 202, p. 9.

Eroglu, H., 1992. *Factors affecting spontaneous combustion liability index,* Johannesburg: University of the Witwatersrand. PhD Thesis.

Fuqiang, Y., 2019. Determination of the influence of pyrite on coal spontaneous combustion by thermodynamics analysis.. *Process Safety and Environmental Protection,* Volume 129, pp. 163-167.

Genc, B., Cook, A., 2015. Spontaneous combustion risk in South African coalfields. *Journal of the Southern African Institute of Mining and Metallurgy*, Volume 117, pp. 563-568.

Ghazi, K., 2007. Gypsum board in fire modelling and experimental validation. *Journal of Fire Science,* Volume 25(3), pp. 267-282.

Gong, B., Pigrams, P.S., Lamb, R.N., 1998. Surface studies of low-temperature oxidation of bituminous vitrain bands using XPS and SIMS. Fuel, Volume 77, pp. 1081-1087.

Hancox, P. & Gotz, A., 2014. South Africa's Coalfields : A perspective. *International Journal of Geology,* Volume 132, pp. 170-254.

Hansel, W., Krause, V., Hoffer, U., 2004. Self-ignition of solid material including dust. *Handbook of Explosion Prevention and Protection*, Volume 1, pp. 227-256.

Hsieh, K. & Wert, C., 1985. Direct determination of organic sulphur in coal. *Fuel,* Volume 64(2), pp. 255-261.

Huffman, G. & Huggins, F., 1985. Comparative sensitivity of various analytical techniques to the low-temperature oxidation of coal. *Fuel,* Volume 64, pp. 849-856.

Humphreys, D., 1979. *A study of the propensity of Queensland coals to spontaneous combustion,* Brisbane: University of Queensland.

Kim, A., 2004. Cryogenic injection to control a coal waste bank fire. *International Journal of Coal Geology,* Volume 1(2), pp. 63-73.

Kucuk, A., Kadioglu, Y., Gulaboglu, M., 2003. A study of the spontaneous combustion characteristics of a Turkish lignite: Particle size, moisture of coal, humidity of air. *Combustion and Flame*, Volume 133(3), pp. 255-261

Lain, A., 2009. *Assessment of spontaneous heating susceptibility of coals using differental thermal analysis,* Rourkela: National Institute of Technology Rourkela. PhD Thesis.

Liodakis, S., Barkirtzis, D., Lois, E. & Gakis, D., 2002. The effect of Ammonium hyposulphate and ammonium sulphate on the spontaneous ignition properties of pinus halepensis pine needles. *Journal of Fire Safety,* Volume 37(5), pp. 481-494.

Li, Q., Xiao, Y. & Zhong, K., 2020. Overview of commonly used materials for coal spontaneous combustion prevention. *Fuel,* Volume 275, pp. 117-981.

Maree, k., 2014. *First steps in research.* 15th Edition. Pretoria: Van Schaik.

Mastalerz, M., Drobniak, A., Hower, J. & O'Keefe, J., 2010. Spontaneous combustion and coal petrology. *Coal-Geology and Combustion,* Volume 1, pp. 47-62.

Miningdata, 2019. *Mingdataonline* [Online] Available at: https://miningdataonline.com/property/1289/Khwezela-Operation.aspx [Accessed 17 December 2019].

Mohalik, N., Panigrahi, D. & Singh, V., 2010. An investigation to optimise the experimental parameters of differential scanning calorimetry method to predict the susceptability of coal to spontaneous combustion. *Archives of Mining Science,* Volume 55, pp. 669-689.

Nimaje, D. & Tripathy, D., 2016. Characterization of some Indian coals to assess their liability to spontaneous combustion. Fuel, Volume 16(3), pp. 139-147.

Olivella, M., Palacious, J. & Vairavamurthy, A., 2002. Astudy of sulphur functionalities in fossil fuels using destructive (ASTM and Py-GC-MS) and non-desructive (SEM-EDX-XANES and XPS) techniques. *Fuel,* Volume 81, p. 405.

Onifade, M., 2018. *Spontaneous combustion of coals and coal shales in the South African coalfields,* Johannesburg: University of the Witwatersrand (PhD Thesis).

Onifade, M. & Genc, B., 2018a. A review of spontaneous combustion studies. *International Journal of Mining, Reclamation and Environment,* Volume 3(8), pp. 527-547.

Onifade, M. & Genc, B., 2018b. Modelling spontaneous combustion liability of carbonaceous materials. *International Journal of Coal Science and Technology,* Volume 5, pp. 191-212.

Onifade, M. & Genc, B., 2018c. Spontaneous combustion of coals and coal-shales. *International Journal of Mining Science and Technology,* Volume 28(6),pp. 933-940.

Onifade, M. & Genc, B., 2019a. Spontaneous combustion liability of coal and coal-shale: A review of prediction methods. *International Journal of Coal Science and Technology,* Volume 6, pp. 151-168.

Onifade, M. & Genc, B., 2019b. *Ash,Volatile Matter and Carbon Content Influence on Spontaneous Combustion Liability of Coal-Shales.* Switzerland, Springler Science and Bussiness Media.

Onifade, M. & Genc, B., 2019c. Spontaneous combustion liability of coal and coal-shales: a review of prediction methods. *International Journal of Coal Science and Technology,* Volume 6, pp. 151-168.

Onifade, M. & Genc, B., 2020. A review of research on spontaneous combustion of coal. *International Journal of Mining Science,*Volume 30(3), pp. 303-311.

Onifade, M., Genc, B. & Bada, S., 2020. Spontaneous combustion liability between coal seams: A thermogravimetric study. *International Journal of Mining Science and Technology.* Volume 30(5),pp. 691-698.

Onifade, M., Genc, B. & Carpede, A., 2018. A new apparatus to establish the spontaneous combustion propensity of coals and coal-shales. *International Journal of Mining Science and Technology,* Volume 28, pp. 151-168.

Onifade, M., Genc,B., Gbadamosi,A.R., Morgan,A., Ngoepe,T., 2021. Influence of antioxidants on spontaneous combustion and coal properties. *Process Safety and Environmental Protection,* Volume 148, pp. 1019-1032.

Onifade, M., Genc, B. & Wagner, N., 2019. Influence of organic and inorganic properties of coal-shale on spontaneous combustion liability. *International Journal of Mining Science,* Volume 29(6), pp. 851-857.

Ozdeniz, A., Sivrikaya, O. & Sensogut, C., 2015. Investigation of spontaneous combustion of coal in undeground coal mining : In Mine Planning and Equipment Selection. *Springer International Publishing Switzwerland,* Volume 7, p. 61.

Phillips, H., Chabedi, K. & Uludag, S., 2011. *Best Practice Guidelines for South African Collieries,* Johannesburg,pp1-129.

Pinheiro, R., 1999. *A techno-economic and historical review of South African coal industry in the 19th century.* Johannesburg, Bulletin, p. 113.

Ray, S. & Singh, R., 2007. Recent developments and practices to control fire in underground coal mines. *Journal of Fire Technology,* Volume 43(4), pp. 285-300.

Ren, L., Li, Q., Deng, J. & Xiao, Y., 2019. Inhibition of carbon dioxide on the oxidative combustion thermodynamics of coal. *Journal of RSC Andvances,* Volume 9(70), pp. 41-126.

Ren, T., Edwards, J. & Clarke, D., 1999. Adiabatic oxidation study on the propensity of pulverized coal to spontaneous combustion. *Fuel,* Volume 78, pp. 1611-1620.

RS Mineral Insulated Thermocouples, 2020. *docs.rs-online.com.* [Online] Available at: https://docs.rs-online.com/96d5/0900766b815e5302.pdf [Accessed 26 September 2020].

RS Thermocouple Selection Guide, 2020. *za.rs-online.com.* [Online] Available at: https://za.rs-online.com/web/p/thermocouples/6212271/ [Accessed 26 September 2020].

Sahu, H., Panigrahi, D. & Mishra, N., 2004. Assessment of heating susceptability of coal seams by differential scanning calorimetry. *Journal of Mines,Metals and Fuels,* Volume 52(7-8), pp. 117-121.

Said, K., Onifade, M., Lawal, A. & Githiria, J., 2020. Computational intelligence-based models for predicting the spontaneous combustion liability of coals. *International Journal of Coal Preparation and Utilization,* Volume 40(12).

Scott, A., 2002. Coal Petrology and the origin of coal macerals. *International Journal of Coal Geology,* Volume 50(4), pp. 119-134.

Shi, B. & Zhou, F., 2014. Impact of heat and mass transfer during the transportation of nitrogen in coal porous media on coal mine fires. *The Scientific World Journal,* Volume 29, pp. 31-42.

Sipila, J. & Auerkari, P., 2012. Risk and mitigation of self-heating and spontaneous combustion in underground mines. *Journal of Loss Prevention in the Process Industries,* Volume 25, pp. 617-622.

Smith, D. & Whittaker, R., 1986. Mineral deposit of south Africa. *The Geological Society of South Africa,* Volume 2, pp. 1969-1984.

Smith, R., 1980. *Inhibiting spontaneous combustion of coal.* United States of America, Patent No. 41993,25,1980.

Snyman, C., 1998. Coal in South Africa. *Journnal of African Earth Sciences,* Volume 16, pp. 171-180.

Srinivasan, K. & Pradeep, K., 1996. Modelling spontaneous combustion in coal stockpiles. *Fuel,* Volume 75(3), pp. 353-362.

Stach, E., Mackowsky, M., Teichmuller, M. & Taylor, G., 1982. *Texbook of Coal Petrology.* 3rd ed. Berlin: Gerbruder Borndraeger.

Sujanti, W. & Zhang, D., 2000. Investigation into the role of inherent inorganic matter and additives in low-temperature oxidation of a Victorian brown coal. *Combustion Science and Technology,* Volume 152(1), pp. 99-114.

Sunjati, W. & Zhang, D., 1999. A laboratory study of spontaneous combustion of coal, the influence of inorganic matter and reactor size. *Fuel,* Volume 78, pp. 549-556.

Taraba, B. & Michalec, Z., 2014. CFD simulation of the effect of wind on the spontaneous heating of coal stockpiles. *Fuel,* Volume 118, pp. 107-112.

Taylor, S., 1984. *Introduction to Qualitative Research Methods.* Third ed. New Jersey: Canadian Center of Science and Education.

Thomas, G., 2002. Thermal properties of gypsum plasterboards at high temperatures. *British Association for the advancement of Science.,* Volume 26(1), pp. 37-45.

Tsai, Y., Yang, Y., Wang, C. & Shu, C., 2017. Comparison of the inhibition mechanism of five types of inhibitors on spontaneous combustion of coal. *International Journal of Energy Research,* Volume 42, pp. 1158-1171.

Uludag, S., 2007. A visit to research on Wits-EHAC Index and it's relationship to inherent coal propoerties for Witbank coalfields. *The South African Institute of Mining and Mettallurgy,* Volume 107, pp. 671-679.

Wade, L., Gouws, M. & Phillips, H., 1987. *An apparatus to establish the spontaneous combustion propensity of South African coals.* Pretoria, Centre for Scientific and Industrial Research.

Wakili, E., 2007. Gypsum board in fire modeling and experimental validation. *Journal of Fire Science,* Volume 25(3), pp. 267-282.

Wang, C., Yang, Y. & Tsai, Y., 2016. Spontaneous combustion in six types of coal by using the simultaneous thermal analysis-fourier transform infrared spectroscopy technique. *Environmental Modelling and Software,* Volume 76, pp. 1-12.

Wang, D. & Dou, G., 2014. An experimental approach to selecting chemical inhibitors to retard the spontaneous combustion of coal. *Fuel,* Volume 117, pp. 218-223.

Weber, B., 2011. Heat transfer mechanisms and models for a gypsum board exposed to fire. *International Journal of Heat and Mass Transfer,* Volume 55, pp. 1661-1678.

Wen, H., Zhang, F., Jin, Y. & Liu, W., 2015. Experimental research on the effect of sulphur on characteristic parameters of coal spontaneous combustion. *Journal of Surface Coal Mines,* Volume 42, pp. 5-7.

Xiao, Y., Ren, S. & Deng, J., 2018. A comparative analysis of thermokinetic behavior and gesous products between first and second coal spontanous combustion. *Fuel,* Volume 227, pp. 325-33.

Yan, F., Lai, Y. & Song, Y., 2019. Determination of the influence of pyrite on coal spontaneous combustion by thermodynamic analysis. *Process Safety and Environmental Protection,* Volume 129, pp. 163-167.

Yang, S., 1996. Experimental study and mechanism analysis of calcium hydroxide as a retarder of high-sulphur coal. *Journal of China University of Mining and Technology,* Volume 4, pp. 68-72.

Zang, Y., Yang, C., Li, Y. & Huang, Y., 2019. Ultrasonic extraction and oxidation characteristics of functional groups during coal spontaneous combustion. *Fuel,* Volume 94, pp. 242-287.

Zheng, L., 2010. Test and analysis on salty retardants performance to restrain coal oxidized spontaneous combustion. *Coal Science and Technology,* Volume 38, pp. 70-72.

Zhu, H., Song, Z. & Tan, B., 2013. Numerical investigation and theoretical prediction of self-ignition characteristics of coarse coal stockpiles. *Journal of Loss Prevention in the Process Industries,* Volume 26, pp. 236-244.

8 APPENDIX

Appendix A: Khwezela Colliery spontaneous combustion

Figure 8.1: Khwezela Colliery spontaneous combustion

Appendix B: Control stockpile burning in day nine

Figure 8.2: Control stockpile burning day 9

Appendix C: Control stockpile burned area

Figure 8.3: Control stockpile burned ash

Appendix D: Temperature measurements of coal the stockpiles

21/08/2020

	S1	S2	S1	S2	S1	S2	S1	S2	S1	S2	S1	S2
A1	60	65	64	68	53	54	47	56	62	70	65	70
A2	48	51	54	56	50	59	50	58	56	62	54	63
A3	41	48	43	49	50	54	48	50	52	55	53	57
A4	40	49	44	50	41	48	40	44	49	54	52	58
A5	48	58	41	64	51	48	40	43	50	64	54	69
A6	52	55	56	67	55	56	43	58	61	68	62	68

22/08/2020

	S1	S2	S1	S2	S1	S2	S1	S2	S1	S2	S1	S2
A1	62	68	66	70	55	56	50	55	65	71	67	71
A2	49	50	55	58	53	60	51	59	56	63	56	64
A3	42	49	45	49	51	53	50	48	51	54	52	55
A4	41	48	43	49	44	47	41	42	50	53	50	56
A5	50	48	42	63	52	46	42	41	53	62	56	68
A6	51	56	55	68	58	58	41	56	62	70	65	69

23/08/2020

	S1	S2	S1	S2	S1	S2	S1	S2	S1	S2	S1	S2
A1	65	70	65	72	56	55	51	56	69	73	70	74
A2	51	54	55	60	55	61	53	59	57	64	59	68
A3	41	50	44	50	52	51	50	49	50	55	53	59
A4	41	51	44	51	46	45	40	42	50	56	52	57
A5	53	62	59	64	58	44	45	42	55	63	57	69
A6	52	70	64	70	60	62	40	57	63	72	65	71

24/08/2020

	S1	S2	S1	S2	S1	S2	S1	S2	S1	S2	S1	S2
A1	68	75	70	75	71	78	69	73	70	73	65	73
A2	63	65	63	66	64	67	63	65	63	66	61	67
A3	53	56	55	60	57	60	57	57	58	56	55	60
A4	48	56	47	56	48	53	46	52	48	54	48	53
A5	60	61	59	65	59	63	57	61	58	60	54	60
A6	65	75	64	76	65	71	63	71	62	73	61	71

25/08/2020

	S1	S2	S1	S2	S1	S2	S1	S2	S1	S2	S1	S2
A1	54	68	54	65	55	62	51	57	51	56	47	53
A2	49	55	48	56	57	60	55	59	54	56	51	54
A3	47	50	43	49	54	55	54	54	53	52	51	49
A4	47	46	47	46	45	48	44	47	43	43	42	39
A5	51	53	49	55	39	47	39	46	39	45	37	42
A6	54	74	55	74	43	67	42	65	37	67	35	63

26/08/2020

	S1	S2	S1	S2	S1	S2	S1	S2	S1	S2	S1	S2
A1	62	64	63	73	68	68	64	71	61	68	65	68
A2	57	62	59	61	61	65	62	67	59	63	62	64
A3	51	56	54	58	56	60	59	62	57	58	57	58
A4	51	54	52	57	50	56	52	56	50	53	49	47
A5	56	59	57	61	54	60	54	59	54	56	51	52
A6	61	77	62	78	59	78	59	77	57	75	57	73

27/08/2020

	S1	S2	S1	S2	S1	S2	S1	S2	S1	S2	S1	S2
A1	48	53	47	53	46	53	46	53	47	53	48	51
A2	46	48	47	48	46	48	46	49	47	48	46	49
A3	45	44	44	45	45	43	45	49	46	43	45	47
A4	41	42	40	44	40	41	40	43	40	44	39	43
A5	43	46	43	45	41	44	41	46	41	46	40	45
A6	45	61	43	62	44	62	44	60	43	60	41	60

28/08/2020

	S1	S2	S1	S2	S1	S2	S1	S2	S1	S2	S1	S2
A1	51	51	54	55	53	56	52	56	52	57	51	54
A2	44	44	44	49	50	47	46	48	47	47	47	49
A3	41	40	45	46	45	44	44	45	46	46	45	48
A4	43	43	45	44	44	44	44	47	44	44	46	47
A5	48	49	47	51	47	51	47	51	47	50	49	51
A6	48	76	52	77	50	76	50	77	50	78	48	78

29/08/2020

	S1	S2	S1	S2	S1	S2	S1	S2	S1	S2	S1	S2
A1	40	525	36	537	32	533	30	536	28	547	30	554
A2	38	38	33	34	30	32	29	32	27	32	30	43
A3	34	34	34	33	38	34	37	35	27	28	32	39
A4	32	32	30	34	30	35	33	34	25	27	28	36
A5	33	38	33	37	28	36	27	33	24	36	30	41
A6	35	549	33	534	29	537	28	524	24	465	26	418

30/08/2020

	S1	S2	S1	S2	S1	S2	S1	S2	S1	S2	S1	S2
A1	57	633	58	583	61	608	62	593	51	607	48	624
A2	52	50	53	57	57	59	60	54	51	51	46	44
A3	44	44	44	47	49	51	50	48	45	46	38	36
A4	35	47	43	46	47	53	44	44	44	41	35	36
A5	44	52	49	53	53	59	54	49	47	48	40	38
A6	45	482	55	458	59	504	59	544	51	530	43	525

31/08/2020

	S1	S2	S1	S2	S1	S2	S1	S2	S1	S2	S1	S2
A1	24	391	24	409	34	426	35	420	37	382	34	412
A2	31	31	28	38	34	41	45	53	37	43	35	35
A3	31	30	29	47	36	46	47	59	35	43	34	35
A4	30	28	29	44	37	43	45	54	34	42	33	34
A5	28	36	29	44	35	40	43	52	32	46	31	44
A6	29	660	27	507	36	526	44	550	33	660	32	660

01/09/2020

	S1	S2	S1	S2	S1	S2	S1	S2	S1	S2	S1	S2
A1	20	263	20	244	20	284	21	275	23	276	22	277
A2	21	40	21	34	22	30	24	33	25	35	23	36
A3	22	24	22	24	23	25	26	27	26	26	25	26
A4	22	22	22	24	23	24	25	26	26	25	25	25
A5	19	45	20	42	21	44	23	43	23	47	23	47
A6	19	498	20	420	20	459	22	428	23	440	22	440

02/09/2020

	S1	S2	S1	S2	S1	S2	S1	S2	S1	S2	S1	S2
A1	20	273	20	264	20	272	19	280	19	273	18	278
A2	21	35	20	33	20	32	19	37	19	30	18	30
A3	22	24	22	24	21	24	21	24	20	24	20	24
A4	22	24	22	23	21	23	21	23	20	23	20	23
A5	20	43	20	42	20	42	19	42	19	41	18	43
A6	19	426	19	422	19	391	19	372	18	373	17	352

03/09/2020

	S1	S2	S1	S2	S1	S2	S1	S2	S1	S2	S1	S2
A1	64	86	64	88	63	89	66	93	67	90	68	93
A2	48	50	51	52	51	54	52	53	52	53	54	55
A3	42	47	44	48	47	49	59	49	60	50	60	51
A4	47	48	48	49	49	51	49	51	51	52	53	54
A5	44	57	46	64	46	57	45	56	45	59	48	60
A6	49	91	50	89	51	91	49	93	50	94	46	95

04/09/2020

	S1	S2	S1	S2	S1	S2	S1	S2	S1	S2	S1	S2
A1	69	93	68	95	68	91	69	89	68	92	66	90
A2	56	55	55	57	55	55	53	55	56	56	54	54
A3	57	52	60	52	62	51	57	50	61	51	60	51
A4	51	54	49	53	51	53	52	52	49	53	50	52
A5	47	59	48	59	46	59	45	57	48	58	45	58
A6	50	94	52	95	51	90	49	87	54	91	51	83

05/09/2020

	S1	S2	S1	S2	S1	S2	S1	S2	S1	S2	S1	S2
A1	67	89	69	91	70	91	68	91	69	93	68	92
A2	54	56	55	58	54	57	56	56	53	56	53	55
A3	60	52	61	52	60	53	61	53	61	51	59	50
A4	51	53	51	53	53	55	52	55	52	53	51	53
A5	43	58	46	59	48	59	47	59	48	57	45	58
A6	51	90	54	83	52	88	52	89	52	88	51	88

06/09/2020

	S1	S2	S1	S2	S1	S2	S1	S2	S1	S2	S1	S2
A1	66	103	67	109	67	110	68	114	69	103	64	103
A2	55	60	60	61	58	61	61	61	61	59	56	58
A3	55	56	56	55	55	58	53	57	57	54	51	51
A4	48	56	50	54	50	56	50	58	50	53	49	50
A5	42	58	43	60	43	61	44	61	45	57	39	55
A6	49	82	52	91	51	89	52	91	51	82	46	96

07/09/2020

	S1	S2	S1	S2	S1	S2	S1	S2	S1	S2	S1	S2
A1	60	189	62	181	64	221	68	245	69	248	70	250
A2	50	53	54	58	53	60	58	61	61	61	60	61
A3	44	49	42	49	47	56	49	57	51	55	52	55
A4	43	51	42	53	45	57	49	54	51	53	53	56
A5	43	57	44	59	46	62	49	61	49	61	48	61
A6	49	157	49	162	50	210	52	211	56	211	56	

08/09/2020

	S1	S2	S1	S2	S1	S2	S1	S2	S1	S2	S1	S2
A1	69	533	65	534	65	527	63	520	64	498	63	509
A2	69	69	67	65	64	67	66	66	65	67	65	68
A3	66	63	62	59	63	59	60	59	61	59	62	61
A4	52	53	50	52	51	50	49	50	50	52	50	51
A5	35	57	37	54	33	54	31	54	33	55	32	55
A6	45	303	43	315	42	301	40	263	41	302	42	311

09/09/2020

	S1	S2	S1	S2	S1	S2	S1	S2	S1	S2	S1	S2
A1	67	204	68	206	69	201	71	203	70	202	68	201
A2	64	72	65	85	67	73	67	73	66	67	66	71
A3	56	59	56	59	60	61	60	61	59	60	60	59
A4	50	53	49	53	50	58	53	56	52	55	51	56
A5	43	62	39	60	43	65	42	65	42	63	40	63
A6	50	93	50	94	50	103	53	114	55	92	52	98

10/09/2020

	S1	S2	S1	S2	S1	S2	S1	S2	S1	S2	S1	S2
A1	61	103	59	104	58	107	60	107	58	106	57	104
A2	64	71	63	69	64	73	64	70	63	71	62	70
A3	60	57	58	58	60	58	59	57	58	57	58	57
A4	46	45	46	49	47	49	47	48	45	48	46	46
A5	33	45	33	46	34	47	36	47	35	46	34	48
A6	42	74	40	74	44	75	42	76	44	76	41	77

Appendix E: Temperature measurements of coal the holes

10/09/2020

																			Average/metre/hole		
	H1	H2	H3	H1	H2	H3	H1	H2	H3	H1	H2	H3	H1	H2	H3	H1	H2	H3	H1	H2	H3
1	39.2	44	43.7	42.3	44.6	44.2	41.5	42.5	41.4	45	44.5	44.2	42.4	44.3	44.3	41.4	45.1	44.3	42	44	44
2	43.2	45.8	45.7	45.1	46	45.5	43.7	44.2	43.7	45.6	46	45.6	44.9	46.2	45.5	43.4	46.6	45.7	44	46	45
3	44.4	47.1	46.4	46.2	41.5	47	44.9	45.1	45.7	46.2	47.2	46.8	45.6	47.5	46.7	44.4	47.7	46.6	45	46	47
4	45.9	48.3	47.6	46.7	48.6	48	46	47.8	47	46.6	48.4	47.8	46.4	48.6	47.6	45.3	48.7	48.2	46	48	48
5	46.6	49.1	48.5	47	49.3	49.1	46.7	48.9	48.1	47.1	49.3	49	47	49.6	48.7	46.4	49.1	49.1	47	49	49
6	47.3	49.6	49.4	47.5	49.8	50	47.5	49.5	49.2	47.6	50	50	47.6	50.2	49.5	47.2	49.9	49.7	47	50	50
7	47.7	50	50	48.3	50.3	50.5	48.1	50.1	50.2	48.1	50.3	50.4	48	50.6	50.4	47.8	50.4	50.2	48	50	50
8	48	50.5	50.4	48.5	50.6	51.2	48.5	50.6	50.7	48.3	50.6	50.9	48.5	51	50.9	48.2	50.8	50.8	48	51	51
9	48.4	50.8	51	48.7	51.1	51.4	48.8	51	51.2	48.7	51.1	51.4	48.7	51.3	51.2	48.8	51.1	51.1	49	51	51
10	48.9	51.2	51.2	49.1	51	51.6	49.2	51.1	51.5	49.1	51.2	51.5	49.2	51.5	51.4	49.3	51.5	51.5	49	51	51
11	49.3	51.2	51.4	49.5	51.3	51.6	49.4	51.3	51.6	49.4	51.4	51.6	49.4	51.7	51.6	49.4	51.4	51.6	49	51	52
12	49.5	51.4	51.4	49.6	51.3	51.7	49.3	51.4	51.8	49.6	51.6	51.8	49.6	51.6	51.6	49.7	51.6	51.7	50	51	52
13	49.5	51.5	51.5	49.7	51.4	51.6	49.6	51.5	51.9	49.5	51.4	51.8	49.7	51.6	51.9	49.8	51.6	51.8	50	52	52
14	49.6	51.4	51.5	49.9	51.3	51.7	49.7	51.1	51.7	49.7	51.5	51.7	49.8	51.5	51.8	49.8	51.6	51.7	50	51	52
15	49.4	51.1	51.4	49.8	51.2	51.6	49.5	51.5	51.6	49.4	51.3	51.7	49.8	51.4	51.7	49.8	51.4	51.5	50	51	52
16	49.5	50	51.2	49.6	50.8	51	49	51.6	51	47.9	51.2	51.3	49.5	51.3	51.3	48.9	51	50.7	49	51	51

09/09/2020

	H1	H2	H3	H1	H2	H3	H1	H2	H3	H1	H2	H3	H1	H2	H3	H1	H2	H3	H1	H2	H3
1	41.9	39.2	42.6	39	40	39	44.1	42	42.3	36.3	31.6	35.6	44.4	42.7	43.1	41.9	44.3	44.3	41	40	41
2	46.1	41.6	44.5	42.3	42.5	42.1	45.6	44.8	44.2	40	34.8	40	45.8	45	44.2	44.2	46	45.3	44	42	43
3	46.8	44.5	45.8	46	44.5	44.2	46.2	46.3	45.5	43.6	37.7	42	46.7	57	45.5	45.1	47.7	46.3	46	46	45
4	47.2	46.2	46.8	47.9	46.2	45.5	46.4	47.5	46.8	44.7	41.6	44.8	47.4	58.3	47	46	48.8	47.5	47	48	46
5	47.5	47.5	47.9	48.2	41.5	47	46.8	48.4	47.7	45.8	44.3	46.4	47.9	59	48	46.6	49.3	49.2	47	48	48
6	47.8	48.5	49.2	48.4	48.6	48.1	47.1	49.1	49	46.4	46.9	47.6	48.2	59.7	48.7	47.2	50	49.5	48	50	49
7	48.2	49.5	50	48.5	49.4	49.2	47.8	49.6	49.8	47.2	48.1	48.7	48.5	50.1	49.6	47.8	40.4	50	48	48	50
8	48.3	50.3	50.4	49	50	50	48.2	50	50.5	47.8	49.2	50	48.8	50.4	50.1	48.1	40.6	50.5	48	48	50
9	48.5	50.6	50.6	49.1	50.4	50.8	48.5	50.4	50.9	48.3	50	50.7	49	50.7	50.5	48.5	41.1	50.9	49	49	51
10	48.7	50.9	51.1	49.5	51	51.1	49.1	50.8	51.1	48.6	50.3	51.2	49.3	51.1	50.9	48.8	41.2	51.1	49	49	51
11	49	51	51.4	49.4	51.1	51.2	49.1	51	51.2	49.1	50.9	51.3	49.6	51.3	51.4	49.1	41.4	51.4	49	49	51
12	49.3	51.2	51.4	49.7	51.2	51.4	49.3	51.1	51.4	49.5	51.1	51.3	49.7	51.2	51.3	49.4	41.5	51.4	49	50	51
13	49.2	51.3	51.4	49.8	51.2	51.5	49.6	51	51.3	49.6	51.3	51.5	49.7	51.3	51.6	49.5	41.4	51.6	50	50	51
14	49.3	51.2	51.2	50.1	51.2	51.4	49.6	51	51.2	49.5	51.2	51.4	49.5	51.3	51.5	49.7	41.4	51.5	50	50	51
15	49.2	51.1	51	50.6	50.9	51.3	49.5	50.9	51.2	49.5	51.1	51	49.9	51.3	51.5	49.8	40.9	51.4	50	49	51
16	47.2	50	51	50.1	49.8	49.9	49.3	50.9	50.3	49.4	50.7	50	50.1	50.7	51.2	49.7	40.7	50.9	49	49	51

08/09/2020

	H1	H2	H3	H1	H2	H3	H1	H2	H3	H1	H2	H3	H1	H2	H3	H1	H2	H3	H1	H2	H3
1	47	39	43.9	39.1	41.9	42.6	40	41.4	40	39	40	41.1	39.1	41.7	41.2	39	43.4	42.1		41	41	42
2	47.4	41.6	44.2	41.7	43.7	44.1	43.2	43.6	42.6	42.7	42	43.5	41.8	44.3	43.2	43.1	45	44		43	43	44
3	47.6	43.7	45.6	43.9	45.9	45.4	45.3	45.5	43.6	44.7	44.5	44.7	45	45.7	44.9	45.4	46.5	45.5		45	45	45
4	47.8	45.8	46.9	45.1	47.3	46.4	45.7	46.9	45.5	45.4	46.3	46.1	45.8	47.2	46.6	46	47.8	46.7		46	47	46
5	48	46.7	48.1	46	48.6	47.9	46.3	48	47	46.4	47.9	47.6	46.7	48.4	47.5	46.5	48.6	48.1		47	48	48
6	48.5	48	49	46.6	49.1	48.8	46.9	48.9	48.1	41	48.8	48.5	47.3	48.7	48.8	47.3	49.1	49.2		46	49	49
7	48.7	48.7	49.5	47.1	49.6	49.6	41.4	49.5	48.9	47.5	49.7	49.6	47.8	49.4	49.8	47.7	49.6	49.7		47	49	50
8	48.6	49.5	50.2	47.8	50	50.2	48	49.9	49.7	47.9	49.8	50.1	48.3	49.8	50.3	48.1	50	50.3		48	50	50
9	49	50.1	50.5	48.4	50.3	50.7	48.3	50.4	50.2	48.5	50.4	50.8	48.7	50.3	50.8	48.7	50.5	50.6		49	50	51
10	49	50.4	50.8	48.7	50.6	51	48.8	50.9	50.7	48.9	50.7	51	49	50.7	51	49	50.8	51		49	51	51
11	49.4	50.3	50.7	48.9	50.8	51.2	49.3	51.1	51.1	49.1	50.8	51.2	49.4	50.9	51.2	49.1	50.9	51.1		49	51	51
12	49.5	50.6	50.8	49.1	51	51.5	49.4	51	51.3	49.3	51	51.4	49.4	51	51.5	49.2	51.1	51.4		49	51	51
13	49.4	50.7	51	49.4	50.9	51.4	49.3	51.2	51.2	49.4	51.2	51.4	49.5	51	51.5	49.3	51.1	51.5		49	51	51
14	49.4	50.7	50.8	49.5	51	51.3	49.4	51	51.1	49.5	51.1	51.4	49.6	51.1	51.3	49.5	51	51.3		49	51	51
15	49.4	50.8	50.4	49.5	50.5	51.2	49.2	50.9	51.1	49.4	50.8	51.2	49.6	51	51	49.6	51	51.3		49	51	51
16	48.3	50.4	48.9	49.5	49.7	51	47.3	50.7	50.5	48.6	51	50.3	49.1	50.8	51	49.6	50.8	51		49	51	50

07/09/2020

	H1	H2	H3	H1	H2	H3	H1	H2	H3	H1	H2	H3	H1	H2	H3	H1	H2	H3	H1	H2	H3
1	41.2	41	39.8	36.9	42	40.8	38.8	42.6	42.3	41.3	43.4	42.4	40.3	41.4	42.5	40.2	44.7	41.8		40	43	42
2	46	44.2	41.6	41.7	44.6	43.1	42.5	43.8	44	43.1	45.3	44.1	42.5	43.7	44	41.7	46.1	43.4		43	45	43
3	47	45	43.1	42.7	46.1	45.1	43.8	45.8	44.9	44	46.6	45.5	44	45.6	45.5	43.5	47.2	45.1		44	46	45
4	47.4	46.9	44.8	44	47.6	46.5	44.9	47.1	46.6	45.5	47.8	46.9	44.8	47	46.9	45	48.3	46		45	47	46
5	47.5	47.9	46.1	45.1	48	47.5	45.1	48.3	47.7	46.3	48.8	48	45.8	48.1	48	45.8	49.2	47.8		46	48	48
6	48	48.7	47.6	46.2	49	48.3	46.5	49	49	47.2	49.4	48.7	46.4	48.9	49.1	46.5	49.7	49		47	49	49
7	48.3	49.5	48.9	47.2	49.2	49.1	47.7	49.6	49.6	47.7	50	49.9	47.3	49.2	49.8	47.5	50	49.6		48	50	49
8	48.7	49.9	49.4	47.6	49.9	50.3	47.9	50.2	50.5	48.2	50.4	50.4	47.7	49.8	50.3	47.9	50.4	50.6		48	50	50
9	49	50.4	50	48.3	50	50.6	48.6	50.5	50.7	48.5	50.7	50.8	48.4	50.4	50.8	48.3	50.7	50.7		49	50	51
10	49.1	50.6	50.3	48.8	50.6	50.9	48.7	50.8	51.2	49.1	50.9	51.1	49	50.6	50.9	48.7	50.9	51.2		49	51	51
11	49.2	50.8	50.8	49.1	50.8	51.2	49.1	51.1	51.3	49.4	51	51.2	49.2	50.9	51.3	49	51.1	51.4		49	51	51
12	49.5	50.9	51	49.3	50.9	51.4	49.2	51	51.5	49.5	51.1	51.5	49.3	51.1	51.5	49.2	51.1	51.6		49	51	51
13	49.6	50.8	51	49.5	51	51.3	49.4	51.1	51.5	49.8	51.3	51.4	49.4	51.1	51.3	49.3	51	51.6		50	51	51
14	49.5	50.9	50.9	49.4	51	51.1	49.5	51.2	51.3	49.7	51.2	51.3	49.5	51	51.4	49.5	51	51.5		50	51	51
15	49.5	50.7	50.9	49.4	50.7	50.7	49.6	51.1	51	49.5	51.1	51.2	49.5	51.2	51.3	49.5	50.8	51.2		50	51	51
16	47.6	50.8	50	48.2	49.2	49.8	49.4	50.9	51.1	49.3	51.2	51	49.6	51	51.1	49.6	50.3	50.8		49	51	51

06/09/2020

	H1	H2	H3	H1	H2	H3	H1	H2	H3	H1	H2	H3	H1	H2	H3	H1	H2	H3	H1	H2	H3
1	37.4	39	41.7	36.3	42.6	42	40.4	43.1	43.2	39.1	41.8	41.2	40.2	43.8	40.6	38.3	42.4	38.1		39	42	41
2	40.5	41.9	43.4	38.7	44	43.8	42	45.2	45.2	45.1	43.9	43.2	41.2	45.4	42.6	41.9	43.8	40.9		42	44	43
3	43.1	44.4	44.9	41.1	46.1	45.6	43.7	46.8	46.5	45	45.8	45.1	43.3	47	44.3	43.4	46	43.8		43	46	45
4	44.2	46.1	46.3	43.4	47.5	46.6	44.9	47.7	47.4	46.2	47.4	46.2	45.1	48	46.1	44.9	47.2	45.2		45	47	46
5	45	47.3	47.2	45	48.3	47.9	45.6	48.8	48.9	46.7	48	47.9	45.9	48.6	47.7	45.9	48	46.9		46	48	48
6	45.9	48	48.1	45.7	49.3	49.1	46.8	49.3	49.7	47.2	49	48.9	46.6	49.3	48.5	46.6	49	48		46	49	49
7	46.8	48.5	49.1	46.6	50	50.2	47.2	49.6	50.3	40.9	49.5	50	47.3	49.9	49.6	47.5	49.5	49		46	50	50
8	47.1	49.3	49.6	47.4	50.1	50.8	48.2	50.3	50.6	48.3	50	50.5	48.1	50.4	50.5	48	50.1	49.9		48	50	50
9	47.7	49.7	49.8	47.8	50.5	51.1	48.8	50.6	51	48.8	50.4	51	48.6	50.7	51	48.5	50.6	50.5		48	50	51
10	48.3	49.9	50.4	48.4	50.8	51.3	49.1	51	51.1	49.1	50.6	51.3	49	50.9	51.2	49	50.1	51		49	51	51
11	48.6	50.3	50.6	48.6	51	51.5	49.3	51.1	51.3	49.4	50.9	51.5	49.2	51	51.4	49.2	51.1	51.2		49	51	51
12	48.9	50.4	50.8	48.8	51.1	51.6	49.5	51.2	51.4	49.6	51.1	51.6	49.3	51.1	51.7	49.3	51	51.5		49	51	51
13	48.9	50.5	50.7	49.2	51.1	51.7	49.6	51.1	51.4	49.4	51	51.6	49.6	51.3	51.7	49.2	51	51.4		49	51	51
14	49.1	50.5	50.6	49.4	51	51.5	49.6	51.1	51.3	49.6	51.1	51.4	49.7	51.2	51.6	49.6	51.1	51.6		50	51	51
15	49.1	50.4	50.4	49.3	51	51.4	49.5	50.9	51	49.3	51.1	51.2	49.6	51.2	51.4	49.4	50.9	51.4		49	51	51
16	49.2	50.3	50.1	49.1	50	51.3	49.2	50.6	50.4	47.7	50.6	49.8	49.2	50.1	49.5	48.9	50.6	50.5		49	50	50

05/09/2020

	H1	H2	H3	H1	H2	H3	H1	H2	H3	H1	H2	H3	H1	H2	H3	H1	H2	H3	H1	H2	H3
1	45.8	44	44.2	42.7	45.4	44.1	42.6	44.6	45.5	38.2	43.3	43	42.8	43.3	42.9	43.8	40.5	42.3		43	44	44
2	46.2	45.6	45.5	44.1	46.8	45.1	44	46	46.7	41.6	44.8	44.2	44.6	45	44.5	45	42.5	44.1		44	45	45
3	46.9	47.1	46.9	44.8	48	46.7	44.8	47.3	48.4	43.4	46.5	45.9	45.4	46.7	45.9	45.8	45	45.7		45	47	47
4	47	48	48.1	45.9	48.9	48.1	46	48.3	48.9	44.7	47.7	46.7	46.1	47.8	46.7	46.6	46.5	47		46	48	48
5	47.4	48.8	48.7	46.8	49.4	49.1	46.8	49	49.5	45.9	48.5	48.3	46.8	48.6	47.7	47	47.9	48		47	49	49
6	48.2	49.5	49.4	47.7	49.7	49.7	47.5	49.6	50.3	46.6	49.2	49.1	47.2	49.2	48.5	47.4	48.7	49.1		47	49	49
7	48.6	49.9	50.1	48	50.4	50.6	48.2	50.2	50.9	47.2	49.7	49.9	47.8	49.7	50	47.8	49.3	49.6		48	50	50
8	48.7	50.3	50.8	48.4	50.7	51	48.5	50.4	51.3	48	50.2	50.7	48.3	50	50.4	48.7	49.8	50.2		48	50	51
9	49.2	50.7	51.2	48.9	50.9	51.4	48.9	50.7	51.4	48.4	50.5	51	48.8	50.3	51.2	48.6	50.1	50.7		49	51	51
10	49.5	50.9	51.3	49.1	51.1	51.7	49.4	51	51.6	48.8	50.9	51.3	49.1	50.7	51.3	49	50.5	50.9		49	51	51
11	49.9	51	51.4	49.5	51.3	51.8	49.6	51.1	51.7	49.2	51.1	51.4	49.4	51	51.5	49.2	50.7	51		49	51	51
12	49.8	51.1	51.5	49.6	51.2	51.9	49.7	51.3	51.8	49.4	51.2	51.6	49.5	51.1	51.6	49.4	50.8	51.3		50	51	52
13	49.8	51.3	51.5	50	51.4	51.8	49.9	51.3	51.7	49.6	51.2	51.7	49.7	51.2	51.5	49.5	50.9	51.5		50	51	52
14	49.9	51.2	51.4	49.9	51.3	51.7	50.1	51.1	51.6	49.7	51.2	51.5	49.9	51	51.4	49.4	51	51.3		50	51	51
15	49.9	51.1	51.3	49.9	51.2	51.6	50.1	51.1	51.2	49.8	51	51.2	49.8	51	51.4	48.9	51	51.2		50	51	51
16	49.8	50.9	50.9	49.6	50.7	51.4	49.9	51.2	50.6	47.6	50.7	49.1	49.6	49.9	51	46	50.9	51		49	51	51

04/09/2020

	H1	H2	H3	H1	H2	H3	H1	H2	H3	H1	H2	H3	H1	H2	H3	H1	H2	H3	H1	H2	H3
1	45.6	43	44.4	44.6	46.5	44	44.1	46	44.2	42.7	45.6	43.6	44.2	43.4	44	43.1	44.2	43.5		44	45	44
2	46.6	45.3	45.4	46.4	47.1	45.5	45	47.2	45.7	44.1	46.8	44.7	44.9	44.9	45.1	44.7	45.7	44.5		45	46	45
3	47.2	47	47.2	46.8	48.5	46.9	45.9	48.4	46.4	45.1	48.4	46.2	45.6	46.7	46.3	45.3	46.9	46		46	48	47
4	47.6	48.1	48	47.5	49	48.3	47	49.3	47.4	46.1	48.8	47.2	46.4	47.9	47.7	45.8	48.3	47.4		47	49	48
5	48	49	49.2	47.7	49.8	49	47.5	49.5	48.7	46.9	49.3	48.2	46.9	48.9	48.7	46.4	48.9	48.6		47	49	49
6	48.3	49.7	50.1	48.3	50.2	50.2	48.2	49.9	49.9	47.6	49.8	49.4	47.5	49.6	49.5	47.3	49.4	49.3		48	50	50
7	48.7	502	50.4	48.7	50.7	50.8	48.5	50.4	50.4	48.3	50.2	50.2	48.2	50	50.2	47.6	50	49.9		48	126	50
8	49.1	50.7	51	49.1	50.9	51.2	49	508	50.9	48.7	50.6	50.6	48.7	50.4	50.8	48.2	50.4	50.5		49	127	51
9	49.2	51.1	51.3	49.4	51.2	51.7	49.3	51.1	51.3	49.1	50.8	50.9	49.1	50.8	51.2	48.6	50.7	51.1		49	51	51
10	49.6	51.2	51.5	49.8	51.4	51.8	49.7	51.2	51.7	49.4	51	51.5	49.3	51	51.5	49	51	51.2		49	51	52
11	49.8	51.4	51.7	50	51.5	52	49.7	51.4	51.8	49.6	51.2	51.6	49.5	51.2	51.4	49.4	51.1	51.4		50	51	52
12	50	51.3	51.6	49.9	51.5	52.1	49.9	51.4	51.9	49.7	51.2	51.7	49.7	51.3	51.5	49.7	51.2	51.4		50	51	52
13	50.2	51.3	51.7	50.2	21.7	52	50.1	51.3	51.8	50.1	51.1	51.7	50	51.4	51.6	49.8	51.4	51.4		50	46	52
14	50.2	51.5	51.6	50	51.5	51.8	50.1	51.3	51.7	49.9	51.2	51.6	49.9	51.3	51.5	49.8	51.3	51.4		50	51	52
15	50.1	51.4	51.5	50	51.6	51.8	50.2	51.4	51.5	50	51	51.4	49.8	51.1	51.4	49.9	51.2	51.1		50	51	51
16	50	51.3	51.5	49.6	51.5	51.2	49.8	51.2	51.2	49.9	50.4	51.1	49.2	51.2	50.6	49.7	50.7	50.3		50	51	51

03/09/2020

	H1	H2	H3	H1	H2	H3	H1	H2	H3	H1	H2	H3	H1	H2	H3	H1	H2	H3	H1	H2	H3
1	44.9	45.1	43.8	43.6	45	42.2	41	45.1	43.5	44.2	45.8	44.4	41.2	45.7	43.6	43.8	45.7	42.4		43	45	43
2	45.5	46.8	45.2	44.5	46.3	44.6	43.1	46.5	45.1	45.4	47.3	45.4	43.8	47	45.6	44.8	46.9	45.7		45	47	45
3	45.9	47.7	46	45.5	47.7	45.8	44.4	47.7	45.4	45.8	48.3	46.4	44.8	47.8	46.6	45.9	48.3	46.4		45	48	46
4	46.5	48.9	47.4	46.5	48.7	47.1	45.2	49	47.6	46.6	48.9	47.8	45.6	48.5	47.4	46.6	49	47.6		46	49	47
5	46.8	49.2	49.1	47.4	49.2	48.5	46.1	49.6	49	47.7	49.4	48.9	46.2	49.4	48.4	47.3	49.5	48.3		47	49	49
6	47.3	49.6	49.7	47.7	49.4	49.4	47.1	50	49.9	48.1	50	49.5	47	50	49.7	47.8	49.8	49.1		48	50	50
7	47.9	49.9	50.1	48.4	50	49.9	47.7	50.4	50.5	48.6	50.2	50.3	47.7	50.3	50.4	48.3	50.2	50.2		48	50	50
8	48.2	50.2	50.2	48.7	50.3	50.5	48.2	50.8	51	48.9	50.6	50.9	48.4	50.5	50.9	48.9	50.6	50.8		49	51	51
9	48.3	50.6	50.9	49.1	50.7	51.1	48.6	51	51.4	49.4	50.9	51.4	48.8	50.9	51.3	49.2	50.9	51.3		49	51	51
10	48.7	50.7	50.9	49.4	50.8	51.2	49.1	51.3	51.6	49.6	51	51.7	49.3	51	51.4	49.4	51.1	51.5		49	51	51
11	49.2	50.8	51.1	49.5	51.1	51.3	49.3	51.4	57.7	49.9	51.2	52	49.5	51.3	51.6	49.6	51.2	51.6		50	51	53
12	49.3	50.9	51	49.7	51	51.5	49.6	51.5	51.8	50	51.3	52.1	49.8	51.2	51.6	50	51.4	51.7		50	51	52
13	49.3	50.8	51.1	49.9	51.2	51.5	49.8	51.5	51.8	50.1	51.3	51.9	49.9	51.3	51.6	49.9	51.3	51.1		50	51	52
14	49.3	50.8	50.8	49.7	51	51.3	49.7	51.4	51.7	50.1	51.3	51.8	50.1	51.2	51.5	50.2	51.2	51.6		50	51	51
15	49.1	50.7	50.6	49.7	50.8	51.1	49.8	51.5	51.5	50	51	51.7	50	51.1	51.4	50.1	51.1	51.3		50	51	51
16	48.2	50.5	50	49.6	49.7	51	49.5	51.1	51	48.8	49.9	51.2	49.6	50.9	50.7	5	50.2	49.8		42	50	51

02/09/2020

	H1	H2	H3	H1	H2	H3	H1	H2	H3	H1	H2	H3	H1	H2	H3	H1	H2	H3	H1	H2	H3
1	44.6	46.3	44.8	43.7	44.3	44.9	42.7	46	45	42.6	46.6	44.6	41.3	46.8	43.9	42	47.6	46		43	46	45
2	45.3	47.2	46	44.7	46.4	46	44	47.5	46.6	44.2	47.6	45.8	42.7	48	45.5	43.8	48.4	47		44	48	46
3	46	48.1	47	45.4	47.5	47.2	45.2	48.4	48	45.3	48.5	47.2	44	48.5	46.8	45	48.8	47.8		45	48	47
4	46.6	48.8	48.1	46.3	48.4	48.2	46.2	49.1	48.6	46.2	49.2	48.2	45.1	49.2	48	45.7	49.4	49		46	49	48
5	47.2	49.2	49.3	46.9	48.8	49	47.3	49.5	49.7	47.1	49.5	49.1	45.8	49.6	49	46.5	49.8	49.5		47	49	49
6	47.5	49.7	49.9	47.5	49.4	50.1	48	49.7	50.3	47.4	50	50.1	46.6	50	49.7	47.4	50.1	50		47	50	50
7	48.2	50.1	50.4	48.1	50	50.4	48.6	50.1	51	48.1	50.3	50.7	47.5	50.2	50.3	48.1	50.4	50.8		48	50	51
8	48.5	50.3	50.7	48.7	50.2	50.7	48.9	50.5	51.3	48.3	50.6	50.9	48.2	50.5	50.7	48.5	50.6	51		49	50	51
9	48.7	50.5	51.1	48.9	50.6	51.2	49.4	50.8	51.6	48.9	50.8	51.1	48.8	50.1	51.2	48.9	50.8	51.2		49	51	51
10	49.3	50.9	51.4	49.4	50.7	51.2	49.8	50.9	51.8	49.3	51	51.5	49.1	51	51.3	49.3	51.1	51.6		49	51	51
11	49.7	50.8	51.5	49.6	51	51.4	50.2	51	51.9	49.6	51.1	51.6	49.4	51	51.4	49.5	51.2	51.7		50	51	52
12	49.8	51	51.5	49.8	51	51.5	50.3	51.1	52	49.9	51.1	51.5	49.7	51.1	51.5	49.8	51.2	51.7		50	51	52
13	49.8	51	51.2	50	50.8	51.4	50.4	51.1	51.9	49.9	51.2	51.5	49.9	51.1	51.5	49.8	51.3	51.7		50	51	52
14	49.9	50.9	51.3	50.2	50.9	51.3	50.5	50.9	51.8	50.1	51.1	51.6	50	51.2	51.4	49.5	51.2	51.6		50	51	52
15	49.8	50.9	51.2	50.1	51	51.2	50.4	50.8	51.7	50	50.8	51.1	49.9	51.1	51.3	48.1	51.1	51.4		50	51	51
16	49.7	50.7	51.3	50.3	50.7	50.1	50.5	51.2	51.4	48.2	49.7	48.8	48.2	50.8	50.2	41.2	51.2	50		48	51	50

01/09/2020

	H1	H2	H3	H1	H2	H3	H1	H2	H3	H1	H2	H3	H1	H2	H3	H1	H2	H3	H1	H2	H3
1	44.8	46	45.6	40.7	44.3	43.3	42.2	48.1	46.3	43.5	46.6	45.3	44.2	46.5	46.1	44.1	46	45.8		43	46	45
2	45.5	47.2	46.8	43.1	46	44.8	43.7	48.7	47.2	44.3	47.7	46.6	45.2	47.7	47.3	44.6	47.3	46.4		44	47	47
3	45.7	48.2	48	44.4	47	46.1	44.7	49.2	48.7	45.2	48.5	47.6	46	48.4	48.3	45.5	48.1	47.7		45	48	48
4	46.2	48.8	48.8	45.5	48.2	47.5	45.6	49.5	49.2	45.7	48.9	48.2	46.6	48.9	49.1	46.6	48.7	48.5		46	49	49
5	47.2	49.2	49.5	46.2	48.7	48.7	46.5	49.8	50	46.7	49.5	49.4	47.4	49.4	49.9	47.4	49.2	49		47	49	49
6	47.7	49.6	50	47.2	49.5	49.6	47.5	50.1	50.5	47.4	49.8	49.9	47.7	49.8	50.3	47.8	49.6	49.9		48	50	50
7	48	50	50.3	48.1	50	50.4	48.1	50.5	50.9	47.8	50.2	50.3	48.2	50.2	50.6	48.1	50.1	50.3		48	50	50
8	48.7	50.2	50.8	48.5	50.3	50.9	48.6	50.7	51.2	48.4	50.4	50.9	48.9	50.5	51	48.5	50.4	50.6		49	50	51
9	49.1	50.4	51	49.2	50.5	51	49	50.9	51.3	49.1	50.7	51	49.3	50.7	51.2	48.9	50.6	51		49	51	51
10	49.4	50.6	51.2	49.5	50.8	51.2	49.6	51	51.5	49.3	50.8	51.1	49.5	50.8	51.4	49.2	50.8	51.2		49	51	51
11	49.6	50.7	51.2	49.9	51	51.5	49.7	51	51.6	49.6	51	51.2	49.6	51	51.4	19.6	51	51.3		45	51	51
12	49.9	50.9	51.3	50.1	51.1	51.6	50.1	51.1	51.6	49.7	51	51.4	50	51	51.5	49.8	51.1	51.4		50	51	51
13	49.8	50.7	51.4	50.1	51.1	51.5	50.3	51.1	51.7	49.8	50.9	51.3	50.1	50.9	51.5	49.9	51	51.4		50	51	51
14	50.1	50.8	51.3	50.2	51	51.2	50.4	51.1	51.6	50	50.8	51.2	50.4	50.8	512	50.1	50.9	51.2		50	51	128
15	50	50.7	51.2	50.3	50.9	51	49.8	51.1	51.4	49.9	50.5	51	50.4	50.5	51	50	50.7	51.1		50	51	51
16	50.2	5.9	511	49.7	51.1	48.7	46.8	51	50.4	49.4	50.3	49.9	50.3	49.4	50.9	49.3	49.6	50.8		49	43	127

31/08/2020

	H1	H2	H3	H1	H2	H3	H1	H2	H3	H1	H2	H3	H1	H2	H3	H1	H2	H3	H1	H2	H3	
1	44.3	47	45	43.4	46.1	44.4	42.4	43.3	44.1	41.3	43.1	43.2	42.9	46.7	44.5	42	45.2	45.1		43	45	44
2	44.8	47.6	46.3	44.3	47.2	46	44	45.8	45.5	42.9	45	44.3	43.6	47.9	45.8	43.2	46.8	46		44	47	46
3	45.6	48.5	47.3	45	48.1	47.2	44.7	47.3	46.7	44.2	46.4	45.1	44.4	48.3	46.5	44.3	47.7	47.2		45	48	47
4	46.5	49	48.5	45.6	49	48.1	45.2	48.1	47.7	45.3	48	46.7	45.4	49	47.7	45.4	48.4	48.1		46	49	48
5	47	49.3	49.6	46.6	49.3	49.2	46.5	48.9	48.4	46.4	48.6	47.7	46.5	49.4	49	46	49.1	49		47	49	49
6	47.7	49.7	49.9	47.4	49.5	49.9	47.3	49.4	49.6	47.2	49.2	49.4	47	49.7	49.7	46.8	49.6	49.9		47	50	50
7	48	50	50.4	47.8	49.9	50.3	47.8	49.8	50	47.7	49.8	49.8	47.5	50	50.2	47.8	50	50.3		48	50	50
8	48.5	50.2	51	48.4	50.2	50.7	48.4	50	50.6	48.1	50.3	50.4	48.2	50.3	50.7	48.4	50.2	50.7		48	50	51
9	49	50.5	51.1	49	50.6	51.1	49.1	50.2	51.1	48.8	50.5	50.8	48.8	50.5	51	49	50.4	51		49	50	51
10	49.5	50.7	51.2	49.5	50.8	51.4	49.4	50.7	51.2	49.3	50.8	51.1	49	50.6	51.2	49.5	50.6	51.2		49	51	51
11	49.7	50.8	51.3	49.7	50.9	51.5	49.9	50.8	51.3	49.7	51.1	51.4	49.8	50.9	51.4	49.8	50.8	51.4		50	51	51
12	50	50.9	51.4	50	50.9	51.4	50.2	50.9	51.5	50	51.2	51.5	49.8	50.8	51.4	50	50.9	51.5		50	51	51
13	49.9	50.9	51.4	50.2	50.9	51.4	50.4	50.8	51.4	50.2	51.2	51.6	50	50.9	51.4	50.2	50.8	51.4		50	51	51
14	50.2	50.9	51.1	50.4	50.9	51.3	50.4	50.6	51.3	50.4	51.1	51.4	50.4	50.9	51.1	50.1	50.8	51.3		50	51	51
15	50.4	50.6	50.7	50.4	50.7	51.1	50.6	50.3	51.3	50.3	51	51.4	50.5	50.8	51.1	50.6	50.7	51.3		50	51	51
16	50.3	49.9	51	50.2	50.7	50.5	50.2	49.7	50.3	49.4	50.5	51.6	50	50.2	50.6	48	50.6	50.9		50	50	51

30/08/2020

	H1	H2	H3	H1	H2	H3	H1	H2	H3	H1	H2	H3	H1	H2	H3	H1	H2	H3	H1	H2	H3	
1	43.3	41.9	42.9	40.1	43	43.5	41.7	42.7	43.3	45.3	43.8	44.9	42.2	44.3	43.7	41.3		45		42	43	44
2	45	44.5	44.9	42.1	45.6	45.1	43.6	45.7	44.5	46.3	45.7	46.5	43.8	46.3	45.3	43.2	46.8	44.6		44	46	45
3	45.2	45.1	46.1	43.4	47.2	45.8	44.8	47.5	46.6	47.1	47.5	47.7	44.9	47.8	47	44.4	48.1	46		45	47	47
4	45.6	47.1	46.9	44.6	48	46.7	45.6	48.2	48	47.6	48.8	48.7	46.4	48.7	48	45.1	49.1	47.6		46	48	48
5	46	48.1	48.1	45.5	48.8	48.4	46.2	49	48.7	48.1	49.8	49.7	47.3	49.2	49.1	46.9	50	48.8		47	49	49
6	47	48.9	49.2	46.5	49.2	49.2	47.4	49.7	49.8	48.8	50.2	50.4	48.1	50.2	49.6	47.8	50	50		48	50	50
7	47.6	49.1	49.5	47.6	49.6	49.7	48.1	50	50.3	49.3	50.6	51.1	48.7	50.6	50.8	48.6	50.8	50.7		48	50	50
8	48	49.7	50.1	48.3	50.1	50.5	48.5	50.5	50.6	49.6	50.9	51.6	49.3	50.8	51.2	49	51.2	51.2		49	51	51
9	48.5	50	50.7	48.8	50.4	50.7	49.2	50.7	51	49.8	51.2	51.9	50	51.2	51.8	49.5	51.3	51.9		49	51	51
10	48.9	50.3	50.8	49.4	50.6	51.1	49.5	50.9	51.5	50.3	51.5	52	50.4	51.4	51.9	50.2	51.9	52.2		50	51	52
11	49.3	50.3	50.8	49.6	50.8	51.2	49.8	51.1	51.6	50.7	51.7	52.2	50.9	51.6	52.2	50.7	52	52.5		50	51	52
12	49.5	50.5	50.9	50	51	51.3	50.1	51.2	51.6	50.8	51.8	52.1	50.9	51.7	52.3	50.9	51.9	52.5		50	51	52
13	49.9	50.6	51	50.2	51	51.4	50.4	51.2	51.6	51	52	52.3	51.3	51.8	52.4	51	52.1	52.5		51	51	52
14	49.8	50.4	50.9	50.4	51.1	51.3	50.6	51.1	51.3	51	51.9	52.1	51.5	51.7	52.2	51.4	52	52.3		51	51	52
15	50.1	50.5	50.5	50.5	51	51	50.5	51.1	51.1	50.8	51.8	52.1	51.5	51.5	51.9	51.5	51.7	51.8		51	51	51
16	49.8	50.5	50.4	50.3	50.8	50.9	49.8	48.7	50.1	49.9	51.9	51.3	50.9	51.6	50.2	51.2	52.2	48.5		50	51	50

29/08/2020

	H1	H2	H3	H1	H2	H3	H1	H2	H3	H1	H2	H3	H1	H2	H3	H1	H2	H3	H1	H2	H3
1	40.4	40.3	37.8	34.4	38	38.2	27	44	40.5	45.2	45.7	45.3	44	44.7	44.2	44.7	45.1	45.8		39	43	42
2	42.9	42.4	40.6	38.5	40.3	40.5	32	45.2	42.2	45.9	46.5	46.4	44.7	46.3	45.6	45.6	47.4	46.7		42	45	44
3	44.4	44.6	43.3	42.1	44	43.5	36.5	46.4	44	46	48	47.6	46	47.8	47	46.4	48.4	47.8		44	47	46
4	45.2	46	44.8	43.3	45.8	45.2	41.1	47.6	45.3	46.2	48.7	48.1	46.5	48.4	48.3	47	48.9	48.9		45	48	47
5	46	47.7	46.3	44.8	47.5	46.5	43.4	43.5	47	47	49.4	49.1	47.5	49.2	48.6	47.6	49.7	49.4		46	48	48
6	46.9	48.3	47.5	45.8	48.2	47.8	44.6	49.2	48.2	47.6	49.6	49.8	48	49.5	49.5	48.1	50	50		47	49	49
7	47.5	49.1	48.7	46.8	48.8	48.7	46	49.6	48.6	48.3	50.2	50.1	48.5	49.8	50.1	48.5	50.5	50.1		48	50	49
8	48.2	49.4	49.4	48	49.4	49.5	47.4	50	49.5	48.6	50.3	50.6	48.8	50.3	50.6	49.2	50.7	51.1		48	50	50
9	48.7	49.6	50.2	48.4	49.9	50.3	48	50.2	50.1	49	50.6	51.1	49.4	50.6	51.2	49.5	51	51.4		49	50	51
10	49.2	50.1	50.5	49.2	50.3	50.6	48.6	50.6	50.8	49.6	507	51.2	49.7	50.9	51.3	50	51.1	51.6		49	127	51
11	49.7	50.3	50.9	49.7	50.6	51	49.3	50.7	51.1	49.9	51.1	51.4	50.1	50.9	51.4	50.4	51.2	51.7		50	51	51
12	50.1	50.4	50.9	49.8	50.7	51.2	49.8	50.7	51.2	50.3	51.2	51.4	50.3	50.9	51.3	50.5	51.4	51.8		50	51	51
13	50.1	50.5	51	50	50.8	51.2	50.3	50.8	51.2	50.4	51.2	51.5	50.4	51	51.6	50.7	51.5	51.8		50	51	51
14	49.9	506	50.9	50.1	50.7	51.1	50.4	50.8	51.2	50.7	51.1	51.4	50.6	51	51.4	50.8	51.4	51.9		50	127	51
15	50.2	50.4	50.7	50.2	50.4	50.9	50.5	50.6	51	50.7	51.1	51.2	50.4	51.1	51.1	50.9	51.3	51.8		50	51	51
16	50.3	50	50.6	50.1	49.2	50.7	48.4	50.1	48.9	50.7	50.9	50.3	48.7	50.8	49.7	51.5	49.9	51.5		50	50	50

28/08/2020

	H1	H2	H3	H1	H2	H3	H1	H2	H3	H1	H2	H3	H1	H2	H3	H1	H2	H3	H1	H2	H3
1	36.6	39.7	39.2	34.5	38.7	43.3	48.4	48.3	36.1	4.03	41.4	43.5	38	40.7	41.8	37.1	42.4	41.8		33	42	41
2	41.7	41.9	41.5	38.6	41.8	43.8	42.5	41.6	41	43	43.8	45	42.2	43.5	44.2	41.4	44.8	43.6		42	43	43
3	44.7	44.2	43	42.1	44.3	45.7	44.6	43.5	43.1	44.9	46.3	46.3	43.8	45.3	45.6	44	46.3	45.5		44	45	45
4	45.9	46.4	45.6	44.8	46.3	47.7	45.8	46.2	45	45.3	47.8	47.6	45.3	46.8	46.5	45.1	47.9	47.3		45	47	47
5	46.2	47.9	46.5	45.6	48.1	48.5	46.5	47.5	46.8	46.3	48.4	49.1	46.1	47.8	48.2	46	48.5	48.3		46	48	48
6	46.5	48.7	48.1	46.2	49.1	49.7	47.2	48.1	47.4	46.8	49.1	49.7	47.3	48.7	49.2	46.9	49	49.3		47	49	49
7	47.4	49.3	49.5	47.7	49.6	50.3	48.3	49.6	48.9	47.6	49.6	50.2	47.9	49.3	49.7	48	49.7	49.8		48	50	50
8	48.3	49.7	50.1	48.6	50	51	48.7	49.5	49.7	48.3	50.1	51	48.7	49.9	50.6	48.5	50.2	50.6		49	50	51
9	48.7	50.1	50.9	49.3	50.5	51.6	49.4	50.1	50.7	49	50.4	51.5	49.1	50.1	51.1	48.9	50.5	51.2		49	50	51
10	49.2	50.4	51.4	50	50.7	51.9	50.2	50.5	51.2	49.6	50.7	51.6	49.9	50.4	51.4	49.5	50.7	51.4		50	51	51
11	49.6	50.5	51.6	50.6	51.1	52	50.7	50.6	51.4	50.1	51	51.6	50.4	50.6	51.8	50.1	51	51.7		50	51	52
12	50	51	51.7	50.9	51.2	52.2	51.1	50.9	51.6	50.4	51.2	51.8	50.6	51	51.9	50.4	51.1	52		51	51	52
13	50.1	51.2	51.7	51.1	51.4	52.1	51.4	50.9	517	50.8	51.2	51.7	50.9	51.1	51.9	50.6	51.2	51.9		51	51	129
14	50.4	51.1	51.5	51.3	51.5	52.2	51.5	51	51.6	50.9	51.3	51.6	51	51	51.8	50.9	51.3	51.8		51	51	52
15	50.3	51.1	51.4	51.3	51.4	52	51.4	50.9	51.4	51.1	51.2	51.4	51	51.1	51.5	50.8	51.2	51.6		51	51	52
16	46.2	51.1	50.6	49.9	50.3	51.3	50.8	50.3	50.1	50.7	50.4	50.6	48.9	51	50.3	49.7	51.3	50.1		49	51	51

27/08/2020

	H1	H2	H3	H1	H2	H3	H1	H2	H3	H1	H2	H3	H1	H2	H3	H1	H2	H3	H1	H2	H3
1	35.1	33.2	35.7	33.1	30.2	37.6	34.8	37.7	37.1	33.8	37.5	37.8	36	37.3	40.4	37.2	36.2	38.2		35	35	38
2	38.1	39.7	39.6	37	38.3	41.3	38.1	41.4	40.5	39.2	42	42	39.8	40.5	43.2	42.2	39.2	43		39	40	42
3	42.9	42.1	42.7	41	40.5	42.8	42.4	43.6	42.5	43.9	43.9	43.8	43.4	44.2	44.6	44.4	41.6	44.3		43	43	43
4	44.3	44.5	45.2	43.7	44	45.4	43.6	46.3	45.2	45.2	45.6	45.6	44.5	46.5	45.6	45.5	43.8	45.4		44	45	45
5	45.5	46.6	46	44.3	45.7	46	44.4	47.3	46.6	45.9	47.6	47.3	46	47.5	47.4	46.4	46.3	47		45	47	47
6	46	48.1	47.5	45.8	47.4	48.4	45.7	48.7	47.9	46.3	48.5	48.6	46.6	48.6	48.4	47.2	48.1	48.3		46	48	48
7	47	48.9	48.9	47.1	48.4	49.2	46.7	49.1	48.2	47.7	49.4	49.3	47.8	49.5	49.3	48.2	48.7	49.6		47	49	49
8	47.8	49.7	49.8	48.3	49.3	50	47.6	49.5	49.5	48.5	49.7	50	48.6	50	50.2	48.5	49.6	50.2		48	50	50
9	48.3	50.2	50.5	48.7	49.9	50.7	48.4	50.1	50.3	49.2	50.4	50.7	49	50.3	50.8	49.3	49.9	50.8		49	50	51
10	49	50.4	51.2	49.3	50.4	51.2	49	50.3	50.7	49.7	50.6	51.2	49.6	50.6	51.3	49.8	50.5	51.3		49	50	51
11	49.6	50.7	51.4	50	50.6	51.4	49.9	50.5	50.9	50.1	51	51.5	50.1	50.9	51.6	50.3	50.9	51.7		50	51	51
12	50	50.9	51.6	50.5	50.8	51.6	50.3	50.6	51.3	50.4	51	51.7	50.6	51.2	51.7	50.7	51	51.7		50	51	52
13	50.2	51.1	51.6	50.8	51	51.6	50.6	50.7	51.4	50.7	51.2	51.8	50.8	51.3	51.8	50.8	51.1	51.8		51	51	52
14	50.5	51	51.5	50.9	51	51.5	50.8	50.7	51.4	50.8	51.1	51.7	51	51.2	51.6	51.1	51.2	51.7		51	51	52
15	50.5	51.1	51.3	51	51	51.4	50.8	50.7	51.2	51.1	51.1	51.5	51.1	51.3	51.7	50.9	51.2	51.6		51	51	51
16	50.6	50.6	51.2	50.4	50.7	50.4	50.8	50	51.1	49.8	50.9	48.2	50.8	51.2	50.9	49.9	51.1	51.5		50	51	51

26/08/2020

	H1	H2	H3	H1	H2	H3	H1	H2	H3	H1	H2	H3	H1	H2	H3	H1	H2	H3	H1	H2	H3
1	34.8	38.6	37.5	36.4	39.5	41.3	35.5	33	35.9	32.5	35.2	29.1	32.3	29.2	34.4	29.8	25.2	29.3		34	33	35
2	39.5	41.4	41.8	42	42.9	43.1	38.7	37.8	4.03	36.6	37.9	33.7	37.1	35.5	37.1	35.5	34.5	35.2		38	38	32
3	43.2	43.5	42.2	42.6	44.8	44.9	41	41.3	42.4	40.4	42.6	39.3	49.3	38.9	40.8	40.5	37.3	39.4		43	41	42
4	44	45.6	45	44.9	46.7	46.5	43.3	43.6	44.2	43.4	45.5	41.5	42.8	43.4	44.1	43.4	43.2	43		44	45	44
5	44	47.3	45.9	45.9	47.9	46.7	45.5	46.1	46.1	45.4	46.7	44.1	44	45.6	45	45.1	45.7	45.1		45	47	45
6	44.9	48.1	47.2	46.4	48.6	48.4	46.1	47.1	47.9	45.8	48.1	45.9	45.7	47.4	46.5	45.7	47.4	46		46	48	47
7	46.1	48.7	48.4	47.4	49.2	49.2	47.7	48.8	49	47.2	48.9	47.2	46.3	48.5	47.8	46.9	48.2	48.1		47	49	48
8	47.2	49.3	49.5	48.3	49.6	50.1	48.3	49.2	49.8	48.3	49.6	48.1	47.9	49.3	48.9	47.8	49.2	49.1		48	49	49
9	47.7	49.8	50	49.1	50	50.7	48.9	49.8	50.5	48.8	50.1	49.7	48.7	49.8	49.9	48.4	49.6	49.4		49	50	50
10	48.6	50.2	50.9	49.5	50.2	51.1	49.5	50.3	51.1	49.6	50.4	50.2	49.5	50.2	50.6	48.9	50.1	50.6		49	50	51
11	49.2	50.3	50.9	50.1	50.5	51.3	50.1	50.6	51.3	50	50.8	51.1	50	50.6	51.1	49.6	50.5	51.2		50	51	51
12	49.6	50.6	51.1	50.3	50.8	51.5	50.5	50.8	51.5	50.2	50.9	51.3	50.4	50.8	51.6	50	50.8	51.3		50	51	51
13	50.1	50.7	51.2	50.6	50.9	51.4	50.6	51	51.6	50.6	51	51.4	50.8	51	51.6	50.5	50.8	51.5		51	51	51
14	50.2	50.7	51.2	50.8	50.9	51.3	50.8	51	51.5	50.7	51	51.3	50.9	50.9	51.5	50.7	51	51.4		51	51	51
15	50	50.8	51	50.7	50.8	51.2	50.8	51.1	51.3	50.7	51.1	51.2	51	51	51.2	50.8	50.9	51.3		51	51	51
16	50.3	50.1	49.8	49.8	50.2	51.1	50.6	50.3	49.5	49.5	50.7	50.7	50.5	50.7	49.8	50.8	50.6	51.1		50	50	50

25/08/2020

	H1	H2	H3	H1	H2	H3	H1	H2	H3	H1	H2	H3	H1	H2	H3	H1	H2	H3	H1	H2	H3
1	35.1	35.1	37	48.8	37.8	40.3	38.4	37.5	39.1	35.2	36	41.1	37	40.1	40.9	34.2	36.6	48.4		38	37	41
2	42.1	39.1	40.8	42.4	42.5	43.3	42.2	40.4	41.5	38.1	38.2	42.9	39.3	43.2	42.5	38.1	49.4	41		40	42	42
3	43	42.6	43.2	43	44.3	43.5	43.5	43.3	43.7	40.7	42.5	43.9	43.1	44.4	45.6	41.5	42.6	44.2		42	43	44
4	43.9	44.5	44.4	44.1	46.1	45.2	44.4	45.7	45.2	43.5	44.3	45.7	44.5	46.5	47.1	43.3	44.5	44.6		44	45	45
5	45.2	46.5	45.2	46.1	47.3	46.4	46.2	47.1	46.1	45.1	45.5	47	45.6	47.3	47.4	45.1	46.2	45.8		46	47	46
6	45.6	47.3	46.4	46.5	48.4	48.2	47.1	48	48.1	46.3	47.4	48.4	47	48.2	49.4	45.9	47.8	47.3		46	48	48
7	47.2	48.1	48.5	47.5	48.7	49.1	48.1	48.8	48.2	47.6	48.5	48.9	48.6	48.8	49.8	47.6	48.7	48.4		48	49	49
8	47.6	48.7	49.1	48.4	49.4	50.1	48.3	49.3	49.6	48.5	49	50.1	49.5	49.3	50.1	48.3	49.4	49.7		48	49	50
9	48.1	49.2	49.7	48.9	49.8	50.4	49.1	49.7	50.5	48.9	49.5	50.4	50.1	49.8	50.5	49	49.9	50.2		49	50	50
10	48.8	49.6	50.4	49.5	50.2	51	49.7	50	51.2	49.9	49.8	51.1	50.9	50.1	51.3	49.7	50.2	51.2		50	50	51
11	49.2	49.9	50.6	49.9	50.5	51.3	50	50.5	51.3	50.4	50.2	51.4	51.3	50.4	51.6	50.2	50.6	51.4		50	50	51
12	49.8	50.1	50.8	50.3	50.7	51.5	50.4	50.7	51.5	50.7	50.6	51.5	51.4	50.5	51.6	50.6	50.8	51.7		51	51	51
13	50	56.4	50.7	50.3	50.9	51.5	50.6	50.8	51.5	50.9	50.7	51.5	51.6	50.6	51.7	50.8	51	51.8		51	52	51
14	50.1	50.5	50.7	50.5	51	51.4	50.8	50.8	51.4	51	50.8	51.5	51.5	50.7	51.7	50.8	51	51.7		51	51	51
15	49.9	50.5	50.6	50.5	51	51.1	50.7	50.9	51.1	51.1	51	51.1	51.4	50.6	51.6	50.8	51	51.4		51	51	51
16	48.6	50.4	49.8	49.4	50.7	50.5	49.9	50	50.8	50.4	51	49.5	51.2	50.3	51	49.7	50.5	51		50	50	50

24/08/2020

	H1	H2	H3	H1	H2	H3	H1	H2	H3	H1	H2	H3	H1	H2	H3	H1	H2	H3	H1	H2	H3
1	35.6	33.5	37.2	29.2	24.8	35	34.3	26.6	36.7	29.9	35.2	37.2	33.1	24.9	37.7	36.1	41.4	40.8		33	31	37
2	40.1	35.9	41.6	34.7	32.6	39.2	38.6	34	41.9	35.4	39.2	41.4	36.9	37.2	41.1	40.4	43.8	42.6		38	37	41
3	44.1	41.4	44	40.5	36.1	42.8	41.9	38.1	42.7	39.6	42.8	43	40.7	41.7	43.4	43	45.3	44.5		42	41	43
4	44.2	43.2	44.3	42.2	40.6	44.5	44.1	42.5	44.6	43.4	44.3	45.2	43.3	44.6	44.6	44.1	46.9	46.3		44	44	45
5	46.1	45.3	46.2	44.2	43.9	45.4	46	44.7	45.7	44.3	46.7	47	44.9	46.2	46.2	45	47.5	47.3		45	46	46
6	46.7	47.2	47.5	45.3	45.6	46.2	46.3	47.2	47.9	45.9	47.6	48	46.4	48	47.5	45.9	48	48.3		46	47	48
7	47.7	48.3	48.1	46.7	47.1	48.6	47.3	47.6	49.3	46.9	48.9	48.7	47.8	48.6	48.6	47	48.7	48.8		47	48	49
8	47.8	48.9	49.5	48.1	49.2	49.5	48.5	48.8	49.6	48.1	49.4	49.7	48.6	49.5	49.2	47.5	49.2	49.6		48	49	50
9	48.3	49.4	50.2	48.8	49	50	49.1	49.2	50.5	49.1	49.9	50.8	49.1	49.8	50	47.9	49.5	50.2		49	49	50
10	49.3	49.7	50.7	49.2	49.5	51	49.8	49.7	51.1	49.7	50.1	51.2	49.9	50.3	50.4	48.5	49.7	50.4		49	50	51
11	49.6	50.1	51.1	50.2	49.9	51.2	50.2	50.3	51.3	50.2	50.5	51.4	50.6	50.5	51.1	49.1	50	50.7		50	50	51
12	49.9	50.5	51.3	50.3	50.3	51.5	50.6	50.5	51.5	50.6	50.7	51.5	50.9	50.8	51.3	49.4	50.1	51		50	50	51
13	50.4	50.6	51.4	50.9	50.6	51.6	51	50.7	51.5	50.9	50.9	51.6	51.1	50.9	51.4	49.6	50.2	50.9		51	51	51
14	50.4	50.7	51.2	50.9	50.6	51.4	51	50.9	51.4	50.9	51	51.5	51.1	51	51.4	49.9	50.1	50.8		51	51	51
15	50.3	50.8	51.1	50.8	50.7	51.3	50.4	50.9	51.2	50.9	50.9	51.2	51.1	51.1	51.3	49.8	50.1	50.6		51	51	51
16	49.5	49.1	48.3	49.8	50.7	50.4	49.5	50.8	50.8	49.9	50.9	51	50.2	50.9	50.5	48.7	50.3	49.1		50	50	50

23/08/2020

	H1	H2	H3	H1	H2	H3	H1	H2	H3	H1	H2	H3	H1	H2	H3	H1	H2	H3	H1	H2	H3
1	36.6	37	39.9	38.5	36.9	39.8	35.2	38.3	41.7	34.6	38.4	41.5	38.6	36.6	37.5	28.8	24.2	28.3		35	35	38
2	40.1	42.6	42.3	41.6	41.2	42.2	38.7	42.7	43.3	39.5	42.3	42.2	41.5	39.6	42.5	34.5	33.5	34.2		39	40	41
3	42.4	44.7	44.6	47	44.3	44.4	41.6	44.5	45.2	42.4	44.4	45.3	43.9	42.7	44.1	39.5	36.3	38.4		43	43	44
4	45.4	46.3	45.3	47.1	46.2	45.8	44.7	46.2	46.2	43.2	45.7	46.3	44.7	44.9	45.2	42.4	42.3	42		45	45	45
5	46.1	47.8	47.8	47.3	48	48.4	45.8	47.5	48.1	46	47.6	47.5	45.9	46.9	45.3	44.1	44.7	44.1		46	47	47
6	45.7	48.6	48.7	46.6	48.6	49.2	46.8	48.3	49	46.4	48.4	48.5	47.4	47.6	47.4	44.7	46.4	45		46	48	48
7	47.1	48.9	49.7	47.7	49.5	49.5	47.6	49.1	49.9	48.1	49.1	49.4	48.1	48.8	48.9	45.9	47.2	47.1		47	49	49
8	48	49.5	50.2	48.6	49.7	50.3	48.9	49.5	50.6	48.3	49.4	49.9	48.5	49.3	49.2	46.8	48.2	48.1		48	49	50
9	48.8	50	50.5	49.3	50.2	51	49.4	50	51.2	49.3	49.8	50.4	49.2	49.6	50	47.4	48.6	48		49	50	50
10	49.9	50.4	51.1	49.6	50.5	51.2	50	50.2	51.5	49.9	50.1	51.1	50.1	50.1	51	47.9	49.1	48.4		50	50	51
11	50.4	50.7	51.5	50.4	50.8	51.5	50.8	50.5	51.7	50.5	50.5	51.4	50.2	50.3	51.4	48.6	49.5	49.6		50	50	51
12	50.8	51	51.6	50.7	51	51.5	51	50.7	51.8	50.9	50.7	51.5	50.7	50.6	51.5	49	49.8	50.2		51	51	51
13	51.1	51.2	51.7	51.3	51	51.5	51.2	50.8	51.8	51.1	50.8	51.5	50.9	50.8	51.5	49.5	49.8	50.3		51	51	51
14	51.1	51.3	51.6	51.3	51.1	51.4	51.1	51.1	51.7	51	50.9	51.4	51	50.9	51.5	49.7	50	50.5		51	51	51
15	50.1	51.3	51.3	51.1	51.3	51.2	50.9	51.1	51.6	51	51	51.3	50.8	50.9	51.1	49.8	49.9	50.4		51	51	51
16	50.3	50.5	50.7	50.1	50.7	50.8	50.1	51	51.3	50.7	50.7	50.6	50.6	50.3	50.6	49.8	49.6	50.3		50	50	51

22/08/2020

	H1	H2	H3	H1	H2	H3	H1	H2	H3	H1	H2	H3	H1	H2	H3	H1	H2	H3	H1	H2	H3
1	44.1	32.1	35.6	31.9	36.2	35.7	30.7	37.8	37.2	32.9	40.1	34.7	40.7	33.7	21.6	33.2	35.6	47.4		36	36	35
2	46.4	36.9	39	359	40.1	38.5	31.1	41.8	40.6	38.5	44.1	38.7	43.8	35.6	23.9	37.1	48.4	40		93	41	37
3	47.6	40.7	43	40.3	42.1	43.2	31.6	42.9	43.4	41.4	44.8	43.5	44.7	39.1	24.5	40.5	41.6	43.2		41	42	40
4	48.1	43.5	45.3	47.3	45.2	45.3	36.3	46.4	44.8	44.2	46.9	44.7	45.5	42.9	25.9	42.3	43.5	43.6		44	45	42
5	49	45.7	45.9	45.5	47.4	45.9	41.9	47.2	46.9	45.4	47.1	46.5	45.6	45.5	33.9	44.1	45.2	44.8		45	46	44
6	49.4	47.6	48	47.3	48.2	47.5	43.8	48.1	47.2	45.8	47.6	46.5	47.3	47	38	44.9	46.8	46.3		46	48	46
7	49.8	48.5	49	47.4	49	49.2	44.9	49.2	49.7	46.5	48.4	48.3	48.3	48.2	42.7	46.6	47.7	47.4		47	49	48
8	50.2	49.1	50.1	49	49.2	49.5	46.8	49.5	50.2	47.8	48.9	49.3	48.7	48.7	45.6	47.3	48.4	48.7		48	49	49
9	50.6	49.8	50.7	49	49.7	50.4	48.8	49.8	50.5	48.7	49.6	50	49.6	49.3	48.7	48	48.9	49.2		49	50	50
10	51	50	51.1	49.9	50.1	51	48.9	50.2	50.9	49.8	49.8	50.8	50	49.8	49.7	48.7	49.2	50.2		50	50	51
11	51.3	50.4	51.7	50.8	50.4	51.5	49.9	50.6	51.4	50.3	50.2	51.2	50.6	50.2	50.8	49.2	49.6	50.4		50	50	51
12	51.3	50.7	51.8	51.2	50.7	51.7	50.7	50.9	51.7	50.7	50.5	51.4	50.7	50.6	51.3	49.6	49.8	50.7		51	51	51
13	51.2	50.8	51.9	51.4	50.9	51.7	51.2	50.9	51.7	51	50.6	51.4	50.7	50.8	51.7	49.8	50	50.8		51	51	52
14	51.1	50.9	51.8	51.2	51	51.6	51.2	51.1	51.6	50.9	50.7	51.3	50.8	50.9	51.5	49.8	50	50.7		51	51	51
15	50.7	50.9	51.5	51.1	50.7	51.3	51.1	51	51.4	50.7	50.7	51.1	50.3	50.7	51.4	49.8	50	50.4		51	51	51
16	50.4	49.8	51	51	50.7	50.6	50.6	50.9	49.9	49.2	49.3	50	48.6	47.5	51.1	48.7	49.5	50		50	50	50

21/08/2020

	H1	H2	H3	H1	H2	H3	H1	H2	H3	H1	H2	H3	H1	H2	H3	H1	H2	H3	H1	H2	H3
1	40.1	40	38.8	35.9	41	39.8	37.8	41.6	41.3	40.3	42.4	41.4	39.3	40.4	41.5	39.2	43.7	40.8		39	42	41
2	45.6	43.2	40.6	40.7	43	42.1	41.5	42.8	43	42.1	44.3	43.1	42.5	42.7	43	40.7	45.1	42.4		42	44	42
3	46	44	42.1	41.7	45.1	44.1	42.8	44.8	43.9	43	45.6	44.5	43	44.6	44.5	42.5	46.2	44.1		43	45	44
4	46.4	45.9	43.8	43	46.6	45.5	43.9	46.1	45.6	44.5	46.8	45.9	43.8	46	45.9	44	47.3	45		44	46	45
5	46.5	46.9	45.1	44.1	47	46.5	44.7	47.3	46.7	45.3	47.8	47	44.8	47.1	47	44.8	48.2	46.8		45	47	47
6	47	47.7	46.6	45.2	48	47.3	45.5	48	48	46.2	48.4	47.7	45.4	47.9	48.1	45.5	48.7	48		46	48	48
7	47	48.5	47.9	46.2	48.2	48.1	46.7	48.6	48.6	46.7	49	48.9	46.3	48.2	48.8	46.5	49	48.6		47	49	48
8	47.7	48.9	48.9	46.6	48.9	49.3	46.9	49.2	49.5	47.2	49.4	49.4	46.7	48.8	49.3	46.9	49.4	49.6		47	49	49
9	48.1	49.4	49	47.3	49	49.6	47.6	49.5	49.7	47.5	49.7	49.8	47.4	49.4	49.8	47.3	49.7	49.7		48	49	50
10	48.1	49.6	49.3	47.8	49.6	49.9	47.7	49.8	50.2	48.1	49.9	50.1	48	49.6	49.9	47.7	49.9	50.2		48	50	50
11	48.2	49.8	49.8	48.1	49.8	50.2	48.1	50.1	50.3	48.4	50	50.2	48.2	49.6	50.3	48	50.1	50.4		48	50	50
12	48.5	49.9	50	48.3	49.9	50.4	48.2	50	50.5	48.5	50.1	50.5	48.3	50.1	50.5	48.2	50.1	50.6		48	50	50
13	48.6	49.8	50	48.5	50	50.3	48.4	50.1	50.5	48.8	50.3	50.4	48.4	50.1	50.3	48.3	50	50.6		49	50	50
14	48.5	49.9	49.9	48.4	50	50.1	48.5	50.2	50.5	48.7	50.2	50.3	48.5	50	50.4	48.5	50	50.5		49	50	50
15	48.5	49.7	49.9	48.4	49.7	49.7	48.6	50.1	50.3	48.5	50.1	50.2	48.5	50.2	50.3	48.5	49.8	50.2		49	50	50
16	46.6	49.8	49	47.2	48.2	48.8	48.4	49.9	50.1	48.3	50.2	50	48.6	50	50.1	48.6	49.3	49.8		48	50	50